Adaptación vascular para irrigar cáncer de colon en humanos: Mecanismos modificados por el ambiente tumoral

Nelson Ivan Cupitra Vergara

Grupo de Investigación en Fisiología y Bioquímica - PHYSIS

Corporación de Ciencias Básicas Biomédicas

Facultad de Medicina

Universidad de Antioquia

Medellín, Colombia

2020

Adaptación vascular para irrigar cáncer de colon en humanos: Mecanismos modificados por el ambiente tumoral

Nelson Ivan Cupitra Vergara. Biólogo.

Tesis sometida en cumplimiento de los requisitos para la obtención del título de Doctor en Ciencias Básicas Biomédicas con énfasis en Bioquímica, Farmacología y Fisiología

DIRECTOR

Raúl Leonardo Narváez Sánchez- MD MSc PhD

Profesor Titular, Universidad de Antioquia, Colombia

Comité Tutorial

Juan Camilo Calderón, MD PhD - Profesor Titular, Universidad de Antioquia, Colombia

Omar Estrada, Químico PhD - Profesor Investigador Instituto Venezolano de Investigaciones científicas, Venezuela

Ángel Luis García Villalón, MD PhD - Catedrático, Universidad Autónoma de Madrid, España

Grupo de Investigación en Fisiología y Bioquímica - PHYSIS

Corporación de Ciencias Básicas Biomédicas

Facultad de Medicina

Universidad de Antioquia

Medellín, Colombia

2020

Nota de aceptación

Nota de aceptación:

_____

_____

_____

_____

_____

_____

_____

Firma del presidente del jurado

_____

Firma del jurado

_____

Firma del jurado

Ciudad y fecha (día, mes, año)

_____

Agradecimientos

A mis padres, hermanos, esposa por apoyarme siempre

A mi hija por ser mi motor y motivarme a ser cada día mejor

A los profesores Raúl Narváez Sánchez y Juan Camilo Calderón por su orientación durante todo este proceso.

A los profesores Omar Estrada y Ángel Luis García-Villalón por su acompañamiento como miembros del comité tutorial.

A mis compañeros y amigos del Grupo PHYSIS.

A la Universidad de Antioquia, al Comité para el Desarrollo de Investigación-Universidad de Antioquia y el Banco de la República por la financiación de este trabajo.

Al sistema de regalías, Universidad del Tolima, Grupo GIPRONUT por la financiación y el apoyo en mi doctorado

A la Universidad de Antioquia y a la Corporación de Ciencias Básicas Biomédicas por aceptarme como su alumno.

A la IPS universitaria- Clínica León XIII en particular Jimmy Paul león su acompañamiento en la obtención de arterias humanas

Resumen

Generar conocimiento acerca del sistema vascular tumoral y su rol en el desarrollo del cáncer tiene potencial impacto en su tratamiento. La virtual totalidad de este tipo de estudios se dedica a caracterizar la angiogénesis, por lo que este trabajo no se enfocará en esta. Dos aspectos poco explorados de las adaptaciones vasculares en cáncer son los cambios en la arquitectura de la pared vascular (en íntima, media y adventicia), y/o en la reactividad vascular (VR) de las arterias que irrigan el tumor. Por ello, se propuso cuantificar estos mecanismos de adaptación vascular en cáncer. Metodología: en arterias tumorales de colon (TU), arterias extratumorales (ET) del mismo paciente y arterias mesentéricas de pacientes sin cáncer (NT), se determinaron por histología (hematoxilina y eosina) los cambios en la morfología vascular; en baño de órgano aislado se evaluó la VR expresada en pD2 y Emax, en respuesta a KCl, fenilefrina (PE), endotelina-1 (ET-1), U46619 (análogo del tromboxano A2), carbacol (CCh), bradikinina (BK), isoproterenol y factor de crecimiento vascular endotelial (VEGF). Además, se cuantificó la expresión de los receptores tromboxano-prostanoides (TP), α1, β2, receptor de endotelina A (ETA) y B (ETB), receptores uno (VEGFR1) y dos (VEGFR2) de VEGF por inmunofluorescencia, normalizando los resultados con la expresión de los receptores en NT. Las comparaciones entre grupos se hicieron con ANOVA. Resultados: se procesaron trece pacientes no tumorales entre 46±9 años, seis mujeres y siete hombres, y Veinticinco pacientes con diagnóstico de adenocarcinoma de CAc, 15 mujeres y 10 hombres. Se encontró hiperplasia del 50% en media y >200% en íntima de arterias de los grupos ET y TU. En VR, se encontraron diferencias significativas en sensibilidad a KCl (pD2: NT, 1.6±0.04; ET, 1.8±0.02; TU, 1.8±0.03, p=0.02). Al estímulo con PE aumentó la pD2 (pD2: NT, 5.7±0.008; ET, 6.2±0.09; TU, 6.1±0.13, p=0.004) y Emax (Emax: NT, 91±12%KCl; ET, 137±6.5% y TU, 117±18%; p=0.04) en ET y TU. A U46619 se presentó un aumento de sensibilidad (pD2: NT, 7.08±0.1; ET, 7.3±0.09; TU, 7.2±0.1, p=0.06) en ET y TU. No se encontraron diferencias en la VR a ET-1. En relajación, el 70% de los pacientes con cáncer presentó Emax a BK inferior al 30% indicando baja viabilidad endotelial, debido a esto los ensayos de relajación se hicieron solo con paciente que presentaran un Emax a BK superior al 30%. Se encontró un aumento en sensibilidad a CCh (Emax: NT, 1.3±8%; ET, 49.6±14% y TU, 41.5±13% de relajación; p=0.009) en ET y TU. Al estímulo con BK disminuyó la pD2 (pD2: NT, 6.2±0.16; ET, 6.01±0.2; TU, 6.05±0.12, p=0.02) y Emax (Emax: NT, 91±20%; ET,

53.4±5.6% y TU, 44.08±1% de relajación, p=0.03) en ET y TU. Al estímulo con isoproterenol aumentó la sensibilidad (pD2: NT, 6.5±0.17; ET, 8.3±0.3; TU, 7.7±0.18, p=0.001) y Emax (Emax: NT, 8.4±2%; ET, 28.2±5% y TU, 29.5±9.2% de relajación; p=0.005) en ET y TU. No se encontraron diferencias en la VR a VEGF. En la cuantificación de expresión se evidenció aumento en la íntima de los receptores α1, TP y VEGFR2 en ET, y TP, β2 y VEGFR1 en TU. En la túnica media aumentó la expresión de α1 y TP en ET y solo TP en TU. No se encontraron diferencias en la expresión de ETA y ETB, ni en adventicia para ningún receptor. Conclusión: el tumor induce engrosamiento de la pared vascular superior al 50% en la íntima y la media, generando cambios en la VR que favorecen la contracción adrenérgica y por tromboxano A2, por aumento de sus receptores y disfunción endotelial. Al tiempo que la arteria favorece la relajación colinérgica y β2-adrenérgica como compensación a la disminución de relajación dependiente de óxido nítrico. Estas modificaciones podrían favorecer un ambiente hipóxico en el tumor retroalimentando así vías de señalización como VEGF/PTEN/GSK3B/NF-kB que facilitan el desarrollo tumoral y las adaptaciones vasculares. A partir de este trabajo se establece una plataforma de investigación basada en los mecanismos de adaptación vascular en cáncer y donde se podría explorar el potencial farmacológico de las vías de contracción/relajación alteradas.

Esta tesis consta de seis capítulos y dos anexos. Los capítulos dos y tres, y los anexos, son artículos que fueron publicados con autoría principal o co-autoría de Nelson Cupitra durante su formación doctoral. Los capítulos cuatro y cinco son dos artículos más que serán sometidos antes de la defensa pública de la tesis, con autoría principal de Nelson Cupitra. En total, con los cuatro artículos ya publicados, esta tesis suma un factor de impacto de 12,05.

Esta tesis fue defendida el 28 de enero de 2021 y obtuvo la calificación *summa cum laude* (4.9 sobre 5)

Abstract

To generate knowledge about the tumor vascular system and its role in the development of cancer has a potential impact on its treatment. Virtually all of these types of studies are dedicated to characterizing angiogenesis, so this work will not focus on it. Two little-explored aspects of vascular adaptations in cancer are changes in the architecture of the vascular wall (intima, media, and adventitia), and/or in vascular reactivity (VR) of the arteries supplying the tumor. Therefore, it was proposed to quantify these vascular adaptation mechanisms in cancer. Methodology: in colon tumor arteries (TU), extratumoral arteries (ET) from the same patient and mesenteric arteries from patients without cancer (NT), the changes in vascular morphology were determined by histology (hematoxylin and eosin); In isolated organ bath, VR expressed in pD2 and Emax was evaluated, in response to KCl, phenylephrine (PE), endothelin-1 (ET-1), U46619 (analog of thromboxane A2), carbachol (CCh), bradykinin (BK), isoproterenol and vascular endothelial growth factor (VEGF). Furthermore, the expression of thromboxane-prostanoid receptors (TP), α1, β2, endothelin receptor A (ETA) and B (ETB), receptors one (VEGFR1) and two (VEGFR2) of VEGF was quantified by immunofluorescence, normalizing the results with the expression of the receptors in NT. Comparisons between groups were made with ANOVA. Results: thirteen non-tumor patients (46±9 years old), six women and seven men, and twenty-five patients with a diagnosis of colon cancer adenocarcinoma (7±3.1 years old), 15 women and 10 men, were processed. Hyperplasia of 50% was found in the middle and> 200% in the intima of arteries of the ET and TU groups. In VR, significant differences were found in sensitivity to KCl (pD2: NT, 1.6±0.04; ET, 1.8±0.02; TU, 1.8±0.03, p=0.02). Upon stimulation with PE increased the pD2 (pD2: NT, 5.7±0.008; ET, 6.2 ± 0.09; TU, 6.1±0.13, p=0.004) and Emax (Emax: NT, 91±12% KCl; ET, 137±6.5% and TU, 117±18%; p=0.04) in ET and TU. U46619 showed an increase in sensitivity (pD2: NT, 7.08±0.1; ET, 7.3±0.09; TU, 7.2±0.1, p=0.06) in ET and TU. No differences were found in VR at ET-1. In relaxation, 70% of cancer patients presented Emax at BK lower than 30% indicating low endothelial viability, due to this the relaxation tests were performed only with patients who presented an Emax at BK greater than 30%. An increase in sensitivity to CCh (Emax: NT, 1.3±8%; ET, 49.6±14% and TU, 41.5±13% relaxation; p=0.009) was found in ET and TU. Upon stimulation with BK, pD2 (pD2: NT, 6.2±0.16; ET, 6.01±0.2; TU, 6.05±0.12, p=0.02) and Emax (Emax: NT, 91±20%; ET, 53.4±5.6%) decreased and TU, 44.08±1% relaxation, p=0.03) in ET and TU. When

stimulated with isoproterenol, sensitivity increases (pD2: NT, 6.5±0.17; ET, 8.3±0.3; TU, 7.7±0.18, p=0.001) and Emax (Emax: NT, 8.4±2%; ET, 28.2±5% and TU, 29.5±9.2% relaxation; p=0.005) in ET and TU. No differences were found in VR to VEGF. In the quantification of expression, an increase in the intima of the α1, TP and VEGFR2 receptors was evidenced in ET, and TP, β2 and VEGFR1 in TU. In the tunica media, the expression of α1 and TP increases in ET and only TP in TU. No differences were found in the expression of ETA and ETB, nor in adventitia for any receptor. Conclusion: the tumor induces thickening of the vascular wall greater than 50% in the intima and media, generating changes in VR that favor adrenergic contraction and by thromboxane A2, due to an increase in its receptors and endothelial dysfunction. At the same time, the artery favors cholinergic and β2-adrenergic relaxation as compensation for the decrease in nitric oxide-dependent relaxation. These modifications could favor a hypoxic environment in the tumor, thus feeding back signaling pathways such as VEGF/PTEN/GSK3B/NF-kB that facilitate tumor development and vascular adaptations. Based on this work, a research platform is established based on vascular adaptation mechanisms in cancer and where the pharmacological role of altered contraction/relaxation pathways could be explored.

This thesis consists of six chapters and two annexes. Chapters two and three, and the annexes, are articles that were published with the main or co-authorship of Nelson Cupitra during his doctoral training. Chapters four and five are two more articles that will be submitted before the public defense of the thesis, with the main authorship of Nelson Cupitra. In total, with the four articles already published, this thesis adds an impact factor of 12.05.

This thesis was defended on January 28, 2021 and qualified as *summa cum laude* (4.9 out of 5)

Índice general

Contenido

Índice de Figuras

Cada figura se denomina por dos números. El primer número corresponde al capítulo de esta tesis, y el segundo número es el de la figura dentro del artículo. Por ejemplo, la figura 1.1 es la primera que aparece en el artículo que constituye el capítulo 1.

Índice de Tablas

Capítulo uno: Introducción, preguntas de investigación y objetivos

1. Introducción

El cáncer (CA) es una forma de crecimiento anormal de las células que genera múltiples complicaciones en los sistemas biológicos. Según la Organización Mundial de la Salud, es la segunda causa de muerte en el planeta. Uno de los CA más comunes en la población es el cáncer de colon (CAc), ocupando el cuarto lugar en incidencia (19.7 por cada 100.000 hab.) y tercero en mortalidad (8.9 por cada 100.000 hab.) a nivel mundial. El CAc es el tercero de mayor incidencia en Colombia (15.8 por cada 100.000 hab.; WHO, 2020). Como tratamiento para el CAc se utiliza cirugía, que remueve el tumor, o radioterapia, que emplea radiaciones ionizantes, y/o quimioterapia, que utiliza fármacos para atacar las células cancerosas. Sin embargo, por la complejidad celular en los tumores sólidos en estadios intermedios y avanzados del CAc u otros cánceres, es frecuente que estos tratamientos sean poco eficaces llevando a una recaída de la enfermedad o la muerte.

En cáncer, la señalización promueve adaptaciones vasculares para tratar de garantizar un mayor suministro de sangre y satisfacer los requisitos de energéticos de la población de células tumorales. Estas adaptaciones se pueden dar por tres vías, angiogénesis, remodelación y reactividad vascular (VR). La angiogénesis es un proceso fisiológico por el cual se forman nuevos vasos sanguíneos a partir de los vasos preexistentes. A la fecha la *Food and Drug Administration-FDA* ha aprobado más de una docena de fármacos como tratamiento anti-angiogénico en cáncer, todos ellos inducen fuertes efectos secundarios y en algunos casos aumentan el riesgo de eventos fatales. Además, en tumores no angiogénicos han llevado a facilitar la progresión de la enfermedad (Lin, 2016). Gran parte de estas complicaciones se deben al desconocimiento de la relación entre el tumor y las modificaciones vasculares asociadas a la enfermedad, lo que puede contribuir a una pobre respuesta del paciente al tratamiento. La mayoría de las investigaciones se han enfocado en el potencial angiogénico de las células tumorales, y en la necesidad del tumor de reclutar vasos sanguíneos para garantizar el suministro de oxígeno y nutrientes en su crecimiento (Nagy, 2012), sin embargo, este trabajo no hará énfasis en la angiogénesis, y se enfocará en la remodelación y la VR.

El tumor también induce remodelación, entendida como la capacidad de una arteria de adaptar su tamaño estructural ante estímulos crónicos, aumentando o reduciendo el tamaño externo para mantener un lumen funcional. En cáncer esta remodelación ha dado como resultado la proliferación de células de músculo liso vascular, síntesis de matriz extracelular y engrosamiento de la adventicia haciendo que la arteria adapte el espesor de su pared a la demanda tumoral. Algunas aproximaciones experimentales histológicas y moleculares han descrito en la vasculatura intratumoral seis tipos de vasos sanguíneos diferentes e irregulares, cuyo crecimiento es estimulado por los altos niveles de expresión del factor de crecimiento vascular endotelial (VEGF) en las células tumorales. Estos vasos se pueden dividir en dos grupos: tempranos (vasos madre, vasos glomeruloides) estimulados por hipoxia y dependientes al estímulo de VEGF, y tardíos (arterias, venas, capilares, malformaciones vasculares), donde al parecer, su proceso de diferenciación es disparado por el estrés de cizalladura generado por fluido (FSS) y el bloqueo de VEGF (Nagy, 2012). Sin embargo, en la vasculatura extratumoral la influencia tumoral vía VEGF u otros inductores de proliferación como la endotelina-1 no está clara, pero dado que en otras enfermedades de carácter inflamatorio se han reportado remodelamiento de la pared vascular mediada por VEGF y endotelina-1 (ET-1), sería esperable que el tumor induzca adaptaciones vasculares en las túnicas íntima y media, alterando posiblemente la función vascular y con ello el flujo de suministros al tumor.

La VR puede considerarse como una medida funcional de la respuesta del vaso sanguíneo, ante el estímulo con agonistas contráctiles como noradrenalina, tromboxano A2 y ET-1, o vasodilatadores como acetilcolina, isoproterenol, bradikinina y VEGF. La VR es definida en términos de sensibilidad –logaritmo negativo en base 10 del EC50 (pD2)- y efecto máximo –Emax-. En cáncer, la VR podría ser un factor limitante de crecimiento del tumor, dado que tejidos altamente proliferativos requieren de mayor irrigación. Los trabajos en el área están enfocados en modelar la morfología y función en la vasculatura intra-tumoral, sólo los trabajos de Ferrero en 2008 y Voss en 2019, usando baño de órgano aislado y cuantificando la expresión de receptores, hacen un primer acercamiento a las diferencias en VR, encontrando aumento en sensibilidad al estímulo con ET-1 y aumento en la vasorelajación

dependiente de óxido nítrico, entre arterias que irrigan tumores en CAc comparados con arterias de pacientes sin cáncer. No obstante, aún los mecanismos involucrados en la respuesta de estos y otros agonistas son desconocidos.

Dado que no hay claridad sobre los cambios en VR en arterias que irrigan tumores, una alternativa para caracterizar el comportamiento vascular en cáncer es comparar la respuesta al estímulo de agonistas fisiológicamente endógenos que a su vez participen en el desarrollo tumoral. Por ejemplo: se han reportado en cultivos celulares un aumento en los niveles de expresión de agonistas y sus receptores en la señalización beta-adrenérgica asociados con crecimiento y metástasis, en cáncer de cerebro, pulmón, riñón, mama, ovario y próstata; modulando la función de miocitos, adipocitos, fibroblastos y pericitos en tumores (Cole, 2012). Se ha reportado el eje tromboxano A2/Ciclooxigenasa-2 como intermediario en migración y angiogénesis en cáncer colorrectal y de mama (Sakai, 2006).

A su vez, para ET-1 y su receptor ET-A se ha descrito que se encuentran sobreexpresada en cáncer de ovario, pulmón, hígado, próstata entre otras, estimulando proliferación, angiogénesis, osteogénesis y supervivencia tumoral y que tienen un efecto principalmente constrictor sobre la pared vascular (Rosanò, 2013). Agonistas de dilatación vascular como acetilcolina, bradikinina (BK), se han asociado como inductores de proliferación, inflamación, crecimiento, y migración tumoral. También se ha reportado que VEGF a través de su receptor 2 (VEGFR2) es potente inductor de proliferación y angiogénesis en cáncer (Rapisarda, 2012) e induce vasodilatación en la circulación pulmonar (Olsson, 2006). Sin embargo, no hay evidencia que respalde los cambios en la VR al estímulo de ninguno de estos agonistas. Al identificar las diferencias funcionales de los vasos en cáncer es posible establecer una plataforma a partir de la cual se gestionen estrategias farmacológicas, que podría enfocarse en promover vasoconstricción en el tumor, reduciendo el suministro de nutrientes y el crecimiento tumoral; o estimulando vasodilatación para aumentar el flujo sanguíneo, coadyuvando en quimioterapia para que los fármacos mejoren su perfusión en células cancerosas y mejore la respuesta al tratamiento.

El VEGF es uno de los blancos farmacológicos en angiogénesis más recurrentes, el VEGF actúa sobre las células endoteliales a través de su receptor VEGFR2, activando la

señalización Akt, que a través de NF-kB, GSK3B y mTOR que estimulan la angiogénesis, facilitan supervivencia, proliferación y migración tumoral. Esta vía es de nuestro particular interés ya que es regulada por la proteína homóloga de fosfatasa y tensina (PTEN), que inhibe la señalización PI3K/Akt/VEGF y con ello no solo la angiogénesis y progresión tumoral, también podría guardar relación con los cambios en función vascular y la remodelación de vasos sanguíneos (Katayama, 2019). Además, al igual que en angiogénesis PTEN actúa como inhibidor, tanto en la proliferación del músculo liso vascular, como de los cambios fenotípicos en el vaso sanguíneo, además de inhibir los procesos trombóticos locales, la adhesión plaquetaria y de macromoléculas y el engrosamiento de la capa media vascular. Por lo anterior queremos describir la relación entre la VR, el remodelamiento y el estadío del tumor en pacientes con CAc.

En el desarrollo de este trabajo se reconocieron limitaciones experimentales que podrían influir en los resultados de la investigación. En experimentación, las arterias humanas regularmente se obtienen en los quirófanos de pacientes con patologías que requieren resección de un segmento del colon o de donantes de órganos, esto implica que el tejido requiere de mínimo 90 minutos de conservación para su transporte al laboratorio e inicio de los experimentos. Adicionalmente, los experimentos en baño de órganos se ven limitados por el número de cámaras del equipo, donde muchas veces la cantidad de arteria excede la capacidad del equipo para montar el tejido en fresco, siendo una posibilidad conservar el tejido a 4°C para aumentar el tiempo de vida útil del vaso, y realizar un nuevo montaje pasadas de 12 a 24 horas desde la resección en quirófano, aumentado así el aprovechamiento de la muestra. Sin embargo, dicha preservación también promueve cambios fisiológicos por activación proteínas de choque térmico, que se activan como respuesta a la hipoxia e hipotermia inducida, y durante el restablecimiento de las condiciones de O_2 y temperatura fisiológica se pueden inducir reacciones inflamatorias crónicas y procesos apoptóticos que dañan el tejido (Rauen, 2004; Buchinger-Kähler, 2016). Por lo anterior y para determinar qué cambios funcionales en los vasos sanguíneos son atribuibles a la influencia del cáncer y no a la preservación, se estableció como objetivo secundario

cuantificar la influencia del tiempo de conservación de 0 a 48 horas sobre la VR y la expresión de receptores en aorta de conejo.

Mientras avanzaba el procesamiento de las arterias de pacientes se identificó otra posible limitación, el grupo de pacientes con cáncer era notablemente más viejo que el grupo control, esto representa un reto experimental ya que se ha reportado que en el envejecimiento se aumenta el riesgo de sufrir enfermedades cardiovasculares, que son responsables del mayor porcentaje de muertes en el mundo, alcanzando el 31% (WHO, 2020). A medida que la población de adultos mayores aumenta, es necesario dilucidar los mecanismos de la disfunción vascular con la edad. Se ha descrito que en el envejecimiento se presenta aumento de la rigidez aórtica y se atribuye principalmente a cambios en la matriz extracelular, a veces denominada elastocalcinosis (Dao, 2005; Donato, 2018). De manera complementaria, el envejecimiento también afecta la VR, al alterar la sensibilidad y el efecto máximo de los agonistas contráctiles estimulantes y vasodilatadores endógenos. Es factible que la rigidez vascular se deba no solo a un mecanismo sino también a la complementariedad de varios, y uno muy importante a tener en cuenta sería el cambio en la VR. Por lo anterior, consideramos que es importante diferenciar los posibles cambios en los vasos sanguíneos causados por el tumor de los causados por el envejecimiento de los vasos, por ello se estableció como objetivo secundario cuantificar la influencia del envejecimiento sobre la VR, el engrosamiento vascular y la expresión de receptores en aorta de conejos jóvenes, adultos y viejos.

La última limitación que se encontró en este trabajo guarda relación con: primero, que la frecuencia de pacientes patológicos no tumorales (grupo control) fue baja (3-4 pacientes por año), reduciendo la potencia estadística, además de inducir riesgo de subestimar o sobreestimar los resultados dado que en ambos casos son grupos con patologías de base. Segundo, la imposibilidad de conseguir arterias de pacientes sanos (donantes de órganos por muerte cerebral) para comparar con el grupo con cáncer. Teniendo en cuenta estas limitaciones, y manteniendo la necesidad un grupo control accesible y comparable, se estableció como una alternativa el uso de modelos animales para caracterizar la función vascular en circulación mesentérica y determinar si hay un modelo que reconociendo las

limitaciones pueda servir como control en este trabajo. En investigación, los modelos *ex vivo* han sido indispensables para caracterizar los mecanismos fisiopatológicos de las ECV y obtener información sobre de eventos específicos, a través de procedimientos precisos, que pueden ser invasivos y difíciles de usar en estudios clínicos (Russell, 2006; Virmani, 2003). No obstante, las diferencias intrínsecas dadas por la biología de cada especie dificultan la extrapolación de resultados, siendo esperable que, entre especies filogenéticamente distintas, sus características puedan condicionar la respuesta a diferentes mecanismos fisiopatológicos o al tratamiento farmacológico. A pesar de las limitaciones genéticas, el modelo vascular en circulación mesentérica más utilizado es la rata, ya que dada las facilidades de crianza, su ciclo de desarrollo y la posibilidad de controlar variables ambientales durante su cría se ha posicionado el modelo estándar en experimentación de fisiopatologías vasculares, sin embargo, algunos resultados promisorios encontrados en ratas no son homologables en humanos. Una posible alternativa para obtener modelos vasculares de mayor tamaño y tal vez mayor comparabilidad con el humano, son cerdos y conejos de granjas tecnificadas, si bien, en estos lugares las variables ambientales no son controladas en su totalidad, son modelos que podrían ser más comparables con el humano. Además, la influencia del medio ambiente en el desarrollo de estos modelos podría aportar información valiosa sobre el comportamiento cardiovascular. Por lo anterior se estableció como objetivo secundario determinar el grado de comparabilidad en la VR y en expresión de receptores en arterias de circulación mesentérica entre el humano, el cerdo, el conejo y la rata.

Esta tesis incluye cuatro capítulos y dos anexos:

- Capítulo 2: Cupitra NI, Calderón JC, Narvaez-Sanchez R, 2020. Increased receptor expression supports vascular reactivity of the rabbit aorta during preservation.
- Capítulo 3: Cupitra NI, Calderón JC, Narvaez-Sanchez, 2020. Influence of ageing on vascular reactivity and receptor expression in rabbit aorta: a complement to elastocalcinosis and smooth muscle mechanisms

- Capítulo 4: Cupitra NI, Calderón JC, León-Rodríguez JP, Narváez-Sánchez R, 2020. Comparability of vascular reactivity and expression of receptors of mesenteric circulation between human, pig, rabbit and rat
- Capítulo 5: Cupitra NI, Calderón JC, León-Rodríguez JP, Narváez-Sánchez R, 2020. Mecanismos de adaptación en remodelamiento y reactividad vascular en arterias que irrigan tumores en cáncer de colon en humanos
- Anexo 1. Estrada O, Giulio C, Dorta-Ledezma R, Gonzalez-Mujica F, Motta N, Zea E, Cupitra NI, Contreras W, Narvaez-Sanchez R, Calderón JC, 2019. Compound Isolated from Phyllanthus tenellus Demonstrates Metabolic and Vascular Effects In Vitro
- Anexo 2. Romero-Imbachi MR, Cupitra NI, Ángel K, González B, Estrada O, Calderón JC, Guerrero-Vargas J, Beltrán J, Narvaez-Sanchez R, 2020. *Centruroides margaritatus* scorpion complete venom exerts cardiovascular effects through alpha-1 adrenergic receptors

2. Preguntas de investigación

Esta investigación gira en torno a la siguiente pregunta:

- ¿Cuáles son los mecanismos de adaptación en remodelamiento y reactividad vascular inducidos por el CAc en humanos sobre los vasos sanguíneos que lo irrigan?

Las siguientes preguntas de investigación responden cuestionamientos operacionales que surgieron en el desarrollo de la pregunta principal

- ¿Cuál es el tiempo óptimo para conservar arterias sin perder reactividad vascular al estímulo con KCl, PE, U46619, CCh, BK e isoproterenol?
- ¿Cómo influye la edad sobre VR al estímulo con KCl, PE, U46619, CCh, BK, isoproterenol y en la expresión de los receptores TP, α1 y β2?
- ¿Cuál es el mejor modelo vascular en VR y expresión de receptores más comparable con los humanos entre cerdos, conejos y ratas?

3. Objetivos

3.1. General:

- Caracterizar mecanismos de adaptación vascular en remodelación y VR inducidos en arterias que irrigan CAc en humanos.

3.2. Específico capítulo 2

- Cuantificar la influencia del tiempo de conservación de 0, 24 y 48 horas sobre la VR y la expresión de receptores en aorta de conejo.

3.3. Específico capítulo 3

- Cuantificar la influencia del envejecimiento sobre la función vascular, el engrosamiento vascular y la expresión de receptores en aorta de conejo.

3.4. Específico capítulo 4

- Determinar el grado de comparabilidad en la VR y en expresión de receptores en arterias de circulación mesentérica entre el humano, el cerdo, el conejo y la rata.

3.5. Específicos capítulo 5 y pregunta principal

- Caracterizar clínica y antropométricamente la población de pacientes a estudiar.
- Medir la respuesta a KCl, fenilefrina, U46619, Endotelina-1, bradikinina, carbacol, isoproterenol y VEGF en presencia y en ausencia de bloqueantes específicos de sus receptores, en arterias tumorales y no tumorales.
- Determinar probables diferencias en la expresión proteica de los receptores α1, β2-1, ETA, ETB, VEGFR1, VEGFR2, y receptor de tromboxano-prostanoides, en arterias tumorales y no tumorales
- Determinar probables diferencias en la expresión proteica de los receptores de PTEN, GSK3β, NF-kB y tubulina, en arterias tumorales y no tumorales
- Determinar probables diferencias en la expresión génica de VEGF, ECE-1, y COX-2, en arterias tumorales y no tumorales
- Buscar asociaciones entre la reactividad vascular, la expresión génica y la estadificación del tumor.

Capítulo dos:

Cupitra NI, Calderón JC, Narvaez-Sanchez R, 2020. Increased receptor expression supports vascular reactivity of the rabbit aorta during preservation.

Capítulo dos:

Cupitra NI, Calderón JC, Narvaez-Sanchez R, 2020. Increased receptor expression supports vascular reactivity of the rabbit aorta during preservation.

Artículo publicado en European Journal of Cardio-Thoracic Surgery; IF:3.48

Enlace: https://academic.oup.com/ejcts/advance-article-abstract/doi/10.1093/ejcts/ezaa386/5982003?redirectedFrom=fulltext

Cuando inició la recolección de arterias humanas en el semestre 2017-1, se encontró la primera limitación en el trabajo, el transporte desde quirófano y montaje de las arterias en el baño de órganos nos tomaba 90 minutos, periodo durante el cual se podrían inducir cambios en la VR que luego afectarán los hallazgos en cáncer, sumado a ello, la productividad en los experimentos era baja debido a que el equipo limitaba los montajes a solo cuatro baños por experimento, obligando en la mayoría de los casos a congelar o eliminar más de la mitad de las arterias obtenidas. Para resolver esta limitación metodológica y buscando ampliar la ventana de tiempo de trabajo con las arterias humanas, nos propusimos determinar cuáles mecanismos en VR se ven afectados durante la preservación y cuáles son atribuibles a la influencia del cáncer, cuantificando la influencia del tiempo de conservación de 0, 24 y 48 horas sobre la VR y la expresión de receptores. Dada la baja frecuencia de pacientes y la imposibilidad de obtener arterias sin preservación para comparar, se escogió como modelo vascular la aorta de conejo, un modelo validado, reproducible y con las dimensiones necesarias para establecer un diseño experimental pareado.

A continuación, el artículo correspondiente al capítulo dos.

European Journal of Cardio-Thoracic Surgery 0 (2020) 1–8
doi:10.1093/ejcts/ezaa386

ORIGINAL ARTICLE

Cite this article as: Cupitra NI, Calderón JC, Narvaez-Sanchez R. Increased receptor expression supports vascular reactivity of the rabbit aorta during preservation. Eur J Cardiothorac Surg 2020; doi:10.1093/ejcts/ezaa386.

EXPERIMENTAL

Increased receptor expression supports vascular reactivity of the rabbit aorta during preservation

Nelson Ivan Cupitra, Juan C. Calderón and Raul Narvaez-Sanchez*

Physiology and Biochemistry Research Group-PHYSIS, Faculty of Medicine, University of Antioquia, Medellin, Colombia

* Corresponding author. Physiology and Biochemistry Research Group-PHYSIS, Faculty of Medicine, University of Antioquia, Carrera 51 D #62-29 office 203, Medellin 050010, Colombia. Tel: +57-4-2196030; e-mail: raul.narvaez@udea.edu.co (R. Narvaez-Sanchez).

Received 21 May 2020; received in revised form 12 August 2020; accepted 5 September 2020

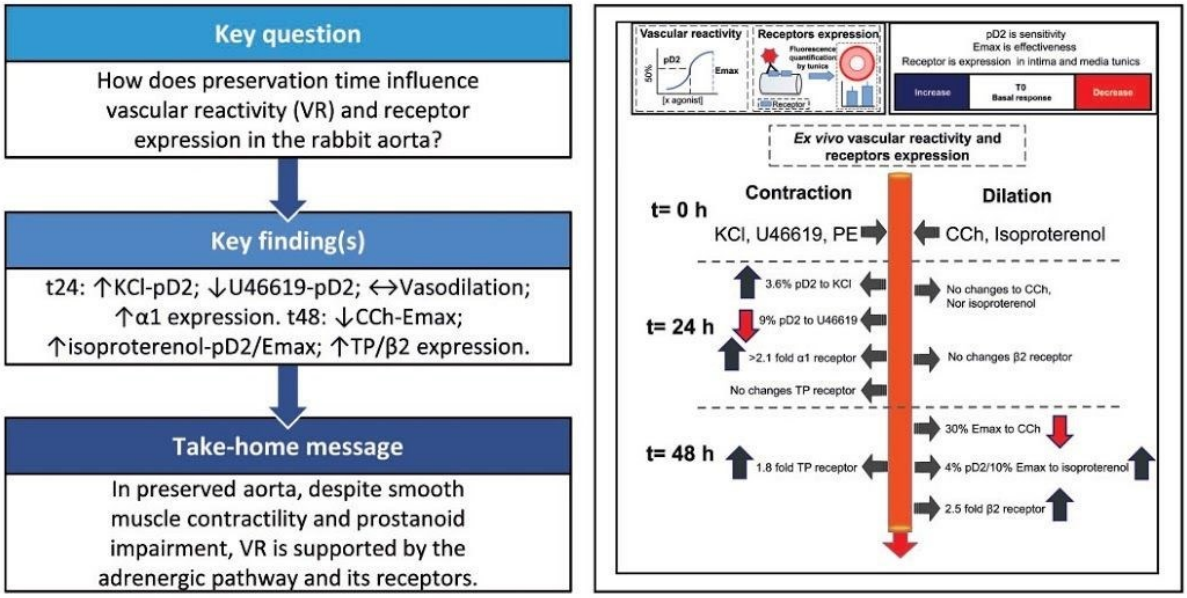

Abstract

OBJECTIVES: The mechanistic understanding of vascular functional impairment during preservation time helps determine the optimal time frame in which explanted arteries can be used. The method of choice is to measure vascular reactivity and receptor expression. Our goal was to study the influence of preservation for 24 and 48 h on vascular reactivity and receptor expression in rabbit aorta.

METHODS: Aortic rings preserved in Krebs–Henseleit solution were evaluated fresh (t0), 24 h (t24) and 48 h (t48) after harvest for (i) vascular reactivity as sensitivity (pD2) and maximum effect in response to potassium chloride, U46619 (thromboxane-A2 agonist), phenylephrine, carbachol and isoproterenol, in an organ bath; and for (ii) expression of α1, β2 and thromboxane-prostanoid receptors, by immunofluorescence.

RESULTS: Compared to the control, after 24 h of preservation, potassium chloride-induced pD2 increased a significant 3.6%, whereas U46619-induced vasoconstriction decreased 9%. None of the agonists affected vasodilation. Intimal and medial α1 receptor expression increased 2.5-fold. After 48 h of preservation, α1 expression and vasoconstrictor responses remained similar to those after 24 h of preservation, but in vasodilation the carbachol-induced maximum effect decreased 30% whereas isoproterenol-induced pD2 increased 4% and the

maximum effect increased 10%. TP and β2 expression in the intima and media increased 1.8- and 2.5-fold, respectively.

CONCLUSIONS: Up to 48 h of preservation, the adrenergic pathway and its receptors support vasoconstriction and vasodilation, despite a significant deterioration in the prostanoid pathway.

Keywords: Aortic rings • Vascular reactivity • Vascular smooth muscle • Cold storage

ABBREVIATIONS

CCh	Carbachol
Emax	Maximum effect
HSPs	Heat shock proteins
KCl	Potassium chloride
KH	Krebs–Henseleit
L-NAME	N(ω)-nitro-L-arginine methyl ester hydrochloride
NO	Nitric oxide
PE	Phenylephrine
ROS	Reactive oxygen species
VR	Vascular reactivity

INTRODUCTION

Tissue preservation for *ex vivo* vascular experiments and transplant operations cannot stop the deterioration of vascular function over time, but a mechanistic understanding of such impairment could help to determine the optimal time frame in which the artery can be used. This knowledge would also guide the interpretation of measurements that compare fresh and preserved arteries and might contribute to knowing how to increase the effectiveness of preservation, since preserving the functionality of the vascular tissue used to reconnect organs can increase survival after the transplant procedure [1, 2].

The protocols used to preserve tissue typically consider temperature, oxygenation, solution and time. The usual temperature for arteries is 4°C; it extends their viability by decreasing the metabolic activity [3]. During this cold preservation, oxygenation is not a critical variable, but when physiological temperature is re-established, reactive oxygen species (ROS) are produced that acutely upregulate mitochondrial and other types of energy metabolism, causing proinflammatory activation and apoptosis that gradually damages the tissue, which would reduce the response of the vessel [4, 5]. Tissue warming additionally activates a protective response via heat shock proteins (HSPs), which, by affecting G protein-coupled receptor signalling [6], can impair cyclic nucleotide-dependent vascular relaxation [7, 8]. Because these processes differentially affect vasomotor-related signalling, the methods of choice to determine the functional state of preserved arteries are vascular reactivity [VR, defined as sensitivity (pD2) and maximum effect (Emax) of vasoconstrictors and dilators in the artery] and receptor expression measurements.

As for the preservation solution, the most used in physiology is Krebs–Henseleit (KH) at 4°C, because the arteries placed in it show just a tendency to decrease VR after 24 h [4, 9, 10]. Physiological saline is not a preservation alternative, not even during the dissection of arteries, because endothelial function begins to decrease after 2 h storage in saline [9]. Other solutions used, primarily in transplants, include TiProtec, University of Wisconsin and Bretschneider histidine–tryptophan–ketoglutarate, but they induce ∼20% contraction and dilation hyper-reactivity during the first 48 h of storage at 4°C [4, 11]. Then, the solution of choice for the present study was KH.

The rabbit aorta has been a good model for macroscopic and microscopic lesions [12, 13], atherosclerosis [14], vascular wall remodelling in diabetes [15] and biomarkers in calcified stenosis [16]. Our group has used it as a model of ageing [17]. To measure the effects of preservation time on *ex vivo* VR, it is interesting to determine smooth muscle reactivity using a receptor-independent contraction inducer, such as potassium chloride (KCl); adrenergic contraction through the α1 receptor, with phenylephrine (PE); and that of the thromboxane prostanoids through the TP receptor, using U46619 (analogue of thromboxane A2—TXA2). Likewise, to determine the cholinergic vasodilator response using carbachol (CCh), and that through the β2 receptor, using isoproterenol. We hypothesized that the arteries keep VR by changing responsible pathways and receptor expression during 48 h of storage in KH at 4°C. Then, we assessed the influence of 24 and 48 h preservation time on VR to the aforementioned agonists, as well as α1, β2 and TP receptor expression, in rabbit aorta.

MATERIALS AND METHODS

Animal model and reagents

Ten adult (6 ± 0.3 months, 2.7 ± 0.18 kg) male New Zealand rabbits were housed in metal cages at a room temperature of 21 ± 2°C, 12 h of light and free access to chow and water. The procedures were approved by the Animal Experimentation Committee of the University of Antioquia (Medellín, Colombia), act 122/2019.

Carbamoylcholine chloride (212385-M), PE hydrochloride (P6126), isoproterenol bitartrate (I2760), N(ω)-nitro-L-arginine methyl ester hydrochloride (N5751, L-NAME), indomethacin (I8280) and seratrodast (SML1379) were obtained from Sigma-Aldrich (St. Louis, MO, USA). U46619 (ab144540) was from Abcam (Cambridge, UK). Stocks were prepared in distilled water with 10 μM ascorbic acid to prevent oxidation. All antibodies were from Abcam.

Dissection

Each animal was anaesthetized with intraperitoneal thiopental, 60 mg/kg. After cervical dislocation, the thoracic aorta was rapidly dissected and cut in 3 segments, preserved at 4°C in KH solution (118 mM NaCl, 4.7 mM KCl, 2.5 mM $CaCl_2$, 1.2 mM $MgSO_4$, 1.2 mM KH_2PO_4, 25 mM $NaHCO_3$, 11.1 mM glucose, pH 7.4) previously bubbled with carbogen (95% O_2, 5% CO_2) until randomly used for baseline (t0), 24 h (t24) and 48 h (t48) measurements. Under a stereo microscope, excess peripheral tissue was removed from the vessel, which was then cut into 15 rings, 3- to 5-mm in length. One ring was embedded in Shandon Cryomatrix (Thermo Fisher Scientific, Waltham, MA, USA) and frozen in liquid

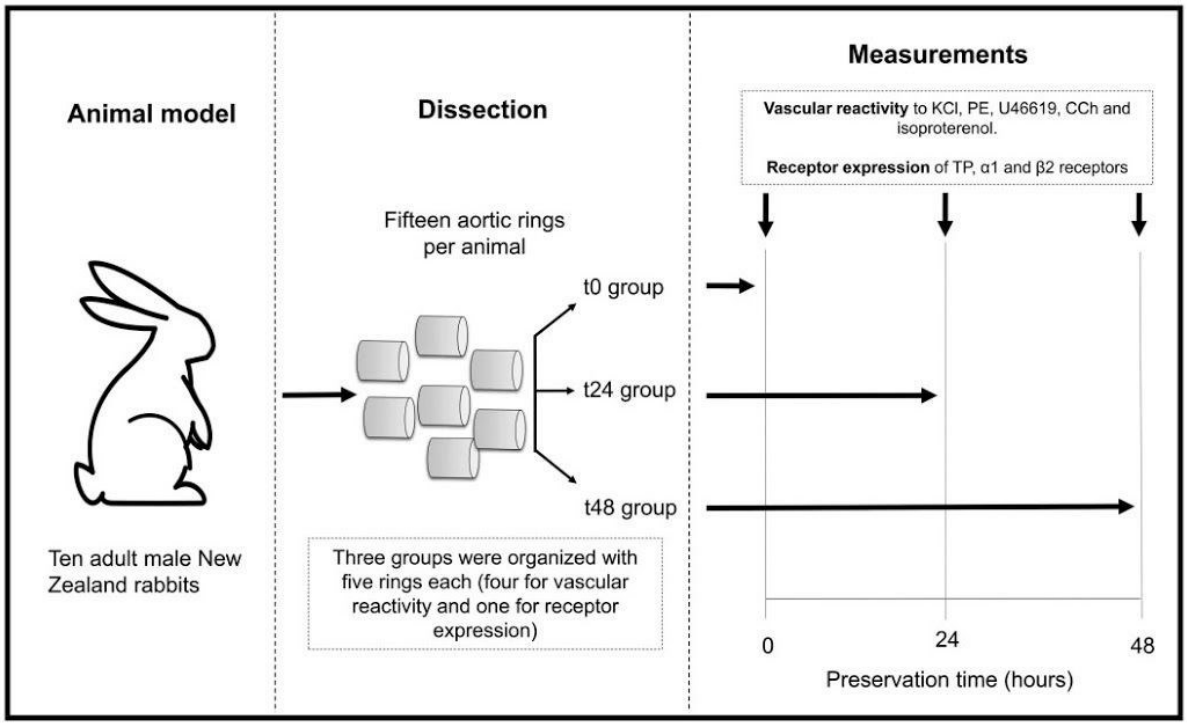

Figure 1: Description of the study and methodological design. CCh: carbachol; KCl: potassium chloride; PE: phenylephrine.

nitrogen for immunofluorescence. Four rings were kept at 4°C and used up to 1 h after sacrifice (t0) for VR experiments. The t24 and t48 rings were kept cold until they were immersed in the organ bath at their respective times (Fig. 1).

Vascular reactivity

The rings were placed in an LE13206 PANLAB (Panlab, Barcelona, Spain) organ bath with 10 ml of KH at 37°C, bubbled with carbogen. The contractile response was digitized with a Powerlab PL-3504 (AD Instruments, Sydney, Australia) and analysed with the dose response module of LabChart 8 software (AD Instruments). Each preparation was stabilized and stimulated as described by Cupitra *et al.* [17]. Each evaluation started by applying a single concentration of 40 mM KCl, followed by a cumulative concentration of KCl ranging from 5 to 60 mM or U46619 ranging from 0.3 nM to 1 μM or PE ranging from 1 nM to 10 μM. Relaxation studies were done in 1 μM PE precontracted rings, using CCh ranging from 1 nM to 10 μM and isoproterenol ranging from 1 nM to 10 μM. The VR to isoproterenol was measured only in relaxation and was suspended at the onset of the contraction due to increased affinity to α receptors. The blockers seratrodast (3 μM), indomethacin (10 μM) or L-NAME (100 μM) were added 20 min before beginning the concentration-response curve.

Immunofluorescence

Frozen arteries were cut in 10 μm sections, each fixed and permeabilized in acetone and then in 0.1% Triton X-100 and blocked with 5% bovine serum albumin in phosphate buffered saline. Different sections were incubated overnight with the following primary antibodies at 4°C (all diluted 1:1000 in the blocking solution): anti-α1 adrenergic receptor (ab3462), anti-β2 adrenergic receptor (ab61778) and anti-thromboxane A2 (TP) receptor (ab233288). After washing, the rings were incubated with a goat anti-rabbit secondary antibody conjugated to Alexa Fluor 594 (red, 1:800 in blocking solution; ab150080) at room temperature for 2 h. As a control, 1 section from each experimental group was not incubated with a primary antibody but with a secondary antibody. Images were obtained with an inverted fluorescence microscope (Axio Observer A1, Carl Zeiss, Oberkochen, Germany), mercury lamp (HXP120, Carl Zeiss) and filter (64-HE MPLUM, Carl Zeiss; emission window 647/70 nm). Micrographs were obtained from three 20× fields. ImageJ v1.52a was used to process the images, using the split channels tool in red-green-blue images. Background fluorescence and fluorescence from the control without secondary antibody were subtracted from each image. Then, we quantified the average intensity of red in 3 regions of interest of the intima, media and adventitia for each image. The expression of receptors quantified by fluorescence in rabbit aorta was normalized with respect to t0. The values of t0 were averaged and normalized based on this average, to show that the differences found were not due to the variability induced during the assembly of the technique.

Statistical analyses

The number of experiments is shown as (#animals, #rings). Complete data were used in the processing of results; the variables are continuous. Results are presented as concentration-

Table 1: Sensitivity and maximum response to KCl, PE, U46619, CCh and isoproterenol in rabbit aortic rings at t0, t24 and t48

Agonist	pD2				Emax (% KCl 40 mM)			
	t0	t24	t48	*P*-value	t0	t24	t48	*P*-value
KCl	1.7 ± 0.04	1.74 ± 0.03	1.8 ± 0.04	0.03[a]	134 ± 1.9	139 ± 4	143 ± 8	0.5
U46619	7.8 ± 0.2	7.1 ± 0.1	7.1 ± 0.1	0.04[a]	141.4 ± 4.8	143 ± 14	125 ± 5	0.43
PE	6.7 ± 0.1	6.6 ± 0.1	6.7 ± 0.08	0.9	169 ± 10	178 ± 10	175 ± 5	0.8
CCh[b]	6.2 ± 0.16	6.2 ± 0.06	6.3 ± 0.03	0.66	84 ± 3	80 ± 5	55 ± 4	0.0001[c]
CCh + L-NAME[b]	5.5 ± 0.13	5.8 ± 0.2	5.5 ± 0.1	0.2	-18.6 ± 4.2	-21 ± 6.2	-14 ± 4.3	0.6
CCh + indomethacin[b]	6.3 ± 0.06	6.2 ± 0.03	6.6 ± 0.4	0.42	48 ± 12	49 ± 11	51 ± 12	0.8
Isoproterenol[b]	6.6 ± 0.08	6.9 ± 0.08	7 ± 0.2	0.043[d]	52 ± 5.2	43 ± 4	63 ± 9	0.048[d]

Results in mean ± SEM.

[a]A higher sensitivity (pD2) to KCl or lower to U46619 in t24 and t48 arteries, compared to t0.

[b]Percent relaxation compared to contraction with PE.

[c]Higher Emax in response to CCh in t0 arteries compared to the responses in t24 and t48.

[d]Higher sensitivity and Emax responses to isoproterenol in t48 arteries compared with those in t0. One-way ANOVA followed by Tukey's *post hoc*, significance level of *P*-value <0.05.

ANOVA: analysis of variance; CCh: carbachol; Emax: maximum effect; KCl: potassium chloride; L-NAME: N(ω)-nitro-L-arginine methyl ester hydrochloride; M: molar concentration; PE: phenylephrine; SEM: standard error of the mean; U46619: thromboxane-A2 agonist; t0: time 0; t24: 24 h after harvest; t48: 48 h after harvest.

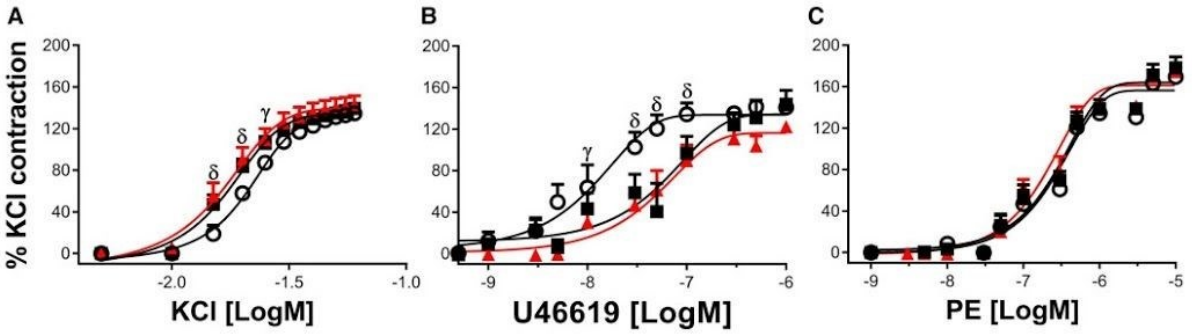

Figure 2: Concentration-response curves to KCl (**A**), the thromboxane-A2 agonist U46619 (**B**) and PE (**C**). t0 (open circle, 5 animals, 10 rings), t24 (filled square, 5, 10) and t48 (filled triangle, 5, 10). [δ]Higher sensitivity to KCl or a lower sensitivity to U46619 in t24 and t48 arteries compared with t0. [γ]A lower sensitivity to U46619 in t48 arteries compared with t0. Two-way analysis of variance followed by Tukey's *post hoc*, significance level of *P*-value <0.05. KCl: potassium chloride; PE: phenylephrine; U46619: thromboxane-A2 agonist.

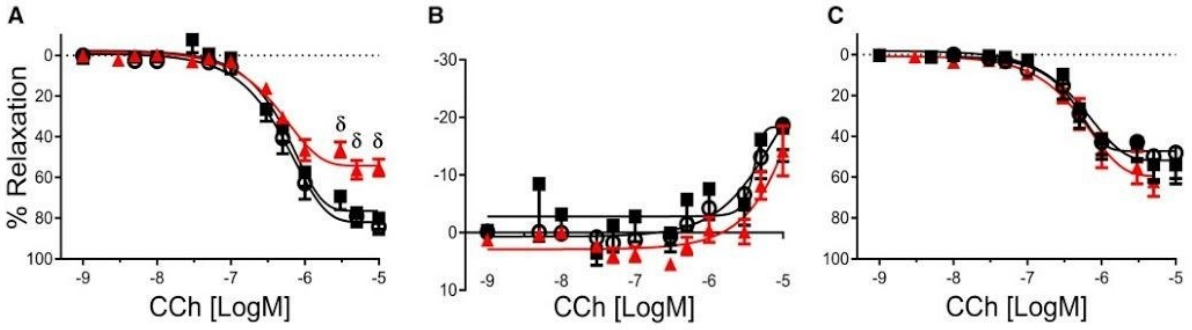

Figure 3: Concentration-response curves to CCh (**A**), blocking with L-NAME (**B**) and indomethacin (**C**). t0 (open circle, 5 animals, 10 rings), t24 (filled square, 5, 10) and t48 (filled triangle, 5, 10). In (**C**), the dotted line corresponds to vascular reactivity of CCh at t0 without blockers (the same as **A**), for the sake of comparison. [δ]A higher sensitivity and maximum effect to CCh in t0 arteries, compared to t24 and t48. Two-way analysis of variance followed by Tukey's *post hoc*; significance level of *P*-value <0.05. CCh: carbachol; L-NAME: N(ω)-nitro-L-arginine methyl ester hydrochloride.

response curves and dot plots with mean ± standard error of the mean. Normality assumptions were confirmed with the D'Agostino–Pearson and Shapiro–Wilk tests. Concentration-response curves were fitted with a non-linear regression using a sigmoidal, four-parameter model of the form Y = Bottom + (Top - Bottom)/(1 + 10^((logIC50-X) × HillSlope)), where Top shows the Emax, and the negative log10 of the molar concentration that produces 50% of the maximum response

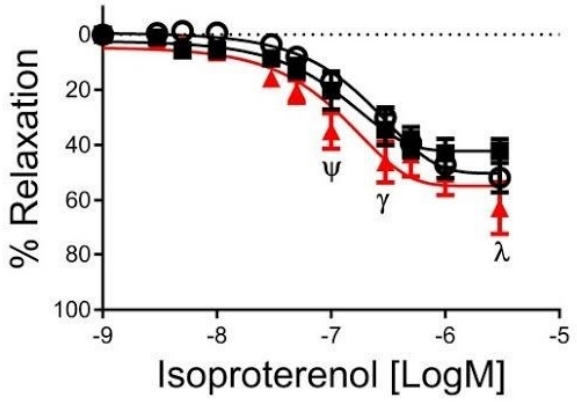

Figure 4: Concentration-response curves to isoproterenol. t0 (open circle, 5 animals, 10 rings), t24 (filled square, 5, 10) and t48 (filled triangle, 5, 10). [ψ]A higher sensitivity to isoproterenol in t48 arteries compared with t0 and t24. [γ]A higher sensitivity to isoproterenol in t48 arteries compared with t0. [λ]A higher maximum effect to isoproterenol in t48 arteries compared with t24. Two-way analysis of variance followed by Tukey's *post hoc*, significance level of *P*-value <0.05.

Table 2: Quantification of expression of thromboxane A2, α1 and β2 receptors in rabbit aortic rings at t0, t24 and t48

Receptor	Tunica	t0	t24	t48	*P*-value
TP	Intima	1 ± 0.2	1.5 ± 0.14	1.8 ± 0.3	0.03[a]
	Media	1 ± 0.16	1.3 ± 0.3	1.9 ± 0.3	0.04[a]
	Adventitia	1 ± 0.14	0.97 ± 0.08	0.9 ± 0.17	0.65
α1	Intima	1 ± 0.12	2.7 ± 0.5	2.4 ± 0.3	0.003[b]
	Media	1 ± 0.2	2.1 ± 0.5	2.1 ± 0.3	0.03[b]
	Adventitia	1 ± 0.12	0.6 ± 0.2	0.56 ± 0.18	0.15
β2	Intima	1 ± 0.15	1.14 ± 0.2	2.6 ± 0.4	0.0001[c]
	Media	1 ± 0.3	1.43 ± 0.2	2.5 ± 0.4	0.0015[c]
	Adventitia	1 ± 0.17	1.3 ± 0.4	1.8 ± 0.46	0.3

Expression of receptors was normalized with respect to t0. t0 values were averaged and normalized based on this average. Results in mean ± SEM.

[a]Higher expression in t48 arteries compared to t0.

[b]Higher expression in t24 and t48 arteries compared to t0.

[c]Higher expression in t48 arteries compared with t0 and t24. One-way analysis of variance followed by Tukey's *post hoc*, significance level of *P*-value <0.05.

SEM: standard error of the mean; t0: time 0; t24: 24 h after harvest; t48: 48 h after harvest.

reflects sensitivity (pD2). pD2, Emax and quantification of receptor expression in the intima, media and adventitia were analysed with a one-way analysis of variance followed by Tukey's *post hoc* test. Concentration-response curves were analysed with a two-way analysis of variance followed by Tukey's *post hoc* test that compares time/concentration. Differences were considered statistically significant at *P*-value <0.05. The GraphPad Prism 7 statistical package v7.0 (GraphPad Software, San Diego, CA, USA) was used.

RESULTS

Contraction

An overview of all data is provided in Table 1. Upon stimulation with KCl, VR in the aorta showed an increase in pD2 at t24 and t48 ($P = 0.03$; Table 1), whereas the Emax remained unchanged ($P = 0.5$; Table 1 and Fig. 2A). The stimulus with U46619 resulted in a decrease in pD2 at t24 and t48 compared to controls ($P = 0.04$; Table 1). The Emax to U46619 did not differ between groups ($P = 0.43$; Table 1 and Fig. 2B). VR with PE of the groups also did not differ in sensitivity and Emax (Table 1 and Fig. 2C). The action of prostanoids in our model only occurred through the TP receptor, since the blocker seratrodast abolished the response in 3 separate experiments (data not shown).

Relaxation

In CCh-induced endothelium-dependent relaxation, no differences were found in sensitivity ($P = 0.66$; Table 1), but Emax decreased at t48 ($P = 0.0001$; Table 1 and Fig. 3A). In addition, the relaxation in response to CCh using L-NAME and indomethacin did not differ among the groups (Fig. 3B and C). To isoproterenol, in t48 were increased both the sensitivity ($P = 0.043$) and Emax ($P = 0.048$; Fig. 4).

Immunofluorescence

The expression of receptors quantified by fluorescence in rabbit aorta was normalized with respect to t0 (Table 2 and Fig. 5A). In the tunica intima and tunica media, the receptor expression increased: 1.8-fold to the TP receptor at t48 ($P < 0.04$; Table 2 and Fig. 5B), 2-fold to the α1 receptor at t24 ($P < 0.03$; Table 2 and Fig. 5C) and 2.5-fold to the β2 receptors at t48 ($P < 0.0015$; Table 2 and Fig. 5D). In the adventitia, no differences were found in receptor expression (Table 2 and Fig. 5C and D).

DISCUSSION

We have shown that in the rabbit aorta preserved for 24 h, smooth muscle and endothelium initiate changes that are accentuated at 48 h, which particularly affect the prostanoid pathway, but are not reflected in large changes in VR because the adrenergic pathway supports function. Receptor expression doubles in the tunicas intima and media, as cholinergic dilation is partially replaced by the action of TP and β2 receptors. This knowledge could help to determine if the functional changes observed in an artery are attributable to the preservation time or to the specific experimental conditions of the study. This knowledge might also be useful in vascular grafts and transplants, because the pathophysiological changes that occur during vascular ischaemia and subsequent reperfusion may cause damage to the harvested arteries that would affect long-term survival of the allograft.

The receptor-independent contraction increases its sensitivity due to preservation time

The initial changes manifest as sensitization of voltage-operated Ca2+ channels in smooth muscle, translocation of proteins from cytosol to plasma membrane and vice versa, activation of kinases and a decrease in endothelium-dependent relaxation, but the damage is not extensive enough to change the Emax, which does decrease after 48 h, as shown, for example, in human saphenous vein preserved in KH at 4°C [5]. Of note, McIntyre *et al.* [18] reported no changes in rat mesenteric artery in response to KCl

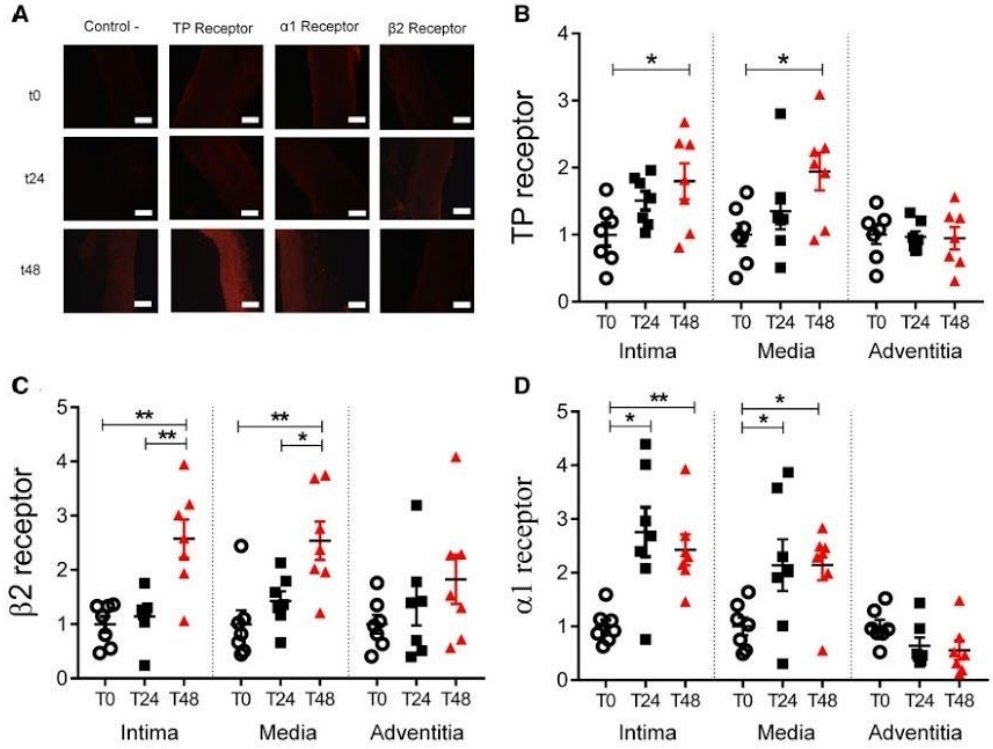

Figure 5: Quantification of protein expression of thromboxane A2 (TP), α1 and β2 receptors in the aortic wall of t0 (open circle), t24 (filled square) and t48 (filled triangle). (**A**) Representative images of immunofluorescence to identify TP, α1 and β2 receptors. The length of the white calibration bars is equivalent to 100 μm. (**B–D**) Quantification of the fluorescence of the TP, α1 and β2 receptors, respectively, in the tunicas of the aortic wall. The number of experiments is 7 in all cases. One-way analysis of variance followed by Tukey's *post hoc*. $^{*}P < 0.05$. $^{**}P < 0.01$. The expression was always normalized to t0. TP: thromboxane A2.

for up to 4 days in saline; such a difference with our results is attributable to the use of different species and different vascular beds.

The prostanoid route is the one most affected by the preservation time

Regarding receptor-dependent mechanisms, our results showed that the rabbit aorta becomes up to seven-fold less sensitive to the TXA2 analogue. It would seem that this decrease of sensitivity is independent of species, arterial original and preservation solution, for example, in University of Wisconsin cold-preserved pig coronary arteries [19]. Interestingly, this decrease in sensitivity was accompanied by progressive increases in the expression of the TP receptor in the tunica intima and media, which in our model is the only receptor for the function of the prostanoids. Increased expression with less functionality suggests a possible internalization or desensitization of this receptor, due to changes in the phosphorylation dynamics caused by hypothermia and cold resistance mechanisms such as HSP27 [20] and by reducing the formation of inositol 1,4,5-triphosphate (IP3) and the affinity for its receptor in the sarcoplasmic reticulum, caused by hypoxia [21], as well as the loss of some mechanical parameters, such as cyclic deformation and shear stress.

α-Adrenergic vascular reactivity tends to be minimally affected despite the preservation time

Contraction via the α1 receptor is similar in the 3 evaluated moments, similar to the situation in human saphenous veins [4], rat mesenteric artery [18] or dog splenic artery [22] preserved in KH at 4°C and in rat aorta in histidine–tryptophan–ketoglutarate [11], showing that the adrenergic pathway is preserved for up to 7 days [22]. We also showed that the VR did not vary although the expression of the α1 receptor doubles in the tunicas intima and media, suggesting decreased receptor functionality, as hypoxia attenuates the coupling of α1 receptors to the synthesis of IP_3 and its downstream activity [23], which would be compensated by increased expression. Despite having intracellular similarities, i.e. coupled G proteins and contractile pathways through IP_3, α1 and TP respond differently to preservation time, suggesting that the receptor or the receptor-dependent pathways have different sensitivities to such stress.

β-Adrenergic signalling is enhanced during the preservation time

The response to isoproterenol increased its sensitivity by 6% and the Emax at t48 by 20% compared to baseline. This same

response was reported by [24] in pig coronary arteries stimulated with isoproterenol, indicating that this result via β receptors is not an exclusive phenomenon of our model. Additionally, in rat aorta preserved for 48 h, an increase in pD2 and Emax was reported when stimulated with forskolin, a cAMP-dependent vasodilator [10], suggesting that preservation favours cAMP-mediated relaxation. Additionally, our work showed that the expression of the β2 receptor triples in the intima and media at t48 (and similarly in the adventitia, although the cellular heterogeneity of this tunica makes it difficult to discriminate which cell groups are sensitive to preservation). Interestingly, during the preservation of intestinal tissues, rabbit jejunum also presents a selective decrease in α but not β function [25], which could indicate that the discussed mechanisms of resilience to preservation stress are comparable between vascular and intestinal smooth muscles.

Preservation time decreases endothelium- and smooth muscle-dependent vasodilation

As mentioned, when discussing non-receptor-dependent VR, the endothelium-dependent vascular relaxation was preserved at t24 and decreased by 35% at t48, similar to the results reported in rat aorta preserved in KH at 4°C [10]. Interestingly, we show that vasodilatation was abolished by blocking endothelial nitric oxide (NO) synthase, but that blocking prostanoid-driven relaxation only partially suppressed arterial relaxation, which was equalized in the 3 groups and diminished to 43% in t0 and to 7% in t48 with respect to non-blocked arteries. Together, this evidence suggests that the prostacyclin pathway comprises nearly half of the relaxation in the rabbit aorta up to t24 but virtually disappears at t48, with relaxation remaining almost exclusively at the expense of NO. Given this result, the reduction in VR is due to the lower bioavailability of NO, possibly as a consequence of an increase in ROS, as previously suggested [4, 5]. Our results may help explain the gain in sensitivity to receptor-independent contractile stimulus at t48 but not at t24, indicating that these changes in contraction are not exclusively dependent on the decrease in endothelial response. Likely, smooth muscle decreases its ability to relax, as hypothermia-induced HSP27 can reduce the availability of relaxing cyclic nucleotides, independent of NO stimulation [7, 8].

The prostanoid and the adrenergic pathways are both evolutionarily ancient defence systems. Both TXA2 and PE induce smooth muscle contraction through the same pathway, associated with G protein-coupled receptors that depend on phosphorylation and ATP for their function, with VR expected to decrease in preservation [26]. However, we demonstrated that the VR to TXA2 is further reduced, as the ROS can decrease the production of thromboxanes due to the reduction of the expression of phospholipase A2 beyond 4 h of preservation [27], whereas vascular control by adrenergic agonists even benefits from the production of mitochondrial ROS, as evidenced, for example, in the rat mesenteric artery [26]. Regarding relaxation, oxidative damage of the endothelium has been described after cold ischaemic storage and reperfusion, increasing the ROS that lead to deterioration of endothelial function, similar to what we found in the present work, but not the non-endothelium-dependent relaxation mechanisms [28], which helps explain why relaxation is partially preserved. Although ROS reduce the bioavailability of NO and prostacyclin, the artery can regulate ROS concentrations sooner, whereas the reconstitution of the prostanoid pathway would depend on recovering phospholipase A2 levels, which is a slower process.

Limitations

Cold storage of animal vessels is a model that replicates only some parts of the clinical artery preservation process. It does not allow inclusion of patient characteristics such as age, underlying disease and genotype. Some mechanical parameters such as cyclic strain and shear stress are also not included.

Future work

Basic experimental work contributes to the understanding of vascular pathophysiology. It also provides elements for future work in the laboratory or clinical setting, for example, with vascular grafts, the use of different preservation solutions and determining the mechanical, metabolic and genetic changes induced by the preservation time. It also includes a more detailed evaluation of receptor function and the evaluation of the functionality of the isolated smooth muscle, in diverse species and vascular beds.

ACKNOWLEDGEMENTS

The authors want to thank the project 'High Level Human Talent Training' approved by the Science, Technology and Innovation Fund (CTeI) of the General Royalty System (SGR)-BPIN:2013000100103, Tolima Governorate and University of Tolima, Colombia, for supporting NIC; the University of Antioquia CODI grants project 2581; the Foundation for the Promotion of Research and Technology, Bank of the Republic of Colombia, agreement 201619/2017; and especially to Marco Harmsen, from the University Medical Center of Groningen, for his valuable comments.

Conflict of interest: none declared.

Author contributions

Nelson Ivan Cupitra: Conceptualization; Data curation; Formal analysis; Investigation; Methodology; Validation; Writing—original draft; Writing—review & editing. **Juan C. Calderón:** Formal analysis; Investigation; Methodology; Supervision; Validation; Writing—original draft; Writing—review & editing. **Raul Narvaez-Sanchez:** Conceptualization; Data curation; Funding acquisition; Investigation; Methodology; Project administration; Resources; Writing—original draft; Writing—review & editing.

Reviewer information

European Journal of Cardio-Thoracic Surgery thanks Omar A. Jarral, Luiz Felipe P. Moreira and the other, anonymous reviewer(s) for their contribution to the peer review process of this article.

REFERENCES

[1] Winkler B, Reineke D, Heinisch PP, Schönhoff F, Huber C, Kadner A *et al.* Graft preservation solutions in cardiovascular surgery. Interact CardioVasc Thorac Surg 2016;23:300–9.

[2] Yuan X, Theruvath AJ, Ge X, Floerchinger B, Jurisch A, García-Cardeña G *et al.* Machine perfusion or cold storage in organ transplantation: indication, mechanisms, and future perspectives. Transpl Int 2010;23:561–70.

[3] Müller-Schweinitzer E. Applications for cryopreserved blood vessels in pharmacological research. Cryobiology 1994;31:57–62.
[4] Buchinger-Kähler V, Stoldt VR, Muth T, Schipke JD. Function and viability of vessels in different preservation solutions—an experimental study on human great saphenous veins. J Angiol Vasc Surg 2016;1:1–7.
[5] Rauen U, Groot H. New insights into the cellular and molecular mechanisms of cold storage injury. J Investig Med 2004;52:299–309.
[6] Storey KB, Storey JM. Heat shock proteins and hypometabolism: adaptive strategy for proteome preservation. Res Rep Biol 2011;2:57–68.
[7] Knoepp L, Beall A, Woodrum D, Mondy JS, Shaver E, Dickinson M *et al.* Cellular stress inhibits vascular smooth muscle relaxation. J Vasc Surg 2000;31:343–53.
[8] Fuchs LC, Giulumian AD, Knoepp L, Pipkin W, Dickinson M, Hayles C *et al.* Stress causes decrease in vascular relaxation linked with altered phosphorylation of heat shock proteins. Am J Physiol Regul Integr Comp Physiol 2000;279:R492–8.
[9] Massa G, Ingemansson R, Sjöberg T, Steen S. Endothelium-dependent relaxation after short-term preservation of vascular grafts. Ann Thorac Surg 1994;58:1117–22.
[10] Stanke-Labesque F, Cracowski JL, Devillier P, Caron F, Bessard G. Functional assessment of rat aorta after cold storage in different media. Fundam Clin Pharmacol 1999;13:310–19.
[11] Corner J, Berwanger CS, Stansby G. Preservation of vascular tissue under hypothermic conditions. J Surg Res 2003;113:21–5.
[12] Zaragoza C, Gomez-Guerrero C, Martin-Ventura JL, Blanco-Colio L, Lavin B, Mallavia B *et al.* Animal models of cardiovascular diseases. J Biomed Biotechnol 2011;2011:1–13.
[13] Fan J, Chen Y, Yan H, Niimi M, Wang Y, Liang J. Principles and applications of rabbit models for atherosclerosis research. J Atheroscler Thromb 2018;25:213–20.
[14] Taylor E, Huang N, Bodde J, Ellison A, Killiany R, Bachschmid M *et al.* MRI of atherosclerosis and fatty liver disease in cholesterol fed rabbits. J Transl Med 2018;16:215.
[15] Tong J, Yang F, Li X, Xu X, Wang GX. Mechanical characterization and material modeling of diabetic aortas in a rabbit model. Ann Biomed Eng 2018;46:429–42.
[16] Mourino-Alvarez L, Baldan-Martin M, Sastre-Oliva T, Martin-Lorenzo M, Maroto AS, Corbacho-Alonso N *et al.* A comprehensive study of calcific aortic stenosis: from rabbit to human samples. Dis Model Mech 2018. https://dmm.biologists.org/content/11/6/dmm033423.
[17] Cupitra NI, Calderón JC, Narvaez-Sanchez R. Influence of ageing on vascular reactivity and receptor expression in rabbit aorta: a complement to elastocalcinosis and smooth muscle mechanisms. Clin Interv Aging 2020;15:537–45.
[18] McIntyre CA, Williams BC, Lindsay RM, McKnight JA, Hadoke PWF. Preservation of vascular function in rat mesenteric resistance arteries following cold storage, studied by small vessel myography. Br J Pharmacol 1998;123:1555–60.
[19] He GW, Yang CQ. Impaired endothelium-derived hyperpolarizing factor-mediated relaxation in coronary arteries by cold storage with University of Wisconsin solution. J Thorac Cardiovasc Surg 1998;116:122–30.
[20] Kinsella BT. Thromboxane A 2 signalling in humans: a 'tail' of two receptors. Biochem Soc Trans 2001;29:641–54.
[21] Zhang L. Adaptation of pharmacomechanical coupling of vascular smooth muscle to chronic hypoxia. Comp Biochem Physiol A Mol Integr Physiol 1998;119:661–7.
[22] Yang XP, Chiba S. Effects of prolonged cold storage on purinergic and adrenergic components of sympathetic co-transmission in isolated canine splenic arteries. Jpn J Pharmacol 1999;81:163–9.
[23] Hu XQ, Yang S, Pearce WJ, Longo LD, Zhang L. Effect of chronic hypoxia on alpha-1 adrenoceptor-mediated inositol 1, 4, 5-trisphosphate signaling in ovine uterine artery. J Pharmacol Exp Ther 1999;288:977–83.
[24] Hashimoto M, Ishida Y, Naruse I, Paul RJ. Prolonged cold storage abolishes endothelium-dependent relaxing responses to A23187 and substance P in porcine coronary arteries. J Vasc Res 1992;29:64–70.
[25] Lum BK, Kermani MH, Heilman RD. Intestinal relaxation produced by sympathomimetic amines in the isolated rabbit jejunum: selective inhibition by adrenergic blocking agents and by cold storage. J Pharmacol Exp Ther 1966;154:463–71.
[26] Hao L, Nishimura T, Wo H, Fernandez-Patron C. Vascular responses to α1-adrenergic receptors in small rat mesenteric arteries depend on mitochondrial reactive oxygen species. Arterioscler Thromb Vasc Biol 2006;26:819–25.
[27] Korbecki J, Baranowska-Bosiacka I, Gutowska I, Chlubek D. The effect of reactive oxygen species on the synthesis of prostanoids from arachidonic acid. J Physiol Pharmacol 2013;64:409–21.
[28] Radovits T, Lin LN, Zotkina J, Koch A, Rauen U, Köhler G *et al.* Endothelial dysfunction after long-term cold storage in HTK organ preservation solutions: effects of iron chelators and N-α-acetyl-L-histidine. J Heart Lung Transpl 2008;27:208–16.

Capítulo tres:

Cupitra NI, Calderón JC, Narváez-Sánchez, 2020. Influence of ageing on vascular reactivity and receptor expression in rabbit aorta: a complement to elastocalcinosis and smooth muscle mechanisms

Capítulo tres:

Cupitra NI, Calderón JC, Narváez-Sánchez, 2020. Influence of ageing on vascular reactivity and receptor expression in rabbit aorta: a complement to elastocalcinosis and smooth muscle mechanisms

Artículo publicado en Clinical Interventions in Aging; IF:3.02

Enlace: https://www.dovepress.com/influence-of-ageing-on-vascular-reactivity-and-receptor-expression-in--peer-reviewed-article-CIA

Hacia diciembre de 2018, cuando se habían recabado arterias de 15 pacientes, se hizo evidente la diferencia etaria de 20 años entre los pacientes con cáncer y el grupo control. Esto representaba para nosotros un reto experimental, dado que el envejecimiento aumenta el riesgo de sufrir enfermedades cardiovasculares. Por ejemplo, aumenta la rigidez aórtica, principalmente debido a cambios en la matriz extracelular, a veces denominada elastocalcinosis. Esto hizo necesario para nosotros dilucidar los mecanismos que se alteran en la función vascular en relación a la edad, ya que estos podrían ser un factor de variabilidad que nos lleven al error a la hora de interpretar los resultados. Por lo anterior, se estableció como objetivo secundario cuantificar la influencia del envejecimiento sobre la función vascular, el engrosamiento vascular y la expresión de receptores. Dado que el flujo de pacientes era insuficiente, se escogió como modelo el conejo a la aorta de conejos jóvenes, adultos y viejos. No se usó el cerdo porque solo se tuvo acceso a tejido en agosto de 2020.

A continuación, el artículo correspondiente al capítulo tres.

Clinical Interventions in Aging

Dovepress
open access to scientific and medical research

Open Access Full Text Article

ORIGINAL RESEARCH

Influence of Ageing on Vascular Reactivity and Receptor Expression in Rabbit Aorta: A Complement to Elastocalcinosis and Smooth Muscle Mechanisms

This article was published in the following Dove Press journal:
Clinical Interventions in Aging

Nelson Ivan Cupitra
Juan C Calderón
Raul Narvaez-Sanchez

Physiology and Biochemistry Research Group-PHYSIS, Faculty of Medicine, University of Antioquia, Medellin, Colombia

Aim: To contribute to the knowledge about the mechanisms involved in aortic stiffness due to ageing.

Materials and Methods: Aortic rings from young (1.5±0.5 months, 0.8±0.2 kg), adult (6 ±0.5 months, 2.7±0.5 kg) and old (28±8 months, 3.2±0.8 kg) male New Zealand rabbits were used to evaluate: 1) intima-media thickness by optical microscopy; 2) vascular reactivity (VR) in terms of sensitivity (pD2) and efficacy (Emax) to KCl; phenylephrine (PE); U-46619, a thromboxane A2 receptor agonist, TXA2; carbachol (CCh), isoproterenol and sodium nitroprusside (SNP), using organ bath experiments; and 3) the expression of receptors α1, β2 and thromboxane-prostanoids (TP), by immunofluorescence.

Results: Ageing 1) did not change the thickness of tunica; 2) significantly reduced the pD2 to KCl, increased the pD2 to PE and reduced both the pD2 and Emax to TXA2, CCh and isoproterenol, and reduced the pD2 to SNP; and 3) significantly increased the expression of α1 and β2 receptors in the intima and adventitia, and the expression of TP only in the adventitia.

Conclusion: Our results suggest that ageing makes the aorta more reactive to α1 adrenergic contraction, and it could be a compensation for lower responsiveness to prostanoids. The aged aorta is less reactive to endothelium-dependent and non-dependent relaxation, and the vessel seems to try to compensate for that stiffness increasing β2 receptors, although probably less functional. These results complement the proposed mechanisms of elastocalcinosis and smooth muscle rigidity, expanding the vision that should guide the treatment of aortic stiffness due to aging.

Keywords: ageing, aortic rings, vascular reactivity, vascular smooth muscle, vascular stiffness

Introduction

Ageing is a natural process that predisposes individuals to cardiovascular disease (CVD), which is responsible for the highest percentage of deaths in the world, reaching 31%.[1,2] As the population of older adults expands, elucidating the mechanisms of vascular dysfunction with age is critical to better direct appropriate and measured pharmacological and lifestyle interventions against CVD risk. Increased aortic stiffness is an important feature of aging and of CVD and is mainly attributed to changes in the extracellular matrix (ECM), sometimes called elastocalcinosis.[3,4] Complementarily, Qiu et al proposed a mechanism due to smooth muscle stiffness.[5] But ageing affects

Correspondence: Raul Narvaez-Sanchez
Carrera 51 D #62-29, Office 203, Medellin, Colombia
Tel +57 42196030
Email raul.narvaez@udea.edu.co

submit your manuscript | www.dovepress.com
DovePress
http://doi.org/10.2147/CIA.S236173

vascular reactivity (VR) too, by altering the sensitivity and maximal effect of stimulating contractile agonists and endogenous vasodilators.[6,7] It is feasible that the vascular stiffness is due not only to one mechanism but also to the complementarity of several, and one very important to take into account would be the change in the VR. Further, in diagnosing or research, it is important to differentiate the possible changes in the blood vessel caused by a disease from those caused by the ageing of the vessels. Moreover, VR is a more plastic factor, while ECM changes require more time and could be less responsive to treatment,[3] which has an impact on therapeutic strategies.

Since a study on vascular ageing in humans is challenging, the rabbit is an interesting model frequently used in research focused on cardiovascular pathophysiologies[8] such as heart damage,[9] hypertension[10] and ageing.[11] This is so because the rabbit has an over 90% homology with humans, is readily available, can be grown in controlled conditions and has a short life span. The rabbit aorta is widely used to quantify the influence of possible drugs on VR and as an initial approach that allows VR to be extrapolated to humans.[12,13] As for ageing, it has been shown in rabbits that it decreases aortic relaxation by reducing β-adrenergic receptors activity.[14] This decrease in vascular function with ageing has also been described in the aorta of male and female rats.[15] We consider important to contribute about the mechanisms and the expression of the receptors involved in the changes of the VR evidenced by the research in rabbits and other models such as mice and rats.

Then, the goal of this study is to characterize the changes in the kinetics of rabbit aortic ring response as a function of ageing and to clarify the mechanisms involved, using one receptor-independent contraction inducer (potassium chloride, KCl), two receptor-dependent contraction inducers (phenylephrine (PE) and U-46619, a thromboxane A2 agonist, TXA2), two receptor-dependent relaxation inducers (carbachol (CCh) and isoproterenol) and independent relaxation inducer (sodium nitroprusside dihydrate, SNP). Complementarily, the wall thickness and expression of the receptors involved in some pathways were measured.

Materials and Methods

Animal Model and Reagents

Ten young ("YO"; 1.5±0.5 months, 0.8±0.2 kg), 10 adult ("AD"; 6±0.5 months, 2.7±0.5 kg) and 7 old ("OL"; 28±8 months, 3.2±0.8 kg) male New Zealand rabbits were obtained from the cuniculture facility of the National Learning Service at La Salada (Antioquia, Colombia). The animals were housed in metal cages, with a room temperature of 21±2°C, under 12 hours of light and with free access to normal chow and water. The use of rabbits was approved by the Animal Experimentation Committee of the University of Antioquia (Medellin, Colombia), act 122 of February 5, 2019 in accordance with law 84 of 1989 "National Statute for Animal Protection" and resolution 8430 of 1993 "Scientific, technical and administrative standards for health research".

Carbamoylcholine chloride (212385-M), phenylephrine hydrochloride (P6126), and isoproterenol bitartrate (I2760), sodium nitroprusside dihydrate (71778) were from Sigma–Aldrich Co. (St. Louis, MO, USA). U-46619 (ab144540) was from Abcam (Cambridge, USA). Stocks were prepared in distilled water with 10 μM ascorbic acid in order to prevent oxidation. All antibodies were from Abcam (see below).

Dissection

Each animal was anaesthetized with intraperitoneal sodium thiopental (60 mg/kg) with subsequent cervical dislocation. The descending aorta was rapidly dissected, without the branching zones, and conserved in Krebs-Henseleit (KH) solution, with the following composition (mM): NaCl, 118; KCl, 4.7; KH2PO4, 1.2; MgSO4, 1.2; NaHCO3, 25.0; glucose, 11.1; CaCl2, 2.5; pH 7. Under magnification, excess peripheral tissue was removed from the aortic segment which was cut into 10 rings, 3–5 mm in length. Four rings were used for relaxation and contraction experiments that began within the first hour after the sacrifice. Four rings were preserved for 24 hours in KH solution previously bubbled with carbonated gas (95% O2–5% CO2) inside a cooler at 4°C and were used only for contraction studies. Other studies have shown that there are no differences in vascular reactivity at 24 hours of preservation in KH at 4°C.[16] The remaining two rings were embedded in Shandon Cryomatrix (Thermo Fisher Scientific, USA) and frozen in liquid nitrogen for immunohistochemistry. Previous results from our laboratory showed that in this type of assay, there is no significant difference with respect to fresh samples.

Vascular Reactivity

The rings were placed in an LE13206 PANLAB organ bath (Barcelona, Spain) with 10 mL of KH at 37°C and bubbled with carbogen, as described.[17] The contractile response was digitized with a Powerlab PL-3504

(Sydney, Australia) and analysed with the dose–response module of LabChart 8 software. Each preparation was stabilized at 2 g of resting tension for 90 minutes before initiating the agonist stimuli; during this period, the KH solution was replaced every 20 minutes. After stabilization, the arterial ring was stimulated twice with 4×10^{-2} M KCl, recording the response for 10 minutes, and washed for 20 minutes between each stimulus. Then, 1×10^{-6} M PE and 1×10^{-5} M CCh were applied to the bath to confirm the presence of the endothelium; this was performed for all arterial rings. Then, the evaluation was started by applying a single dose of 4×10^{-2} M KCl; a cumulative dose of KCl ranging from 5 to 60 mM; a cumulative dose of PE ranging from 1×10^{-9} M to 1×10^{-5} M; and a cumulative dose of U-46619 ranging from 1×10^{-10} M to 1×10^{-6} M. Relaxation studies were performed with 1×10^{-6} M PE precontracted rings, using CCh at doses ranging from 1×10^{-9} M to 1×10^{-5} M, isoproterenol at doses ranging from 1×10^{-9} M to 1×10^{-5} M, SNP at doses ranging from 1×10^{-10} M to 1×10^{-5} M. The VR to isoproterenol was measured only in relaxation and was suspended at the onset of contraction because precontraction with an α1 agonist could have affected this contractile VR.

Histology and Immunofluorescence

Frozen arteries were cut in 10-µm thick sections. For histology, they were fixed in Carnoy's solution (ethanol, chloroform and acetic acid, 6:3:1) and stained with haematoxylin and eosin to evaluate changes in morphology, and with Van Gieson and a modified Van Gieson (with orcein) to qualitatively evaluate collagen and elastic fibers, respectively. Evaluation of the images was performed under a 20× objective. ImageJ v1.52a was used to process the images by quantifying the thickness of the intima-media in 2 random regions for each image.

For immunofluorescence, the sections were fixed in acetone, permeabilized with 0.1% Triton X-100 and blocked with 5% bovine serum albumin in phosphate-buffered saline. Different sections were incubated with the following primary antibodies at 4°C overnight (all diluted 1:1000 in blocking solution; Abcam): anti-α1 adrenergic receptor (ab3462, Abcam), anti-β2 adrenergic receptor (ab61778, Abcam), anti-thromboxane A2 (TP) receptor (ab233288, Abcam). After washing, the rings were incubated with goat anti-rabbit secondary antibody conjugated to Alexa Fluor 594 (red, 1:800 in blocking solution; ab150080, Abcam) at room temperature for 2 hours. As a control, one section from each experimental group was not incubated with a primary antibody but was incubated with a secondary antibody. Images were obtained using an inverted fluorescence microscope (Axio Observer A1, Carl Zeiss), a mercury lamp (HXP120, Carl Zeiss) and a filter (64 HE MPLUM, Carl Zeiss; emission window 647/70 nm). Evaluation of the images was performed under a 20× objective. ImageJ v1.52a was used to process the images using the Split channels tool in RGB images, quantifying the average intensity of red in 3 regions of interest of the intima, media and adventitia for each image.

Statistical Analysis

The results are presented as the mean ± SEM of the maximum contraction (Emax) and the negative logarithm of the molar concentration of agonist producing 50% of the maximum response (pD2). pD2 was calculated by nonlinear regression of the concentration–response curves. The groups were compared using two-way ANOVA followed by post hoc Tukey's test, considering a significance level of $P<0.05$. The statistical package GraphPad Prism 6 Statistics, version 6.01, was used.

Results

Intima-Media Thickness

In the quantification of vascular thickness, no differences were found between YO, AD and OL (YO, 126±6 µM; AD, 125.7±7.2 µM; and OL, 133±5.5 µM; n=5 for all the experiments. Figure 1; p=0.62). In addition, in the histology results by Van Gieson and modified Van Gieson (with orcein), no qualitative differences were found between the groups.

Contraction

Upon stimulation with KCl, VR in the aorta showed a decreased sensitivity in AD and OL (p=0.01). However, no significant differences were found in the maximal response (Figure 2A, p=0.1). VR with PE showed significant differences in sensitivity between YO and AD compared with OL (Figure 2B; p=0.002), together with an increase in the Emax of OL versus YO (Figure 2B; p=0.01). The stimulus with U-46619 resulted in a decrease in the pD2 of OL compared with that in YO and AD (p=0.001). The maximum response to the stimulus with U-46619 was higher in YO than in AD and OL (Figure 2C; p=0.001). A summary and number of experiments can be found in Table 1.

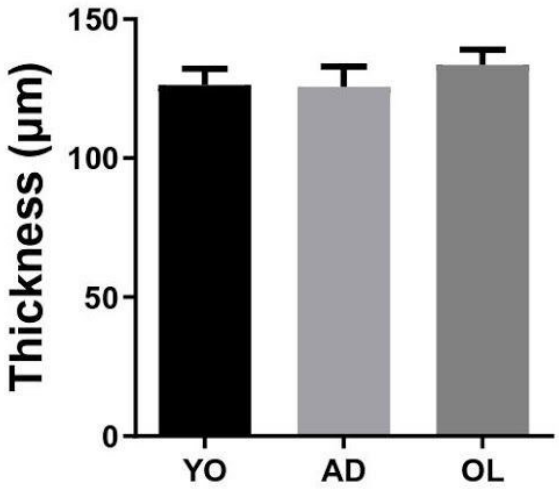

Figure 1 Quantification of the thickness of the vascular wall of aortic rings of YO, AD and OL rabbits. Results on average ± SEM. The number of experiments is 4 in all cases.

Relaxation

In the CCh-induced endothelium-dependent relaxation showed a decreased sensitivity (Table 1; p=0.05) and maximal response in OL (Figure 3A; p=0.03). When stimulated with isoproterenol showed significant differences in sensitivity between YO compared with AD and OL. The maximal relaxation was found decreased in OL (Emax: YO, 73±12%; AD, 50±6%; and OL, 30±3% of maximum relaxation) compared to the other groups (Figure 3B, p=0.001). VR with SNP showed significant differences in sensitivity between YO compared with AD and OL (Figure 3C; p=0.01). However, no significant differences were found in the maximal response (Figure 3C; p=0.2). A summary and number of experiments can be found in Table 1.

Immunofluorescence

The expression of receptors quantified by fluorescence in rabbit aorta was normalized with respect to YO (Figure 4A). For the α1 receptor, the values for the intima were 1 ±0.2 for YO (n=4 for all the experiments), 2.3±0.9 for AD and 3±0.5 for OL, with no significant differences among the groups (Figure 4B, p>0.05); for the media, the values were 1±0.5 for YO, 3.44±1.3 for AD and 4.04±2.4 for OL, without significant differences among the groups (Figure 4B, p>0.05); and for the adventitia, the values were 1±0.3 for YO, 20.7±10.2 for AD and 13.4±5.8 for OL, with significant differences between YO and AD and between YO and OL (Figure 4B, p<0.01). For the β2 receptor, the values for the intima were 1±0.6 for YO, 1.9±0.55 for AD and 5.2±1.4 for OL, with significant differences between YO and OL and between AD and OL (Figure 4C, p<0.05); for the media, the values were 1±0.7 for YO, 0.65±0.13 for AD and 1.08±0.4 for OL, with no significant differences among groups (Figure 4C, p>0.05); and for the adventitia, the values were 1±0.8 for YO, 1.4±0.2 for AD and 4.3±1.2 for OL, with significant differences between YO and OL and between AD and OL (Figure 4C, p<0.01). For the TP receptor, the values for the intima were 1±0.2 for YO, 1.7±0.8 for AD and 0.75±0.3 for OL, without significant differences among the groups (Figure 4D, p>0.05); for the media, the values were 1±0.4 for YO, 1.75±0.6 for AD and 1.2±0.4 for OL, without significant differences among the groups (Figure 4D, p>0.05); and for the adventitia, the values were 1±0.5 for YO, 5.7±1.9 for AD and 7.6±2 for OL, with significant differences between YO and AD and between YO and OL (Figure 4D, p<0.01).

Discussion

We assessed the effect of ageing on structure, VR and receptor expression in rabbit aorta. Our main findings were as follows: 1) there were no structural changes in the ageing aorta, 2) ageing causes a decrease in the sensitivity of the aorta to KCl, U-46619 and isoproterenol, and 3) there was an increase in the adrenergic response with ageing, associated to an increased α1 receptor expression.

Structural Vascular Changes with Ageing

We performed a histological approach in order to establish whether there was vascular remodeling attributable to ageing, but we found no differences in intima-media thickness, as showed in Figure 1. We stained with Van Gieson and a modified Van Gieson (with orcein) to qualitatively evaluate collagen and elastic fibers, respectively, without finding a difference either.

Functional Vascular Changes with Ageing

We demonstrated that ageing causes a decrease in the sensitivity of aortic smooth muscle to receptor-independent agonists; however, Emax did not change. This result contrasts with,[6] which showed an increase in sensitivity and Emax to KCl in SAMR1 and SAMP8 mouse aorta (senescence model). This difference in results is expected because[6] used female mice in an accelerated senescence model, that could not exactly meet natural

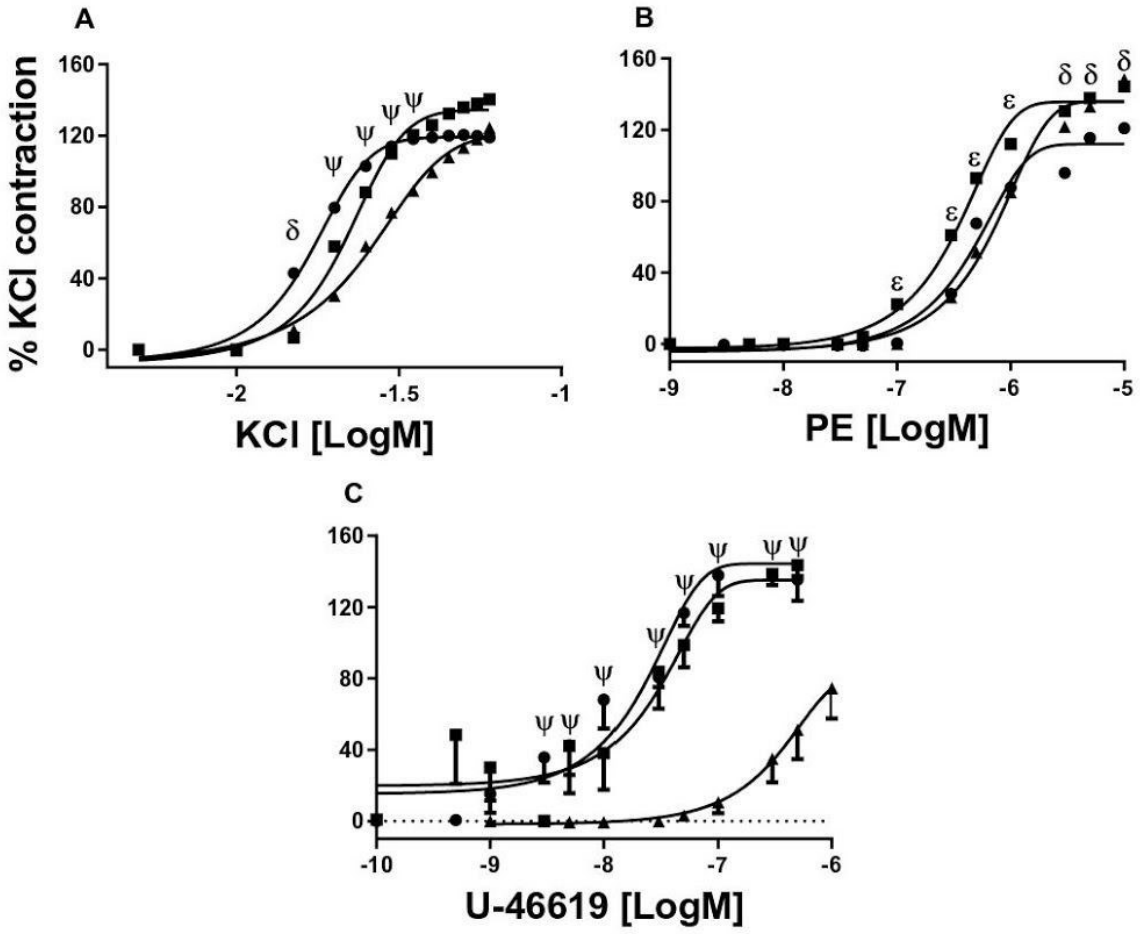

Figure 2 Concentration–response curves to KCl (**A**), PE (**B**) and U-46619 (**C**). YO (●, 4 animals, 8 rings), AD (■, 4,8) and OL (▲, 4,8). δ indicates a higher sensitivity to KCl and lower Emax to PE in YO arteries, compared to AD and OL. ψ indicates a higher sensitivity to KCl and to U-46619, and a higher Emax to U-46619, in YO and AD arteries compared with OL. In panel B, ε indicates a higher sensitivity to PE in AD, compared to YO and OL. pD2 and Emax values in all conditions can be seen in Table 1. Significance level of $P<0.05$.

ageing processes. Another important finding of the present study is the lack of differences between adult and old subjects, in agreement with[18] and,[19] who showed identical results in the aorta of healthy young vs old Sprague-Dawley rats; however, they did find differences in Emax at 18 months in SHR rats (hypertensive model).

Table 1 pD2 and Emax to KCl, FE, U-46619, CCh Isoproterenol and SNP in Aortic Rings in YO, AD, and OL Rabbits

Agonist	pD2				Emax (%KCl 40mM)			
	YO	AD	OL	p	YO	AD	OL	p
KCl	1.8±0.03	1.65±0.03	1.6±0.05	0.01	119±11	140±5	124±5	0.1
PE	6.3±0.03	6.5±0.6	6.1±0.04	0.002	121±12	144±2.2	148±6	0.01
U-46619	8±0.3	7.9±0.5	6.5±0.1	0.001	149±14	129±9	74.5±11	0.001
CCh	6.3±0.1	6.5±0.05	6.2±0.01	0.05	86±3[a]	83±4[a]	73±3[a]	0.03
Isoproterenol	7±0.1	6.6±0.08	6.1±0.4	0.01	73±12[a]	50±6[a]	31±12[a]	0.001
SNP	8.5±0.03	6.5±0.07	7.2±0.1	0.01	127±6	124±4	108±4	0.2

Notes: [a]% Relaxation with respect to the maximum contraction with PE. Results on average ± SEM. The n of KCl, PE and U-46619 are respectively the same as in Figure 2; The n of CCh, isoproterenol and SNP is the same as in Figure 3.

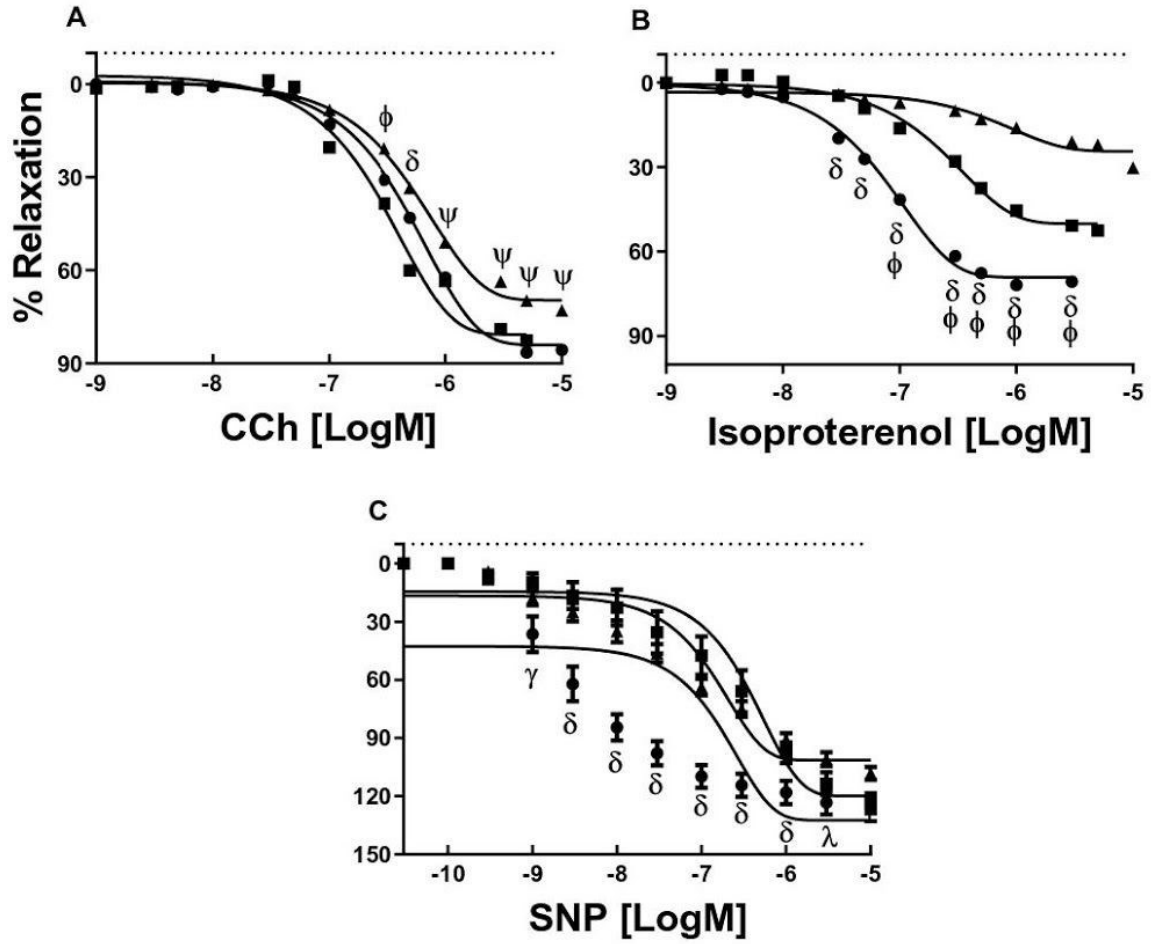

Figure 3 Concentration–response curves to CCh (**A**), isoproterenol (**B**) and SNP (**C**). YO (•, 4 animals, 8 rings), AD (■, 4,8) and OL (▲, 4,8). δ indicates a lower sensitivity in YO to CCh than AD and higher than OL, and a higher sensitivity to isoproterenol and SNP and higher Emax to isoproterenol in YO compared with AD and OL. ψ indicates a higher sensitivity to CCh in YO and AD compared with OL. ϕ indicates a higher sensitivity to CCh and isoproterenol and higher Emax to isoproterenol in AD compared with YO and OL. γ indicates a lower sensitivity in AD to SNP than YO. λ indicates a lower relaxation in OL to SNP than YO. pD2 and Emax values in all conditions can be seen in Table 1. Significance level of $P<0.05$.

We observed an increase in the adrenergic response with ageing, consistent with the increased expression of the α1 receptor in the tunica intima and media (observed as a trend) and in the adventitia (significant increase); however, cellular diversity of this external layer makes it difficult to establish how this increase in α1 expression contributes to the changes seen in VR. The increase in adrenergic response that we observed contrasts with,[20] which found decreased sensitivity to stimulation with norepinephrine (NE) in adult rat aorta, but it is probably due to NE has an α and β effect, while the PE used in the present study has specific affinity for α1. Our results also differed from,[21] which did not find differences in VR to PE in rat coronary artery, but agreed with,[22] which showed an increase in the α1 receptor in the human mammary artery in relation to age, and with,[23] which observed an increase in the reactivity of the renal artery to the sympathetic stimulus in humans over 50 years of age. Notably, the results involve different vascular beds and different species. The diversity of results justifies new complementary studies in arteries of distribution of various species, for example, in the mesenteric arteries of humans, rabbits and rats, to further clarify this scenario.

The VR to the TXA2 analogue, normalized to KCl, showed a marked difference in contraction between young and old rabbits and between adult and old rabbits, suggesting that sensitivity to prostanoids remains until six months of

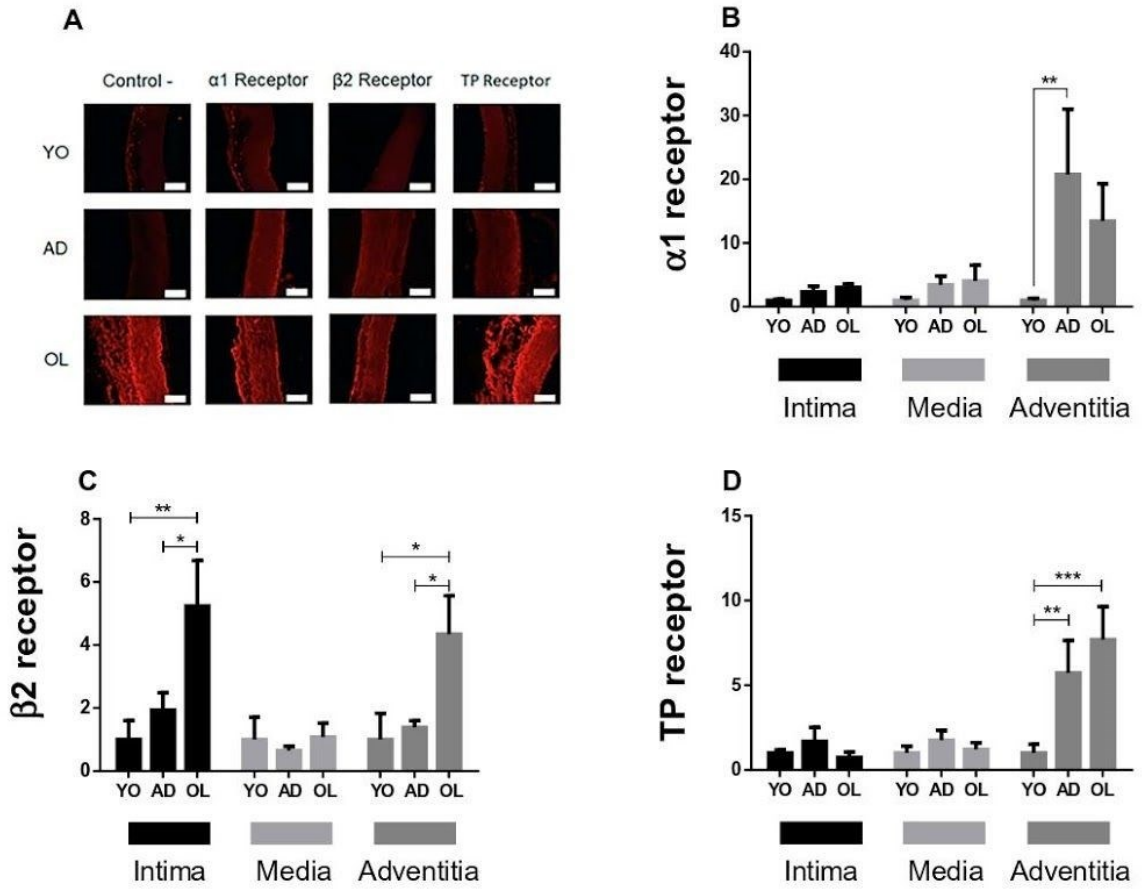

Figure 4 Quantification of protein expression of α1, β2 and thromboxane A2 (TP) receptors in the aortic wall of YO, AD, and OL rabbit. (**A**) representative images of immunofluorescence to identify α1, β2 and thromboxane A2 (TP) receptors. (**B–D**) Quantification of the fluorescence of the α1, β2 and TP receptors, respectively, in the tunica of the aortic wall. The number of experiments is 4 in all cases. **(A)** The length of the white calibration bars are equivalent to 100 μm. *Indicates $p<0.05$. **$p<0.01$. ***$p<0.001$. The expression was always normalized to YO.

development in rabbits, which would be equivalent to approximately 14 human years.[13] However, the sensitivity deteriorates in old age. This result is reinforced by the tendency to decrease in the expression of the TP receptor in the intima and media after adulthood, and coincides with that reported in the female SAMR1 and SAMP8 mouse aorta, attributing this increase in sensitivity and maximum effect to the stimulus with U-44619 to a decrease in the availability of nitric oxide and increase in contractile prostanoid synthesis.[6] Strikingly, there is a significant increase in the expression of the TP receptor in the vascular adventitia, but again, the cellular diversity of this external layer makes it difficult to define how this increase in TP contributes to the changes seen in VR. Our results for the intima match those reported in,[24] which did not find differences in the expression of the TP receptor in endothelial cells of SHR and WKY rats between 36 and 72 weeks, and contrasts with those reported in,[25] which did not find differences to the stimulus with U-46619 in male 6 and 22 months old Fischer F344 rat aorta, and with those reported in,[26] which did not find differences with the same agonist in rat cerebral arterioles. These results suggest that this contrast may be due to the animals and vessels used, in addition to different ages, but could also be related to the amount of perivascular tissue removed during the cleaning and mounting procedure.

We add that such changes in VR, at least in the aorta, may have other origins, for example, in the dynamics of phosphorylation at the cellular level, the availability of second messengers and other downstream mechanisms, which we did not explore but are reviewed in.[3]

It is important to take into account that the gain in contraction could be accentuated by the decrease in endothelial compensation.[24] In our relaxation results, VR with CCh

showed a tendency to decrease sensitivity to stimulation in old rabbits, coinciding with studies that showed decreased endothelial-dependent vasodilatory response to stimulation with acetylcholine or CCh in coronary[21] and mesenteric[27] arteries related to ageing in rats. This deterioration of relaxation is usually attributed to oxidative processes in the vascular wall.

In the present study, when we applied isoproterenol, a vascular relaxant that acts through the β2 receptor, we found a significant decrease in sensitivity and a maximum effect that was accentuated as age progressed, in contrast with the increase in β2 receptor expression in the endothelium and adventitia, suggesting that there is less β-adrenergic receptor activity as an individual ages, as discussed in[14] and.[22] It is feasible that the vessel responds by increasing the number of β receptors in adults and older patients especially in the endothelium and adventitia; however, each unit is relatively less functional, at least in this vascular bed. These results are similar to those reported in,[28] which showed a decrease in the vasorelaxant response in the human coronary artery in relation to ageing, although this decrease is much more pronounced in response to an endothelium-dependent vasodilator than to an endothelium-independent vasodilator. Additionally, our results would contribute to understanding the reduction of vascular stiffness when sympathetic denervation is made[29] although apparently not when baroreflex activation therapy is performed,[30] suggesting that vascular stiffness does not depend exclusively on sympathetic control.

When testing the non-endothelium-dependent relaxation response, the present work evidenced a marked decrease in SNP sensitivity in AD and OL with respect to YO, suggesting a reduction in the ability of vascular smooth muscle to relax in aging, complemented by a structural change of the vessel that makes it more rigid, known as elastocalcinosis.[3,4] These results contrast with studies that did not find such differences in the SNP response between young and old animals, in soleus feed arteries of Fisher 344 rats,[31] in aorta of Wistar rats[32] and in carotid of Albino rats.[33] The evidence strongly suggests that stiffening due to aging occurs differently depending on the vascular territory, as,[34] co-authored by the same author of,[31] showed in aorta, iliac, femoral and gastrocnemius feed arteries of Fisher 344 rats, that deterioration of the dilatation to the SNP did occur in large/elastic arteries, but not in resistance arteries. According to this, and to our results, vascular stiffening due to aging is not only due to endothelial changes but to a structural and functional changes of the different layers of the artery. Additional studies are required to characterize the involved mechanisms.

Conclusion

In a rapidly ageing world, it is critical to know more about the mechanisms by which blood vessels harden with age. Our results suggest that ageing makes the aorta more rigid not only mechanically but, in addition, more reactive to α1 adrenergic contraction, perhaps as compensation for lower responsiveness to the prostanoid contractile pathway. In the same sense, the aorta is less reactive to endothelium-dependent and non-dependent relaxation, which could not be attributable only to oxidative stress. The vessel seems to try to compensate for that stiffness with increased receptors, with little success due to their probable lower functionality. The evidence here presented complements the view that there is a deterioration of the ECM (elastocalcinosis) and an increase in the rigidity of vascular smooth muscle. In this way, we hope to contribute to a better rationale of lifestyle and pharmacological interventions which attempt to treat/prevent CVD. Our quantification could also contribute to improving the comparability of vascular outcomes between groups of people with different ages. In addition, if experimental animals are used, our results insist on the necessity to ensure that the age of the animals used is equivalent to the age range of incidence of the disease in humans, to decrease a probable bias when extrapolating the findings.

Acknowledgments

We want to thank the project "High Level Human Talent Training" approved by the Science, Technology and Innovation Fund (CTeI) of the General Royalty System (SGR)-BPIN 2013000100103, Tolima Governorate and University of Tolima, Colombia; the CODI grants, 2014-University of Antioquia; and the Foundation for the Promotion of Research and Technology, 2017-Bank of the Republic of Colombia.

Disclosure

The authors report no conflicts of interest in this work.

References

1. Childs BG, Durik M, Baker DJ, Van Deursen JM. Cellular senescence in aging and age-related disease: from mechanisms to therapy. *Nat Med*. 2015;21(12):1424. doi:10.1038/nm.4000
2. WHO. WHO | cardiovascular diseases (CVDs). 2018. Available from: https://www.who.int/cardiovascular_diseases/en/. Accessed June 18, 2019.
3. Donato AJ, Machin DR, Lesniewski LA. Mechanisms of dysfunction in the aging vasculature and role in age-related disease. *Circ Res*. 2018;123(7):825–848. doi:10.1161/CIRCRESAHA.118.312563
4. Dao HH, Essalihi R, Bouvet C, Moreau P. Evolution and modulation of age-related medial elastocalcinosis: impact on large artery stiffness and isolated systolic hypertension. *Cardiovasc Res*. 2005;66(2):307–317. doi:10.1016/j.cardiores.2005.01.012

5. Qiu H, Zhu Y, Sun Z, et al. Short Communication: vascular smooth muscle cell stiffness as a mechanism for increased aortic stiffness with aging. *Circ Res*. 2010;107(5):615–619. doi:10.1161/CIRCRESAHA.110.221846
6. Novella S, Dantas AP, Segarra G, et al. Aging enhances contraction to thromboxane A 2 in aorta from female senescence-accelerated mice. *Age*. 2013;35(1):117–128. doi:10.1007/s11357-011-9337-y
7. Hongo K, Nakagomi T, Kassell N, et al. Effects of aging and hypertension on endothelium-dependent vascular relaxation in rat carotid artery. *Stroke*. 1988;19(7):892–897. doi:10.1161/01.STR.19.7.892
8. Kokozidou M, Katsargyris A, Verhoeven EL, Schulze-Tanzil G. Vascular access animal models used in research. *Ann Anat*. 2019;225:65–75. doi:10.1016/j.aanat.2019.06.002
9. Lapenna D, Ciofani G, Pierdomenico SD, Giamberardino MA, Porreca E. Iron status and oxidative stress in the aged rabbit heart. *J Mol Cell Cardiol*. 2018;114:328–333. doi:10.1016/j.yjmcc.2017.11.016
10. Ning B, Chen Y, Waqar AB, et al. Hypertension enhances advanced atherosclerosis and induces cardiac death in Watanabe heritable hyperlipidemic rabbits. *Am J Pathol*. 2018;188(12):2936–2947. doi:10.1016/j.ajpath.2018.08.007
11. Orlandi A, Francesconi A, Marcellini M, Ferlosio A, Spagnoli LG. Role of ageing and coronary atherosclerosis in the development of cardiac fibrosis in the rabbit. *Cardiovasc Res*. 2004;64(3):544–552. doi:10.1016/j.cardiores.2004.07.024
12. Russell JC, Proctor SD. Small animal models of cardiovascular disease: tools for the study of the roles of metabolic syndrome, dyslipidemia, and atherosclerosis. *Cardiovasc Pathol*. 2006;15(6):318–330. doi:10.1016/j.carpath.2006.09.001
13. Woodruff-Pak DS. Aging and classical conditioning: parallel studies in rabbits and humans. *Neurobiol Aging*. 1988;9:511–522. doi:10.1016/S0197-4580(88)80108-8
14. Fleisch JH, Hooker CS. The relationship between age and relaxation of vascular smooth muscle in the rabbit and rat. *Circ Res*. 1976;38(4):243–249. doi:10.1161/01.RES.38.4.243
15. Sullivan JC, Loomis ED, Collins M, Imig JD, Inscho EW, Pollock JS. Age-related alterations in NOS and oxidative stress in mesenteric arteries from male and female rats. *J Appl Physiol*. 2004;97(4):1268–1274. doi:10.1152/japplphysiol.00242.2004
16. Buchinger-Kähler V, Stoldt VR, Muth T, Schipke JD. Function and viability of vessels in different preservation solutions-an experimental study on human great saphenous veins. *J Angiol Vasc Surg*. 2016;1(003):1–7. doi:10.24966/AVS-7397/100003
17. Estrada O, González-Guzmán JM, Salazar-Bookaman M, Fernández AZ, Cardozo A, Alvarado-Castillo C. Pomolic acid of Licania pittieri elicits endothelium-dependent relaxation in rat aortic rings. *Phytomedicine*. 2011;18(6):464–469. doi:10.1016/j.phymed.2010.10.008
18. Soltis EE. Effect of age on blood pressure and membrane-dependent vascular responses in the rat. *Circ Res*. 1987;61(6):889–897. doi:10.1161/01.RES.61.6.889
19. Ponte A, Sánchez-Ferrer CF, Hernández C, Alonso MJ, Marín J. Effect of ageing and hypertension on endothelial modulation of ouabain-induced contraction and sodium pump activity in the rat aorta. *J Hypertens*. 1996;14(6):705–712. doi:10.1097/00004872-199606000-00005
20. Feletou M, Köhler R, Vanhoutte PM. Nitric oxide: orchestrator of endothelium-dependent responses. *Ann Med*. 2012;44(7):694–716. doi:10.3109/07853890.2011.585658
21. Su N, Narayanan N. Age related alteration in cholinergic but not α adrenergic response of rat coronary vasculature. *Cardiovasc Res*. 1993;27(2):284–290. doi:10.1093/cvr/27.2.284
22. Rudner XL, Berkowitz DE, Booth JV, et al. Subtype specific regulation of human vascular α1-adrenergic receptors by vessel bed and age. *Circulation*. 1999;100(23):2336–2343. doi:10.1161/01.CIR.100.23.2336
23. Boddi M, Sacchi S, Lammel RM, Mohseni R, Gastone G, Serneri N. Age-related and vasomotor stimuli-induced changes in renal vascular resistance detected by Doppler ultrasound. *Am J Hypertens*. 1996;9(5):461–466. doi:10.1016/0895-7061(96)00027-1
24. Tang EH, Vanhoutte PM. Gene expression changes of prostanoid synthases in endothelial cells and prostanoid receptors in vascular smooth muscle cells caused by aging and hypertension. *Physiol Genomics*. 2008;32(3):409–418. doi:10.1152/physiolgenomics.00136.2007
25. Shams G, Wallace LJ, Miller DD, Feller DR. Effects of thromboxane A2 on thoracic aorta of young and old rats: use of selective thromboxane receptor antagonists. *Pharmacology*. 1990;40(1):27–32. doi:10.1159/000138635
26. Mayhan WG, Faraci FM, Baumbach GL, Heistad DD. Effects of aging on responses of cerebral arterioles. *Am J Physiol Heart Circ Physiol*. 1990;258(4):H1138–H1143. doi:10.1152/ajpheart.1990.258.4.H1138
27. Atkinson J, Tatchum-Talom R, Capdeville-Atkinson C. Reduction of endothelial function with age in the mesenteric arterial bed of the normotensive rat. *Br J Pharmacol*. 1994;111(4):1184–1188. doi:10.1111/j.1476-5381.1994.tb14870.x
28. Egashira K, Inou T, Hirooka Y, et al. Effects of age on endothelium-dependent vasodilation of resistance coronary artery by acetylcholine in humans. *Circulation*. 1993;88(1):77–81. doi:10.1161/01.CIR.88.1.77
29. Brandt MC, Reda S, Mahfoud F, Lenski M, Böhm M, Hoppe UC. Effects of renal sympathetic denervation on arterial stiffness and central hemodynamics in patients with resistant hypertension. *J Am Coll Cardiol*. 2012;60(19):1956–1965. doi:10.1016/j.jacc.2012.08.959
30. Gronda E, Brambilla G, Seravalle G, et al. Effects of chronic carotid baroreceptor activation on arterial stiffness in severe heart failure. *Clin Res Cardiol*. 2016;105(10):838–846. doi:10.1007/s00392-016-0992-y
31. Woodman CR, Price EM, Laughlin H. Selected contribution: aging impairs nitric oxide and prostacyclin mediation of endothelium-dependent dilation in soleus feed arteries. *J Appl Physiol*. 2003;95(5):2164–2170. doi:10.1152/japplphysiol.01073.2002
32. Kim SY, Park JT, Park JK, Lee JS, Choi JC. Aging impairs vasodilatory responses in rats. *Korean J Anesthesiol*. 2011;61(6):506–510. doi:10.4097/kjae.2011.61.6.506
33. Omar NM, Abbas AM, Abdel-Malek H, Suddek GM. Effect of age on the contractile response of the rat carotid artery in the presence of sympathetic drugs and L-NAME. *Acta Physiol Hung*. 2013;100(3):266–279. doi:10.1556/APhysiol.100.2013.3.3
34. Luttrell M, Kim H, Shin SY, Holly D, Massett MP, Woodman CR. Heterogeneous effect of aging on vasorelaxation responses in large and small arteries. *Physiol Rep*. 2020;8(1):e14341. doi:10.14814/phy2.14341

Capítulo cuatro:

Cupitra NI, León-Rodríguez JP, Calderón JC, Narvaez-Sanchez R, 2020. Comparability of vascular reactivity and expression of receptors of mesenteric circulation between human, pig, rabbit and rat.

Capítulo cuatro:

Cupitra NI, León-Rodríguez JP, Calderón JC, Narvaez-Sanchez R, 2020. Comparability of vascular reactivity and expression of receptors of mesenteric circulation between human, pig, rabbit and rat

Terminado el desarrollo del trabajo, en diciembre de 2019 se encontró la última limitación, siendo ésta la baja frecuencia de pacientes patológicos no tumorales (grupo control; 3-4 pacientes por año), que redujo la potencia estadística al 60% en los experimentos de VR con bloqueantes específicos, induciendo riesgo de sub o sobreestimar los resultados. Además, no había forma de conseguir arterias de pacientes sanos (donantes de órganos por muerte cerebral) para comparar con el grupo con cáncer, obligando tener como control fisiológico "sano" los pacientes patológicos. Ante la necesidad de un grupo control accesible y comparable, se estableció como alternativa el uso de modelos animales para caracterizar la función vascular en circulación mesentérica y determinar si hay un modelo que pueda servir como control en este trabajo. Los modelos vasculares como cerdos, conejos y ratas han sido indispensables para caracterizar los mecanismos fisiopatológicos de las ECV a pesar de las limitaciones genéticas. Se incluye la rata ya que dada las facilidades de crianza, su ciclo de desarrollo y la posibilidad de controlar variables ambientales durante su cría se ha posicionado el modelo estándar en experimentación de fisiopatologías vasculares, por lo que es interesante cuantificar el grado de comparabilidad de la VR con el humano y otros modelos, ya podría ayudar a entender por qué algunos resultados promisorios encontrados en ratas no son homologables en humanos. Proponemos como una posible alternativa para obtener modelos vasculares de mayor tamaño y tal vez de mayor comparabilidad con el humano, los cerdos y conejos de granjas tecnificadas, si bien, en estos lugares las variables ambientales no son controladas en su totalidad, son modelos que podrían ser más comparables con el humano. Además, la influencia del medio ambiente en el desarrollo de estos modelos podría aportar información valiosa sobre el comportamiento cardiovascular. Por lo anterior establecimos como objetivo secundario determinar el grado de comparabilidad en la VR y en expresión de receptores en arterias de circulación mesentérica entre el humano, el cerdo, el conejo y la rata.

Artículo correspondiente al capítulo cuatro

Comparability of vascular reactivity and expression of receptors of mesenteric circulation among human, pig, rabbit and rat

Nelson Ivan Cupitra [1]; Jimmy P. León-Rodríguez [2]; Juan C. Calderón [1]; Raul Narvaez-Sanchez[1]

[1] Physiology and Biochemistry Research Group-PHYSIS, Faculty of Medicine, University of Antioquia, Medellin, Colombia.
[2] Trauma and surgery Research Group, Department of Surgery, School of Medicine, Universidad de Antioquia, Medellín, Colombia.

Graphical Abstract:

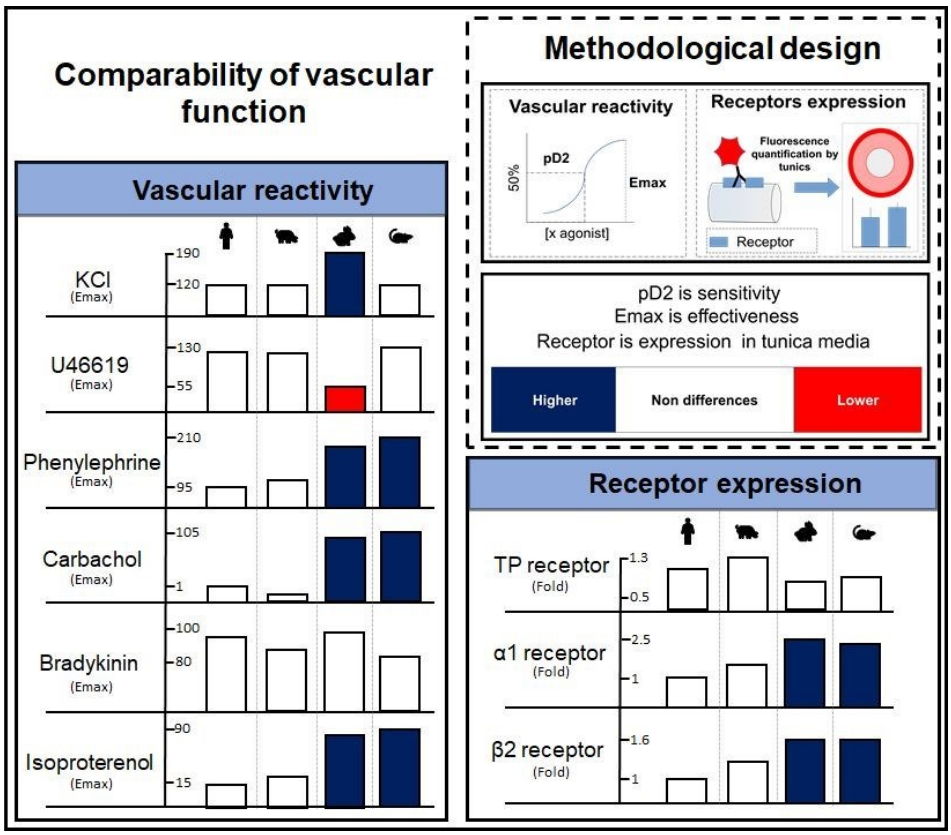

Abstract:

Los modelos *ex vivo* son indispensables porque permiten caracterizar los mecanismos fisiopatológicos de enfermedades cardiovasculares, pero es esperable que en especies filogenéticamente distintas se encuentren diferencias entre los modelos y el humano que pueden condicionar la respuesta de mecanismos fisiopatológicos o del tratamiento farmacológico. Nosotros caracterizamos la comparabilidad en reactividad vascular en baño de órganos a KCl, U46619, phenylephrine, carbacol, bradikinina e isoproterenol en arterias mesentéricas de cerdos, conejos y ratas frente al humano. Se obtuvieron curvas concentración-respuesta a los agonistas se estimaron Emax y pD2. Además, se hizo la cuantificación de receptores α1, β2 y TP en la pared vascular por microscopía de fluorescencia. En contracción, los conejos tuvieron mayor Emax a KCl y PE, pero menor eficacia a U46619; las ratas mostraron mayor Emax a PE. En relajación, conejos y ratas tuvieron más dilatación a carbacol e isoproterenol. Conejos y ratas presentan mayor expresión de los receptores α1 y β2 en la túnica media. Los cerdos no presentaron diferencias vasculares frente a los humanos. La respuesta vascular en arterias de la mesentérica en cerdo, conejo y rata no son completamente comparables al humano, pero el modelo vascular de mayor comparabilidad es el cerdo.

Introducción

Las enfermedades cardiovasculares (ECV) son la principal causa de muerte a nivel mundial (OMS, 2020). Las ECV son patologías complejas multifactoriales, en las que están implicados factores genéticos y ambientales, pero a pesar de grandes esfuerzos mundiales para prevenirlas, su prevalencia sigue en aumento (Zaragoza, 2011). El desarrollo de modelos animales ECV ha proporcionado importantes conocimientos sobre la fisiopatología cardiovascular. Los modelos *ex vivo* son indispensables porque permiten caracterizar los mecanismos fisiopatológicos y obtener información directa de eventos específicos, con la posibilidad de controlar las variables mientras se aplican procedimientos precisos, que pueden ser invasivos y difíciles de usar en estudios clínicos (Chorro, 2009).

Es esperable que en especies filogenéticamente distintas se encuentren diferencias entre la enfermedad humana y la enfermedad inducida experimentalmente, donde las características de cada modelo pueden condicionar la respuesta de mecanismos fisiopatológicos o al tratamiento farmacológico (Chorro, 2009). Por esto, la extrapolación de los resultados a la fisiopatología humana debe realizarse con precaución, además, se justifica caracterizar comportamientos fisiológicos en las especies más utilizadas. A pesar de las diferencias biológicas, ratones y ratas son los modelos vasculares más utilizados en investigación, por encima de modelos como cerdos y conejos. Desde un punto de vista evolutivo es esperable que murinos y conejos tengan mayor homología con el humano, sin embargo, se desconoce el grado de similitud en la respuesta vascular entre estas especies y el humano lo que podría llegar a limitar la extrapolación de resultados.

A su vez, la aorta es el lecho vascular más utilizado para medir las adaptaciones funcionales en VR asociadas a fenómenos fisiopatológicos y como modelo en la evaluación de sustancias con potencial farmacológico sobre aterosclerosis e hipertensión. No obstante, los fenómenos ateroscleróticos en aorta y sus grandes ramas son ampliamente conocidos, pero poco se sabe de estos fenómenos en vasos de menor calibre y más musculares. Además, al ser la aorta un vaso sanguíneo de conducción relativamente elástico, su rol en el control de la presión arterial es menor que el de vasos musculares –de resistencia-, eso hace preferible usar como modelo arterias con mayor proporción de músculo liso como las coronarias, las carótidas, arterias de circulación periférica y las mesentéricas, ya que irrigan amplias zonas, son altamente reguladas, y guardan relación con enfermedades prevalentes como el cáncer. La arteria mesentérica es una excelente opción, por accesibilidad y porque distribuye sangre hacia un área con mayor participación en el control del flujo sanguíneo. Sin embargo, aunque hay un acercamiento sobre este lecho vascular en cerdo, conejo y rata (Russell, 2006; Virmani, 2003), no hay trabajos que caractericen los modelos y por tanto su capacidad para extrapolar las respuestas en ese lecho vascular en humanos. Lo anterior justifica caracterizar el vaso sanguíneo con el fin de establecer la comparabilidad de dicha respuesta vascular arterias de la mesentérica entre el humano y los modelos vasculares cerdo, conejo y rata.

Proponemos caracterizar las diferencias en la VR de arterias de la circulación mesentérica de humanos, cerdos, conejos y ratas a contracción independiente de receptor con cloruro de potasio (KCl), contracción dependiente de receptor con fenilefrina (PE) y U-46619 (agonista de tromboxano A2 –TXA2), y relajación dependiente de receptor con carbacol (CCh), bradikinina (BK) e isoproterenol. Complementariamente se compara la expresión de receptores de estas vías de señalización en la pared vascular por inmunofluorescencia.

Materiales y métodos

Modelo animal y reactivos

Los ensayos en humanos y animales fueron aprobados por el Comité de Bioética y el Comité de Experimentación Animal de la Universidad de Antioquia (Medellín, Colombia) de acuerdo con la declaración de Helsinki, ley 84 de 1989 y la resolución 8430 de 1993. Acta 14 del 27 de agosto de 2015; Acta 122 del 5 de febrero de 2019; Acta 134 del 4 de agosto de 2020. Los segmentos arteriales fueron obtenidos de cuatro grupos experimentales: A. Ocho humanos de 46±9 años, tres mujeres y cinco hombres. Tres pacientes fueron colectomizados por diverticulitis, dos por obstrucción por bridas, dos por traumatismo y uno por donación de órganos en la Clínica León XIII. B. Diez cerdos machos PIC-410 (100±4 kg, 4±0,5 meses) de Supercerdo Paisa S.A.S.. C. Diez conejos machos Nueva Zelanda (2,7±0,5 kg, 4±0,5 meses) de la instalación de cunicultura del Servicio Nacional de Aprendizaje-La Salada. D. Diez ratas Wistar macho (350±40 g, 3,5±0,5 meses) del bioterio de la SIU-Universidad de Antioquia. Todos de Antioquia, Colombia.

Carbamoylcholine chloride (212385-M), phenylephrine hydrochloride (P6126), Bradykinin acetate salt -BK-(B3259) and Isoproterenol bitartrate (I2760) were from Sigma–Aldrich Co. (St. Louis, MO, EE.UU.). El U46619 (ab144540) de Abcam (Cambridge, EE. UU.). Las soluciones Stock se prepararon en agua destilada con ácido ascórbico 10 µM para evitar la oxidación. Todos los anticuerpos eran de Abcam (ver más abajo).

Disección

Se obtuvieron segmentos arteriales de humanos en quirófanos y se almacenaron durante dos horas en solución de Krebs-Henseleit (HK), con la siguiente composición (mM): NaCl, 118; KCl, 4,7; KH2PO4, 1,2; MgSO4, 1,2; NaHCO3, 25,0; glucosa, 11,1; CaCl2, 2,5; pH 7 a 4 °C. Los segmentos arteriales de cerdo se obtuvieron de animales sacrificados en una granja tecnificada y se almacenaron durante dos horas en HK. El tejido de conejos y ratas se obtuvo de animales sacrificados en el laboratorio con tiopental sódico intraperitoneal (60 mg/kg) y posterior dislocación cervical. Las ramas mesentéricas se disecaron rápidamente y se conservaron HK. Los segmentos arteriales tenían 0.5-1 mm de diámetro interno en humanos y cerdos o 0.3-0.5 en conejos y ratas. Se eliminó el exceso de tejido periférico y se cortaron en 10 anillos de 3-5 mm de longitud. Se utilizaron cuatro anillos para experimentos de relajación y contracción. Se conservaron cuatro anillos durante 24 horas en solución HK previamente burbujeada con gas carbonatado (95% O2-5% CO2) a 4 °C y se usaron solo para estudios de contracción. Otros estudios han demostrado que no existen diferencias en la reactividad vascular a las 24 horas de conservación en solución de Krebs a 4 °C (Buchinger-Kähler, 2016; Cupitra, 2020A). Los dos anillos restantes se embebieron en Shandon Cryomatrix (Thermo Fisher Scientific, EE. UU.) y se congelaron en nitrógeno líquido para inmunohistoquímica.

Reactividad vascular

Los anillos fueron montados en un baño de órganos LE13206 PANLAB (Barcelona, España) de 10 ml con HK a 37 °C y burbujeo con carbogeno, como se describió previamente (Cupitra, 2020B). La respuesta contráctil se digitalizó con Powerlab PL-3504 (Sydney, Australia) y se analizó en el módulo de respuesta a dosis del software LabChart 8. Cada preparación se estabilizó a 2 g de tensión en reposo durante 90 minutos antes de iniciar los estímulos agonistas; durante este período, la solución de HK se reemplazó cada 20 minutos. Después de la estabilización, el anillo arterial se estimuló dos veces con KCl 40 mM, registrando la respuesta durante 10 minutos y se lavó por 20 minutos entre cada estímulo. Luego, se aplicó al baño U46619 300 nM en humanos y cerdos o PE 30 µM en conejos y ratas, seguido de

BK 10 µM para humanos y cerdos o CCh 10 µM para conejos y ratas para confirmar la presencia del endotelio; esto se realizó para todos los anillos arteriales. Luego, se aplicó una dosis única de KCl 40 mM; dosis acumulativa de KCl 5 a 60 mM; dosis acumulativa de U46619 0,1 nM a 1 µM, y dosis acumulativa de PE 10 nM a 100 µM. Los estudios de relajación se realizaron con anillos precontraídos con U46619 300 nM (humanos y cerdos) o PE 10 µM (conejos y ratas), usando CCh 1 nM a 10 µM; isoproterenol 1 nM a 10 µM y BK 1 nM a 10 µM. La VR a CCh e isoproterenol se midió sólo en relajación y se suspendió al inicio de la contracción porque la precontracción podría haber afectado está VR contráctil.

Inmunofluorescencia

Las arterias congeladas se cortaron en secciones de 10 µm de espesor y se fijaron en acetona, se permeabilizaron con Triton X-100 al 0,1% y se bloquearon con albúmina de suero bovino al 5% en solución salina tamponada con fosfato. Se incubaron diferentes secciones con los siguientes anticuerpos primarios a 4 °C durante la noche (diluidos 1:1000 (humanos, cerdos y ratas) o 1:1500 (conejos) en solución de bloqueo): receptor adrenérgico anti-α1 (3462, Abcam), receptor anti-β2 adrenérgico (AB61778, Abcam), receptor anti-tromboxano A2 (TP) (233288, Abcam). Después del lavado, los anillos se incubaron con anticuerpo secundario anti-conejo conjugado con Alexa Fluor 488 (verde, 1:800 en solución de bloqueo; AB150077, Abcam) a temperatura ambiente durante 2 horas. Como control, una sección de cada grupo experimental no se incubó con un anticuerpo primario, solo se incubó con un anticuerpo secundario. Las imágenes se obtuvieron utilizando un microscopio invertido de fluorescencia (Axio Observer A1, Carl Zeiss), una lámpara de mercurio (HXP120, Carl Zeiss) y un filtro (488009-9901, Carl Zeiss; ventana de emisión >515 nm). La evaluación de las imágenes se realizó con un objetivo de 20X. Se utilizó ImageJ v1.52a para procesar las imágenes utilizando la herramienta Split channels en imágenes RGB, se normalizó la fluorescencia contra el background del control sin primario, cuantificando la intensidad promedio del verde en 3 regiones de interés de la íntima, media y adventicia para cada imagen respecto a NT.

Análisis estadístico

El número de experimentos se muestra cómo (#animales, #anillos). En el procesamiento de resultados se utilizaron datos completos, las variables son continuas. Los resultados se presentan como curvas de concentración-respuesta y gráficos de puntos con media±SEM. Los supuestos de normalidad se confirmaron con las pruebas de D'Agostino-Pearson y Shapiro-Wilk. Las curvas de concentración-respuesta se ajustaron con una regresión no lineal utilizando un modelo sigmoidal de cuatro parámetros (4PL) con fórmula Y=Bottom+(Top-Bottom)/(1+10^((LogIC50-X)*HillSlope)), donde Top muestra la Emax y el Log10 negativo de la concentración molar que produce el 50% de la respuesta máxima refleja la sensibilidad (pD2). Se analizaron pD2, Emax y la cuantificación de la expresión del receptor en la íntima, media y adventicia con un ANOVA de una vía seguido de la prueba post hoc de Dunnett. Las curvas de concentración-respuesta se analizaron con un ANOVA de dos vías seguido de la prueba post-hoc de Dunnett que compara modelo/concentración. Las diferencias se consideraron estadísticamente significativas a $p<0,05$. Se utilizó el paquete estadístico GraphPad Prism 7 v7.0.

Resultados

Contracción

En la Tabla 1 se muestra una descripción general de todos los resultados. Tras la estimulación con KCl, la VR no mostró diferencias en pD2 entre los grupos ($p =0,29$), mientras que los conejos mostraron un 40% más Emax que los humanos ($p = 0,0002$; Tabla 1; figura 1A). El pD2 a U46619 no difirió entre grupos ($p = 0.055$). El estímulo con U46619 mostró una Emax más baja en conejos en comparación con los humanos ($p = 0,02$; Tabla 1; Fig. 1B). La VR con PE de los grupos tampoco difirió en sensibilidad, pero mostró más Emax en conejos y ratas en comparación con los humanos ($p = 0,02$; Tabla 1; Fig. 1C).

Relajación

En la relajación dependiente del endotelio inducida por CCh, no se encontraron diferencias en la sensibilidad (p =0,057; Tabla 1) pero mostró más dilatación en conejos y ratas en comparación con los humanos (p=0,0001; Tabla 1; Fig. 2A). La relajación a BK no presentó diferencias en pD2 y Emax entre los grupos (p>0.05; Tabla 1; Fig. 2B). Al isoproterenol, la sensibilidad fue menor en los cerdos en comparación con los humanos (p=0,005; Tabla 1). La dilatación a isoproterenol en conejos y ratas fue mayor que en humanos (p=0,0001; Fig. 2C).

Inmunofluorescencia

La expresión de receptores cuantificada por fluorescencia en cerdos, conejos y ratas se normalizó con la expresión en humanos (Fig. 3A). En la expresión del receptor TP no se encontraron diferencias (Tabla 2; Fig. 2B). En túnica media, la expresión del receptor α1 fue 1,5 y 1,38 veces mayor en conejos y ratas en comparación con los humanos (p<0,0014; Tabla 2; Fig.2C), y el receptor β2 fue 1,5 veces mayor en conejos y ratas en comparación con los humanos (p <0,009; Tabla 2; Fig. 3D). En la íntima y la adventicia no se encontraron diferencias en la expresión de los receptores (Tabla 2; Fig. 3C-D).

Discusión

Este es el primer trabajo que hace una comparación de la RV y la expresión de receptores en los vasos mesentéricos de humano, cerdo, conejo y rata. Nuestros principales hallazgos fueron: i) El conejo es más reactivo a KCl y menos sensible a U46619 que los humanos, cerdos y ratas, ii) el conejo y la rata presentan mayor respuesta adrenérgica en contracción a PE y relajación a isoproterenol, asociado a un aumento de la expresión del receptor α1 y β2, respectivamente, iii) el conejo y la rata aumentaron los mecanismos de relajación colinérgica al separarse evolutivamente de los humanos y cerdos. Se encontraron diferencias interesantes entre los modelos vasculares, pero por el enfoque de este trabajo la discusión se centrará en las diferencias frente al humano.

La contracción independiente del receptor es mayor en modelos de conejos que en humanos, cerdos o ratas

La RV a KCl no mostró diferencias en sensibilidad, pero sí en respuesta máxima, donde el conejo tuvo mayor respuesta contráctil frente al humano. En conejo, la sensibilidad a KCl que describimos en conejo es similar a la encontrada por (Asano, 1983) y (Field, 1985) quienes evaluaron el efecto potenciador de agentes sulfidrilo y el efecto del estrés por alta presión y el calcio extracelular sobre la VR, respectivamente, mostrando en sus hallazgos una sensibilidad a KCl comparable (pD2: 1.8 y 1.52) con nuestros resultados. Por otro lado, no es posible comparar nuestros valores en Emax con los de (Asano, 1983) debido a que normalizaron la VR tomando la Emax a KCl como el 100%, sin embargo, es probable que las diferencias en Emax se deban al condicionamiento fisiológico por estrés, inducido en los conejos durante el transporte desde la zona de cría hasta el bioterio. La VR a KCl en cerdo y rata parece ser comparable con el humano. En cerdo no hemos encontrado trabajos para comparar, sin embargo, se han encontrado trabajos donde utilizan la VR a KCl como normalizador de contracción o evaluando su efecto a dosis única (McAllister, 1985; González-Luis, 2019). Lo anterior sugiere que la maquinaria contráctil posee mecanismos preservados a lo largo del desarrollo de estas especies, siendo esta VR susceptible de alterarse por la influencia del ambiente.

La vía de los prostanoides es menos sensible en conejos que en humanos, cerdos o ratas

Las diferencias estadísticas en la VR a U46619, mostraron que la vía de contracción por TXA2 en humano es más comparable con cerdo y rata que con conejo, y que este último sería un modelo pobre para trabajar TXA2, al menos en el territorio mesentérico. También, se observó una tendencia hacia menor expresión del receptor TP en conejo y rata, explicando parcialmente las diferencias en sensibilidad al estímulo, particularmente en conejo donde se indica una menor participación de los receptores de tromboxano-prostanoides. Sin embargo, se ha reportado en otras investigaciones que el uso de U46619 tienen un rol como potenciador en la contracción inducida por serotonina (Trachte, 1989; Choppin, 1995), sugiriendo que TXA2 participa en el control vascular en arteria mesentérica

de conejo de forma pasiva. Complementariamente, las diferencias en sensibilidad entre humano y cerdo podrían deberse a la condición fisiopatológica de las arterias humanas, esto teniendo en cuenta que la VR a U46619 de nuestro único donante de órganos de 32 años de edad, no presentó diferencias estadísticas con el modelo porcino (pD2= 6.4±0.02; Emax: 141.4±9.5; datos no mostrados) y que se ha descrito que la VR a TXA2 es susceptible a disminuir en ambientes inflamatorios (Ricciotti, 2011) y por el envejecimiento (Cupitra, 2020). No hemos encontrado bibliografía que establezca claramente la razón de estas diferencias, más allá de que el comportamiento vascular quizá ha sido influenciado por la evolución y la dieta particular de las especies.

La rata y el conejo son más reactivos a los agonistas α-adrenérgicos que los humanos y los cerdos

La respuesta a PE sugiere fuertemente que conejos y ratas modulan el territorio mesentérico principalmente por vía adrenérgica más que el humano. Complementariamente, se encontró una mayor expresión del receptor α1 conejo y rata en el músculo liso vascular, lo que explicaría la mayor Emax en ambos modelos. La mayor afinidad a la contracción adrenérgica en lo modelos más pequeños podría guardar relación con su evolución y su adaptación al entorno, dado que en condiciones silvestres conejos y ratones son susceptibles a muchos depredadores, siendo esperable un condicionamiento a favor de su biología que favorezca reacciones de defensa o huida. El hecho que este mismo fenómeno no se evidencie en cerdos también sugiere que esta ganancia de reactividad en conejos y ratas es más reciente que su separación con el cerdo (80 millones de años), y que se presentó luego de su separación evolutiva con los humanos (60 millones de años; Upham, 2019). Además, otro factor que pudo influir en la preservación de la VR en cerdos fue el proceso de domesticación inducido por el hombre, donde se eliminaron de base los depredadores y se redujo considerablemente el estrés ambiental. Destacamos que, aunque no son concluyentes por ser un solo individuo, nuestros resultados de VR en humanos no presentan diferencias con el paciente donante y son comparables con los de (Medina, 1997), que reportó en pacientes con cáncer gástrico una pD2 de 5.5±0.1 y una Emax 110±5 % de KCl 100 mM. Esto sugiere

que el control vascular α1 adrenérgico preserva su función independiente de la influencia inflamatoria o cancerosa.

Los humanos reducen la vasodilatación colinérgica dependiente del endotelio en comparación con conejos y ratas

En los resultados de relajación, la RV a CCh mostró diferencias entre conejo y rata con relación al humano y el cerdo, siendo evidente la ganancia de dilatación a CCh conejos y ratas luego de su separación con los humanos. Al ser conejo y rata los modelos más recurrentes en investigación vascular hay suficientes trabajos que describen y concuerdan con la relajación a CCh mencionada previamente (Chiba, 1990; Wu, 1997; Fujimoto, 2001; Angulo, 2019; Harry, 2019). No hemos encontrado bibliografía sobre la VR a CCh en circulación mesentérica de cerdo, sin embargo, es evidente que el comportamiento vascular de este modelo es diferente al de conejos y ratas y comparable con la VR en humanos. Nuestros resultados en humanos coinciden con lo mostrado por (Hall, 2006) y (Tottrup, 2004) quienes reportan ausencia de relajación a CCh en mesentéricas humanas, soportando la idea de que la débil relajación a CCh en cerdos y humanos es un mecanismo preservado a lo largo de su evolución.

La vasodilatación dependiente del endotelio a bradikinina es la vía de control vascular mejor conservada entre los modelos

En la VR a BK no se evidenciaron diferencias estadísticas entre el humano y los demás modelos animales. Estos resultados son similares a los reportados por (Liu, 2006) en ratas Sprague-Dawley (pD2: ±7.4; Emax: ±90%) y (Churchill, 1986) en conejos Nueva Zelanda (pD2: ±7.2; Emax: ±90%). En cerdos Yorkshire se reportó una VR con mayor sensibilidad, pero con la misma eficacia (Ohgushi, 1993), esta diferencia en sensibilidad probablemente esté dada por la raza del animal o su alimentación. No obstante, nuestros resultados indican que la VR a BK es un mecanismo preservado y comparable entre estas especies. Complementariamente, (Törnebrandt, 1987; Chadha, 2010), en arterias mesentéricas de pacientes, reportaron menor sensibilidad y la misma eficacia a BK (pD2: >8; Emax: >80%).

Estas diferencias en sensibilidad podrían deberse a la condición fisiopatológica de los pacientes utilizados, en el grupo evaluado por (Törnebrandt, 1987), las arterias fueron de pacientes con cáncer gástrico e intestinal y en (Chadha, 2010), el 70% de los pacientes fueron tratados para CAc, Esto indicaría que los tumores indujeron mayor sensibilidad a BK, probablemente mejorando con ello la irrigación hacia el tumor. Se debe destacar que, a pesar de tener el mismo mecanismo de relajación, la VR a BK es contrastante con la VR a CCh, donde no se encontró mayor similitud entre la VR en humanos y cerdos comparados con conejos y ratas, esto sugiere que esta ganancia en relajación compensa desde la respuesta colinérgica la ganancia en contracción mostrada en conejos y ratas.

La señalización β-adrenérgica es menor en humanos y cerdos que en conejos y ratas

En humanos y cerdos hay menor VR a isoproterenol (Emax y pD2) comparadas con conejos y ratas. La mayor VR en conejos y ratas se podría explicar por la mayor expresión del receptor β2 en la túnica media. Esta mayor VR en el modelo murino concuerda con lo reportado por (Briones, 2005), quien presentó una VR con mayor sensibilidad y similar eficacia a isoproterenol (pD2: 7.7±0.1; Emax: 97.2±0.7%), y estableció que la relajación β adrenérgica en mesentérica de rata, está dada principalmente por los receptores presentes en el músculo liso. A su vez, varios trabajos han reportado VR a isoproterenol en circulación mesentérica de conejo, con eficacias comparables a las encontradas en nuestro trabajo (60-80% de relajación) (Brodde, 1981; Itoh, 1985; Wilson 1993). Lo anterior, asociado con los resultados de PE permite establecer que el control del tono vascular en circulación mesentérica de conejo y rata es principalmente adrenérgico y no es comparable con el humano. Por otro lado, en cerdos anestesiados, (Molinari, 1999) reportó que isoproterenol induce vasodilatación en el lecho mesentérico. No obstante, al ser realizado en un modelo *in vivo*, sus resultados no son necesariamente comparables con los nuestros. Complementariamente, las diferencias entre humanos y cerdos podrían deberse a una disminución en función del receptor β2 producto del envejecimiento en los pacientes, esto debido a que reportamos en aorta de conejo que durante el envejecimiento hay una reducción de la VR a isoproterenol asociado con aumento en la expresión del receptor β2 como mecanismo compensatorio (Cupitra, 2020). Esto implicaría que se están subestimando

los niveles de expresión en cerdo, conejo y rata al compararse con pacientes relativamente más viejos.

Con lo anterior es posible determinar que las diferencias biológicas a nivel vascular están fuertemente definidas entre conejos y ratas frente a los humanos y cerdos. Estableciendo a su vez que la VR en cerdo, conejo y rata no es completamente comparable con el humano en contracción o relajación vascular, aunque el modelo más comparable es el cerdo. Complementariamente, nuestros resultados en cerdos y conejos, y otras experiencias como las de Sakai, 2003; Herrera, 2008; Llanos, 2012 que utilizaron en ovejas y llamas como modelos vasculares, demuestran que los animales de granjas tecnificadas pueden ser modelos vasculares reproducibles, comparables y económicos en el estudio de la fisiología vascular humana.

Limitaciones

En el presente trabajo la edad de estos animales no es exactamente comparable con las arterias humanas, sin embargo, en los trabajos de (Ohgushi, 1993), (Greenberg, 2017) y (Morita, 2014) se utilizaron cerdos (4–6 meses), conejos (4–5 meses) y ratas (2-3 meses) como modelos vasculares, con edad comparable con la utilizada en esta investigación. El conejo es el único modelo usado en este estudio que fue sacrificado en las instalaciones de la universidad, aunque fueron mantenidos en bioterio por 5 días para que se acostumbraron al ambiente, no podemos asegurar que el estrés generado por el transporte e instalación en el bioterio no haya inducido cambios en la VR o expresión de receptores. Debido a la emergencia sanitaria por COVID-19 fue restringido el acceso arterias humanas lo que no nos permite realizar nuevos experimentos para aumentar la potencia estadística en humanos.

Conclusión

Los modelos vasculares cerdo, conejos y rata no son completamente comparables al humano, sin embargo, los cerdos presentan la mayor comparabilidad dado que no presentaron diferencias vasculares frente a los humanos. Además, las marcadas diferencias entre el grupo de humanos y cerdos frente a conejos y ratas, sugiere que estas diferencias

vasculares se deben a una ganancia de función adrenérgica y colinérgica en los conejos y las ratas luego de separarse evolutivamente de los humanos hace 60 millones de años.

Agradecimientos

Queremos agradecer a Supercerdo Paisa SAS por la donación de arterias de cerdo. El proyecto “Formación de Talento Humano de Alto Nivel” aprobado por el Fondo de Ciencia, Tecnología e Innovación (CTeI) del Sistema General de Regalías (SGR) -BPIN: 2013000100103, Gobernación de Tolima y Universidad del Tolima, Colombia, para el apoyo al NIC; Proyecto 2581 Becas CODI Universidad de Antioquia; y a la Fundación para el Fomento de la Investigación y la Tecnología, Banco de la República de Colombia, convenio 201619/2017.

Bibliografía

Angulo J, El Assar M, Sevilleja-Ortiz A, Fernández A, Sánchez-Ferrer A, Romero-Otero J, Martínez-Salamanca JI, La Fuente JM, Rodríguez-Mañas L (2019). Short-term pharmacological activation of Nrf2 ameliorates vascular dysfunction in aged rats and in pathological human vasculature. A potential target for therapeutic intervention. Redox Biol. 26:101271. doi: 10.1016/j.redox.2019.101271. Epub 2019 Jul 5. PMID: 31302408; PMCID: PMC6626891.

Asano M, Hidaka H (1983). Potentiation in various agonists-induced contractions of rabbit mesenteric artery by sulfhydryl reagents. Jpn J Pharmacol. 33(1):145-154. doi:10.1254/jjp.33.145

Briones, A. M., Daly, C. J., Jimenez-Altayo, F., Martinez-Revelles, S., Gonzalez, J. M., McGrath, J. C., & Vila, E. (2005). Direct demonstration of β1-and evidence against β2-and β3-adrenoceptors, in smooth muscle cells of rat small mesenteric arteries. British journal of pharmacology, 146(5), 679-691.

Brodde, O. E., Meyer, F. J., Schemuth, W., & Freistühler, J. (1981). Demonstration of specific vascular dopamine receptors mediating vasodilation on the isolated rabbit mesenteric artery. Naunyn-Schmiedeberg's archives of pharmacology, 316(1), 24-30.

Buchinger-Kähler V, Stoldt VR, Muth T, Schipke JD. Function and viability of vessels in different preservation solutions-an experimental study on human great saphenous veins. J Angiol Vasc Surg. 2016;1(003):1–7. doi:10.24966/AVS-7397/100003

Chadha, P. S., Liu, L., Rikard-Bell, M., Senadheera, S., Howitt, L., Bertrand, R. L., … Sandow, S. L. (2010). Endothelium-Dependent Vasodilation in Human Mesenteric Artery Is Primarily Mediated by Myoendothelial Gap Junctions Intermediate Conductance Calcium-Activated K+ Channel and Nitric Oxide. Journal of Pharmacology and Experimental Therapeutics, 336(3), 701–708. doi:10.1124/jpet.110.165795

Chiba, Y., Mikoda, N., Kawasaki, H., & Ito, K. (1990). Endothelium-dependent relaxant action of platelet activating factor in the rat mesenteric artery. Naunyn-Schmiedeberg's Archives of Pharmacology, 341-341(1-2). doi:10.1007/bf00195060

Choppin A, O'Connor SE (1995). Presence of vasoconstrictor 5HT1-like receptors revealed by precontraction of rabbit isolated mesenteric artery. Br J Pharmacol.

Chorro, F. J., Such-Belenguer, L., & López-Merino, V. (2009). Animal models of cardiovascular disease. Revista Española de Cardiología (English Edition), 62(1), 69-84.

Churchill, L., & Ward, P. E. (1986). Relaxation of isolated mesenteric arteries by des-Arg9-bradykinin stimulation of B1 receptors. European journal of pharmacology, 130(1-2), 11-18.

Cupitra NI, Calderón JC, Narvaez-Sanchez R. Increased receptor expression supports vascular reactivity of the rabbit aorta during preservation. Eur J Cardiothorac Surg. 2020A Nov 14:ezaa386. doi: 10.1093/ejcts/ezaa386. Epub ahead of print. PMID: 33188691.

Cupitra NI, Calderón JC, Narvaez-Sanchez R. Influence of Ageing on Vascular Reactivity and Receptor Expression in Rabbit Aorta: A Complement to Elastocalcinosis and Smooth Muscle Mechanisms. Clin Interv Aging. 2020B Apr 20;15:537-545. doi: 10.2147/CIA.S236173. PMID: 32368020; PMCID: PMC7182455.

Estrada O, González-Guzmán JM, Salazar-Bookaman M, Fernández AZ, Cardozo A, Alvarado-Castillo C (2011). Pomolic acid of Licania pittieri elicits endothelium-dependent relaxation in rat aortic rings. Phytomedicine.

Field, F. P., & Soltis, E. E. (1985). Vascular reactivity in the spontaneously hypertensive rat. Effect of high pressure stress and extracellular calcium. Hypertension, 7(2), 228–235. doi:10.1161/01.hyp.7.2.228

Fujimoto, S., Asano, T., Sakai, M., Sakurai, K., Takagi, D., Yoshimoto, N., & Itoh, T. (2001). Mechanisms of hydrogen peroxide-induced relaxation in rabbit mesenteric small artery. European Journal of Pharmacology, 412(3), 291–300. doi:10.1016/s0014-2999(00)00940-7

Gao YJ, Lee RM (2001). Hydrogen peroxide induces a greater contraction in mesenteric arteries of spontaneously hypertensive rats through thromboxane A2 production. Br J Pharmacol.

González-Luis, G., Pérez-Vizcaíno, F., García-Muñoz, F. et al (2005). Age-Related Differences in Vasoconstrictor Responses to Isoprostanes in Piglet Pulmonary and Mesenteric Vascular Smooth Muscle. Pediatr Res 57, 845–852. https://doi.org/10.1203/01.PDR.0000161411.01208.83

Greenberg HZE, Carlton-Carew SRE, Khan DM, Zargaran AK, Jahan KS, Vanessa Ho W-S, et al (2017). Heteromeric TRPV4/TRPC1 channels mediate calcium-sensing receptor-induced nitric oxide production and vasorelaxation in rabbit mesenteric arteries. Vascul Pharmacol [Internet]. Elsevier; 96–98:53–62. Available from: https://www.sciencedirect.com/science/article/pii/S1537189117301453

Hall, J., Jones, T. H., Channer, K. S., & Jones, R. D. (2006). Mechanisms of agonist-induced constriction in isolated human mesenteric arteries. Vascular Pharmacology, 44(6), 427–433. doi:10.1016/j.vph.2006.02.004

Harry Z.E. Greenberg, Simonette R.E. Carlton-Carew, Alexander K. Zargaran, Kazi S. Jahan, Lutz Birnbaumer & Anthony P. Albert (2019). Heteromeric TRPV4/TRPC1 channels mediate calcium-sensing receptor-induced relaxations and nitric oxide production in mesenteric arteries: comparative study using wild-type and TRPC1−/- mice, Channels, 13:1, 410-423, DOI: 10.1080/19336950.2019.1673131

Herrera, E. A., Reyes, R. V., Giussani, D. A., Riquelme, R. A., Sanhueza, E. M., Ebensperger, G., ... & Pulgar, V. M. (2008). Carbon monoxide: a novel pulmonary artery vasodilator in neonatal llamas of the Andean altiplano. Cardiovascular research, 77(1), 197-201.

Itoh, T., Sasaguri, T., Makita, Y., Kanmura, Y., & Kuriyama, H. (1985). Mechanisms of vasodilation induced by vasoactive intestinal polypeptide in rabbit mesenteric artery. American Journal of

Physiology-Heart and Circulatory Physiology, 249(2), H231–H240. doi:10.1152/ajpheart.1985.249.2.h231

Kozłowska H, Schlicker E, Kozłowski M, Siedlecka U, Laudański J, Malinowska B. Ligands at β2-, β3-, and the low-affinity state of β1-adrenoceptors block the α1- adrenoceptor-mediated constriction in human pulmonary and rat mesenteric arteries. J Cardiovasc Pharmacol. 2005;

Liu, C., Huang, Y., Ngai, C. et al (2006). TRPC3 is involved in flow- and bradykinin-induced vasodilation in rat small mesenteric arteries. Acta Pharmacol Sin 27, 981–990. https://doi.org/10.1111/j.1745-7254.2006.00354.x

Llanos, A. J., Ebensperger, G., Herrera, E. A., Reyes, R. V., Cabello, G., Díaz, M., ... & Parer, J. T. (2012). The heme oxygenase–carbon monoxide system in the regulation of cardiorespiratory function at high altitude. Respiratory physiology & neurobiology, 184(2), 186-191.

McAllister RM, Kimani JK, Webster JL, Parker JL, Laughlin MH (1985). Effects of exercise training on responses of peripheral and visceral arteries in swine. J Appl Physiol . 80(1):216-25. doi: 10.1152/jappl.1996.80.1.216. PMID: 8847306.

Medina P, Noguera I, Aldasoro M, Vila JM, Flor B, Lluch S (1997). Enhancement by vasopressin of adrenergic responses in human mesenteric arteries. Am J Physiol.

Molinari, C., Battaglia, A., Grossini, E., Mary, D. A. S. G., Surico, N., & Vacca, G. (1999). The role of β2-adrenergic vascular receptors in the peripheral vasodilation caused by 17β-estradiol in anesthetized pigs. Life Sciences, 65(15), 1545–1552. doi:10.1016/s0024-3205(99)00399-9

Morita T, Okada M, YAmawaki H (2014). Mechanisms Underlying a Decrease in KCl-Induced Contraction after Long-Term Serum-Free Organ Culture of Rat Isolated Mesenteric Artery. J Vet Med Sci.

Ohgushi, M., Yasue, H., Kugiyama, K., Murohara, T., & Sakaino, N. (1993). Contraction and endothelium dependent relaxation via a adrenoceptors are variable in various pig arteries. Cardiovascular research, 27(5), 779-784.

Ricciotti, E., & FitzGerald, G. A. (2011). Prostaglandins and inflammation. Arteriosclerosis, thrombosis, and vascular biology, 31(5), 986-1000.

Russell JC, Proctor SD (2006). Small animal models of cardiovascular disease: tools for the study of the roles of metabolic syndrome, dyslipidemia, and atherosclerosis. Cardiovascular Pathology.

Sakai, A., Matsumoto, T., Saitoh, M., Matsuzaki, T., Koizumi, T., Ishizaki, T., ... & Wang, X. Q. (2003). Cardiopulmonary hemodynamics of blue-sheep, Pseudois nayaur, as high-altitude adapted mammals. The Japanese journal of physiology, 53(5), 377-384.

Törnebrandt, K., Nobin, A., & Owman, C. (1987). Contractile and dilatory action of neuropeptides on isolated human mesenteric blood vessels. Peptides, 8(2), 251–256. doi:10.1016/0196-9781(87)90099-4

Tottrup A, Kraglund K (2004). Endothelium-dependent responses in small human mesenteric arteries. Physiol Res. 53(3):255-63. PMID: 15209532.

Trachte GJ, Stein EA (1989). Thromboxane receptor agonists enhance adrenergic neurotransmission in rabbit isolated mesenteric arteries. J Pharmacol Exp Ther. 249(1).

Upham, N. S., Esselstyn, J. A., & Jetz, W. (2019). Inferring the mammal tree: Species-level sets of phylogenies for questions in ecology, evolution, and conservation. PLoS biology, 17(12), e3000494.

Virmani R, Kolodgie FD, Farb A, Lafont A (2003). Drug eluting stents: are human and animal studies comparable? Heart [Internet]. BMJ Publishing Group Ltd; 89(2):133–8. Available from: http://www.ncbi.nlm.nih.gov/pubmed/12527658

WHO (2020). Cardiovascular diseases (CVDs). WHO [Internet]. World Health Organization; [cited 2020 Sep 18]; Available from: https://www.who.int/cardiovascular_diseases/en/

Wilson AJ, Warren JB (1993). Adenylate cyclase-mediated vascular responses of rabbit aorta, mesenteric artery and skin microcirculation. Br J Pharmacol. 110(2):633-8. doi: 10.1111/j.1476-5381.1993.tb13858.x. PMID: 7902177; PMCID: PMC2175949.

Wu, Chin-Chen; Chen, Shiu-Jen; Yen, Mao-Hsiung (1997) Loss of Acetylcholine-Induced Relaxation by M3-Receptor Activation in Mesenteric Arteries of Spontaneously Hypertensive Rats, Journal of Cardiovascular Pharmacology: Volume 30 - Issue 2 - p 245-252

Zaragoza, C., Gomez-Guerrero, C., Martin-Ventura, J. L., Blanco-Colio, L., Lavin, B., Mallavia, B., ... & Egido, J. (2011). Animal models of cardiovascular diseases. Journal of Biomedicine and Biotechnology.

Tablas.

Tabla 1. Respuesta vascular en arteria mesentérica de humanos, cerdos, conejos y ratas a la estimulación con KCl, FE, U46619, CCH, BK e isoproterenol.

Agonist	pD2					Emax (%KCl 40mM)				
	Human	Pig	Rabbit	Rat	p	Human	Pig	Rabbit	Rat	p
KCl	1.63±0.07	1.58±0.03	1.5±0.03	1.7±0.03	0.29	127.9±10	136±7.2	191±14.4	127.5±8.1	0.0002[α]
U46619	7.05±0.17	6.6±0.07	6.3±0.05	7.1±0.4	0.055	128.6±8.5	113.6±16	54.75±25.6	135±9.3	0.02[δ]
PE	5.68±0.1	5.82±0.09	5.35±0.2	6,1±0.2	0,058	95.9±14	132.8±16.7	176.5±32	208±13	0.02[δ]
CCh[a]	6.48±0.14	5.93±0.17	6.3±0.38	6.7±0.2	00.57	1.3±8	-8±8.4	94,6±4.5	105±7.5	0.0001[γ]
BK[a]	6.6±0.25	7.3±0.33	6.9±0.6	6.4±0.26	0.06	96.4±17	86±7.5	98.5±4.03	82.2±5.8	0.3
Isoproterenol[a]	7.36±0.12	6.36±0.17	7.5±0.03	6.8±0.28	0.005[λ]	13.6±3.6	27.4±9.9	76.4±7.7	87.4±7.3	0.0001[γ]

M: Concentración molar. [a]% de relajación en relación con la precontracción con U46619 en humanos y cerdos o PE en conejos y ratas. Resultados en media±SEM. δ indica una efectividad menor (Emax) para KCl o menor para U46619 en conejos en comparación con humanos; γ indica mayor Emax a PE, CCh o isoproterenol en conejos y ratas, en comparación con humanos; λ menor sensibilidad al isoproterenol en arterias de cerdo en comparación con humanos. Oneway ANOVA seguido del post-hoc de Dunnett, nivel de significancia P <0,05.

Tabla 2. Cuantificación de la expresión de receptores TP, α1 y β2 en arteria mesentérica de humanos, cerdos, conejos y ratas.

Receptor	Tunica	Human	Pig	Rabbit	Rat	p
TP	Intima	1±0.09	1.2±0.13	0.9±0.16	1.07±0.11	0.42
	Media	1±0.11	1.13±0.14	0.6±0.16	0.8±0.1	0.06
	Adventitia	1±0.14	1.07±0.11	0.9±0.14	0.85±0.18	0.75
α1	Intima	1±0.08	1.27±0.15	1.43±0.12	1.13±0.2	0.24
	Media	1±0.18	1.5±0.3	2.5±0.23	2.38±0.28	0.0014[γ]
	Adventitia	1±0.17	1.36±0.2	1.03±0.12	1.08±0.22	0.11
β2	Intima	1±0.07	0.65±0.11	1.39±0.13	1.38±0.14	0.09
	Media	1±0.11	1.3±0.14	1.6±0.08	1.6±0.12	0.009[γ]
	Adventitia	1±0.16	0.9±0.16	0.9±0.16	0.75±0.16	0.7

La expresión de los receptores se normalizó con respecto a los humanos. Los valores humanos se promediaron y normalizaron en base a este promedio. Resultados en media±SEM. γ indica mayor expresión en arterias de conejo y rata en comparación con los humanos. Oneway-ANOVA seguido del post-hoc de Dunnett, nivel de significancia P <0,05.

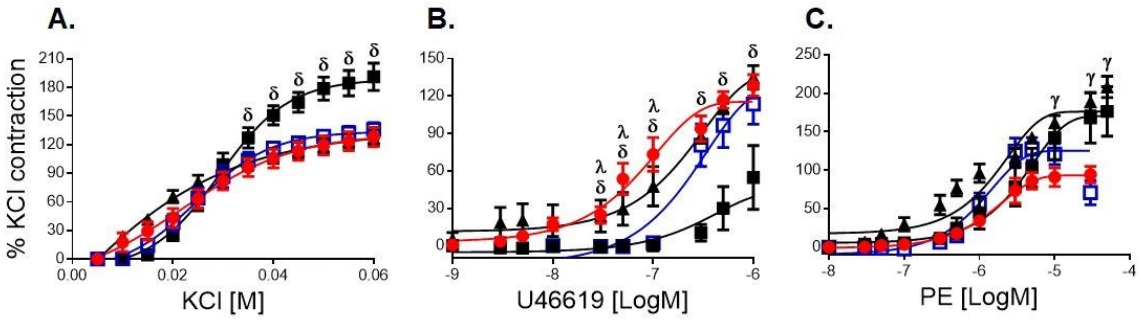

Figura 1. Curvas de concentración-respuesta a KCl (A), U46619 (B) y PE (C). Humano (●, 5 pacientes, 10 anillos), cerdo (□, 5,10), conejo (■, 5,10) y rata (▲, 5,10). δ indica mayor Emax a KCl o pD2 y Emax más bajos a U46619 en conejos, en comparación con los humanos. λ indica una menor sensibilidad al U46619 en cerdos en comparación con los humanos. γ indica mayor Emax a PE en conejos y ratas en comparación con los humanos.
Oneway-ANOVA seguido del post-hoc de Dunnett, nivel de significancia P <0,05.

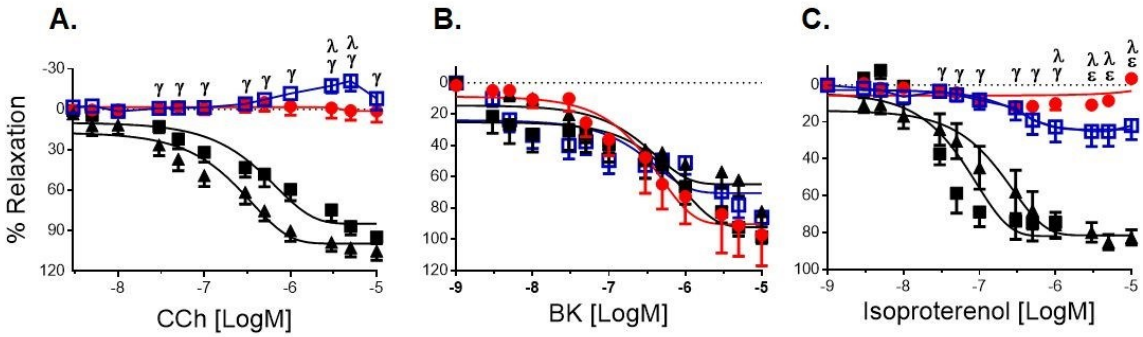

Figura 2. Curvas de concentración-respuesta a CCh (A), BK (B) e isoproterenol (C). Humano (●, 5 pacientes, 10 anillos), cerdo (□, 5,10), conejo (■, 5,10) y rata (▲, 5,10). γ indica mayor sensibilidad y eficacia a CCh o mayor pD2 a isoproterenol en conejos y ratas en comparación con los humanos. λ indica menor sensibilidad a CCh o menor efectividad a BK o pD2 y mayor Emax a isoproterenol en cerdos en comparación con humanos. ξ indica mayor eficacia del isoproterenol en ratas, en comparación con los humanos. Oneway ANOVA seguido del post-hoc de Dunnett, nivel de significancia P <0,05.

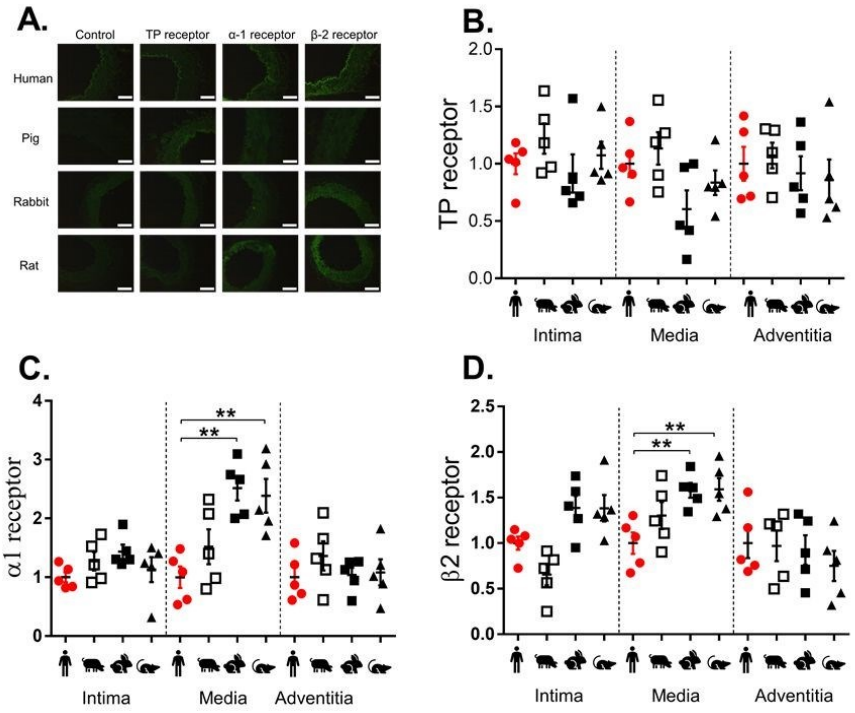

Figura 3. Cuantificación de la expresión proteica de los receptores tromboxano A2 (TP), α1 y β2 en arteria mesentérica de humanos (), cerdos (), conejos () y ratas (). A, imágenes representativas de inmunofluorescencia para identificar receptores TP, α1 y β2. B, C y D, cuantificación de la fluorescencia de los receptores TP, α1 y β2, respectivamente, en las túnicas de la pared mesentérica. El número de experimentos es cinco en todos los casos. (A) La longitud de las barras de calibración del blanco es equivalente a 100 µm. Oneway-ANOVA seguido del post-hoc de Dunnett, * indica $p<0,05$. ** indica $p<0,01$. La expresión se normalizó con los humanos.

Capítulo cinco:

Cupitra NI; León-Rodríguez JP; Calderón JC; Narvaez-Sanchez R, 2020. Mecanismos de adaptación en remodelamiento y reactividad vascular en arterias que irrigan tumores en cáncer de colon en humanos

Mecanismos de adaptación en remodelamiento y reactividad vascular en arterias que irrigan tumores en cáncer de colon en humanos

Nelson Ivan Cupitra[1]; Jimmy Paúl León[2]; Juan C. Calderón[1]; Raul Narvaez-Sanchez[1]*

1Physiology and Biochemistry Research Group-PHYSIS, Faculty of Medicine, University of Antioquia, Medellín, Colombia
2Department of Surgery, Faculty of Medicine, University of Antioquia.
E-mail address: raul.narvaez@udea.edu.co (R. Narvaez-Sanchez).
URL: http://www.udea.edu.co/physis

Introducción

El cáncer (CA) es una forma de crecimiento anormal de las células que genera múltiples complicaciones en los sistemas biológicos. Según la Organización Mundial de la Salud, es la segunda causa de muerte en el planeta. Uno de los CA más comunes en la población es el cáncer de colon (CAc), ocupando el cuarto lugar en incidencia (19.7 por cada 100.000 hab.) y tercero en mortalidad (8.9 por cada 100.000 hab.) a nivel mundial, y el tercero de mayor incidencia en Colombia (15.8 por cada 100.000 hab.; WHO, 2020). Como tratamiento para el CAc se utiliza cirugía, que remueve el tumor, radioterapia, que emplea radiaciones ionizantes, y/o quimioterapia, que utiliza fármacos para atacar las células cancerosas, sin embargo, por la complejidad celular en los tumores sólidos en estadios intermedios y avanzados del CAc u otros cánceres, es frecuente que estos tratamientos sean poco eficaces llevando a una recaída de la enfermedad o la muerte (Wagland, 2016).

Al identificar las diferencias funcionales de los vasos en cáncer una posible estrategia farmacológica podría enfocarse en promover vasoconstricción en el tumor, reduciendo el suministro de nutrientes y el crecimiento tumoral; o estimulando vasodilatación para aumentar el flujo sanguíneo, coadyuvando en quimioterapia para que los fármacos mejoren su perfusión en células cancerosas y mejore la respuesta al tratamiento (Sonveaux, 2008).

Una alternativa para caracterizar el comportamiento vascular en cáncer es comparar la respuesta al estímulo de agonistas fisiológicamente endógenos que a su vez participen en el desarrollo tumoral. Algunos ejemplos de la función de estos agonistas sobre el cáncer se presentan a continuación: se han reportado sobre cultivos celulares, cambios en los niveles de expresión en la señalización beta-adrenérgica asociados con crecimiento y metástasis, en cáncer de cerebro, pulmón, riñón, mama ovario y próstata; modulando la función de miocitos, adipocitos, fibroblastos y pericitos en tumores (Cole, 2012). A su vez, se ha relacionado la señalización de tromboxano A2como intermediaria en migración y angiogénesis en cáncer colorrectal y de mama (Sakai, 2006) y endotelina-1 como inductor de proliferación, angiogénesis, osteogénesis y supervivencia tumoral en cáncer de ovario, pulmón, hígado, próstata entre otras (Rosanò, 2013). De igual manera otros agonistas de dilatación vascular como acetilcolina, bradikinina (BK), se han reportado como inductores de proliferación, inflamación, crecimiento, y migración tumoral (Maeda, 1996; Stewart, 2006). También se ha reportado que el factor de crecimiento vascular endotelial (VEGF) además de ser potente inductor de proliferación, y angiogénesis en cáncer, es inductor de vasodilatación en circulación pulmonar (Olsson, 2006; Rapisarda 2012). Sin embargo, pese a que en estos trabajos se establece su participación en el desarrollo en cáncer de colon y otros tipos de cáncer, en ninguno de ellos se evalúan los cambios en la VR de estos agonistas. Tomando como modelo cáncer de colon, por su alta incidencia y mortalidad en la población, y por la facilidad quirúrgica de obtener la vasculatura que irriga sus tumores. consideramos necesario determinar las adaptaciones vasculares en remodelación y reactividad vascular (VR) inducidas por estos tumores.

El presente trabajo propone cuantificar la remodelación en histología, VR, expresión de receptores y determinar sus mecanismos en arterias de tumores de colon comparadas con arterias no tumorales en humanos. En VR se compara la contracción independiente de receptor con KCl; dependiente de receptor con fenilefrina (PE), ET-1, y U-46619 (análogo de tromboxano A2); y relajación dependiente de receptor con VEGF, isoproterenol, BK y Carbacol (CCh, análogo de acetilcolina).

Materiales y métodos

Modelo animal y reactivos

Los ensayos en humanos fueron aprobados por el Comité de Bioética de la Facultad de Medicina de la Universidad de Antioquia (Medellín, Colombia) de acuerdo con la declaración de Helsinki, y la resolución 8430 de 1993 "Normas científicas, técnicas y administrativas para la investigación en salud". Los segmentos arteriales fueron obtenidos en la Clínica León XIII: A. trece pacientes no tumorales de 46±9 años, seis mujeres y siete hombres. Cuatro pacientes fueron colectomizados por diverticulitis, cinco por obstrucción por bridas, tres por traumatismo y uno por donación de órganos. B. Veinticinco pacientes con diagnóstico de adenocarcinoma de CAc, 15 mujeres y 10 hombres. Las muestras fueron colectadas de 10 de marzo de 2017 al 19 de septiembre de 2020.

Disección

Se obtuvieron segmentos arteriales humanos de pacientes en quirófanos y se almacenaron durante dos horas en solución de Krebs-Henseleit (HK), con la siguiente composición (mM): NaCl, 118; KCl, 4,7; KH_2PO_4, 1,2; $MgSO_4$, 1,2; $NaHCO_3$, 25,0; glucosa, 11,1; $CaCl_2$, 2,5; pH 7 a 4 °C. Las ramas mesentéricas se disecaron de 0.5-1 mm de diámetro interno. Se disecaron rápidamente y se conservó la solución de HK. Se eliminó el exceso de tejido periférico y se cortó en 10 anillos de 3-5 mm de longitud. Se utilizaron cuatro anillos para experimentos de relajación y contracción. Se conservaron cuatro anillos durante 24 horas en solución HK previamente burbujeada con gas carbonatado (95% O_2-5% CO_2) a 4 °C y se usaron solo para estudios de contracción. Nuestro grupo demostró que no hay diferencias en la reactividad vascular a fenilefrina y carbacol a las 24 horas de conservación en solución en Krebs a 4 °C (Cupitra, 2020A). Los dos anillos restantes se incrustaron en Shandon Cryomatrix (Thermo Fisher Scientific, EE. UU.) y se congelaron en nitrógeno líquido para inmunohistoquímica. Resultados previos de nuestro laboratorio mostraron que en este tipo de ensayo no hay diferencia significativa con respecto a las muestras frescas (Cupitra, 2020B).

Reactividad vascular

Los anillos fueron montados en un baño de órganos LE13206 PANLAB (Barcelona, España) de 10 ml con HK a 37 °C y burbujeo con carbogen, como se describe en (Cupitra, 2020B). La respuesta contráctil se digitalizó con Powerlab PL-3504 (Sydney, Australia) y se analizó en el módulo de respuesta a dosis del software LabChart 8. Cada preparación se estabilizó a 2 g de tensión en reposo durante 90 minutos antes de iniciar los estímulos agonistas; durante este período, la solución de HK se reemplazó cada 20 minutos. Después de la estabilización, el anillo arterial se estimuló dos veces con KCl 40 mM, registrando la respuesta durante 10 minutos y se lavó por 20 minutos entre cada estímulo. Luego, se aplicó al baño U46619 300 nM en humanos y cerdos o PE 30 µM en conejos y ratas, seguido de BK 10 µM para humanos y cerdos o CCh 10 µM para conejos y ratas para confirmar la presencia del endotelio; esto se realizó para todos los anillos arteriales. Luego, se aplicó una dosis única de KCl 40 mM; dosis acumulativa de KCl 5 a 60 mM; dosis acumulativa de U46619 0,1 nM a 1 µM, y dosis acumulativa de PE 10 nM a 100 µM. Los estudios de relajación se realizaron con anillos precontraídos de U46619 300 nM (humanos y cerdos) o PE 10 µM (conejos y ratas), usando CCh 1 nM a 10 µM; isoproterenol 1 nM a 10 µM y BK 1 nM a 10 µM. La VR a CCh e isoproterenol se midió sólo en relajación y se suspendió al inicio de la contracción porque la precontracción podría haber afectado está VR contráctil.

Histología e Inmunofluorescencia

Las arterias congeladas se cortaron en secciones de 10 µm de espesor y se separaron en dos grupos. Los cortes del primer grupo fueron fijados con Carnoy y el análisis histológico se realizó por el método de hematoxilina & eosina. Las arterias del segundo grupo se fijaron en acetona, se permeabilizaron con Triton X-100 al 0,1% y se bloquearon con albúmina de suero bovino al 5% en solución salina tamponada con fosfato. Se incubaron diferentes secciones con los siguientes anticuerpos primarios a 4 °C durante la noche (todos diluidos 1:1000 (humanos, cerdos y ratas) o 1:1500 (conejos) en solución de bloqueo): receptor adrenérgico anti-α1 (3462, Abcam), receptor anti-β2 adrenérgico (AB61778, Abcam), receptor anti-tromboxano A2 (TP)(233288, Abcam); NF-kB (16502, Abcam); PTEN (32199,

Abcam); GSK3 (15314, Abcam); ETA (85163, Abca); ETB (129102, Abcam); VEGFR1 (2893, Cell signaling), VEGFR2 (2472, Cell signaling). Después del lavado, los anillos se incubaron con anticuerpo secundario anti-conejo conjugado con Alexa Fluor 488 (verde, 1:800 en solución de bloqueo; AB150077, Abcam) a temperatura ambiente durante 2 horas. Como control, una sección de cada grupo experimental no se incubó con un anticuerpo primario, solo se incubó con un anticuerpo secundario. Las imágenes se obtuvieron utilizando un microscopio invertido de fluorescencia (Axio Observer A1, Carl Zeiss), una lámpara de mercurio (HXP120, Carl Zeiss), un filtro de emisión de fluorescencia en rojo (64 HE MPLUM, Carl Zeiss; ventana de emisión 647/70 nm) y un filtro de emisión de fluorescencia en verde (488009-9901, Carl Zeiss; ventana de emisión >515 nm). La evaluación de las imágenes se realizó con un objetivo de 20X. Se utilizó ImageJ v1.52a para procesar las imágenes utilizando la herramienta Split channels en imágenes RGB, cuantificando la intensidad promedio del rojo o verde en 3 regiones de interés de la íntima, media y adventicia para cada imagen.

Análisis estadístico

El número de experimentos se muestra cómo (#pacientes, #anillos). En el procesamiento de resultados se utilizaron datos completos, las variables son continuas. Los resultados se presentan como curvas de concentración-respuesta y gráficos de puntos con media±SEM. Los supuestos de normalidad se confirmaron con las pruebas de D'Agostino-Pearson y Shapiro-Wilk. Las curvas de concentración-respuesta se ajustaron con una regresión no lineal utilizando un modelo sigmoidal de cuatro parámetros (4PL) con fórmula Y=Bottom+(Top-Bottom)/(1+10^((LogIC50-X)*HillSlope)), donde Top muestra la Emax y el Log10 negativo de la concentración molar que produce el 50% de la respuesta máxima refleja la sensibilidad (pD2). Se analizaron pD2, Emax y la cuantificación de la expresión del receptor en la íntima, media y adventicia con un ANOVA de una vía seguido de la prueba post hoc de Dunnett. Las curvas de concentración-respuesta se analizaron con un ANOVA de dos vías seguido de la prueba post-hoc de Dunnett que compara modelo/concentración.

Las diferencias se consideraron estadísticamente significativas a p<0,05. Se utilizó el paquete estadístico GraphPad Prism 7 v7.0.

Resultados

Antropometría

Los pacientes con cáncer (CA) tenían una edad promedio de 67±3.1 años, fueron diagnosticados con adenocarcinoma predominante en colon derecho, cuya patología arrojó pT3N0, pT3N1 y pT4N0 en el 80% de los casos (Tabla 1). En nueve de estos pacientes había concomitante hipertensión arterial, en seis había tabaquismo por más de 10 años y en dos había hipercolesterolemia. Los pacientes sin patología tumoral (NT) tenían edad de 49±5 años. Uno solo presentó hipertensión arterial y uno manifestó tabaquismo por más de 10 años. Solo uno de los pacientes fue donante de órganos por muerte cerebral.

Histología

A nivel morfológico se evidenció hiperplasia en las túnicas media (NT, 121.6±5.1 µm; ET, 162.5±6.3 µm; TU, 176.6±7.7 µm; p=0.0001; fig. 1A-B) y en la íntima (NT, 18.5±3.6 µm; ET, 66.8±12.7 µm; TU, 101.2±15.3 µm; p=0.002; fig. 1A-C).

Reactividad vascular

Contracción

Se encontraron diferencias significativas en sensibilidad a KCl (pD2: NT, 1.6±0.04; ET, 1.8±0.02; TU, 1.8±0.03, p=0.02; Tabla 2; fig. 2A). No se encontraron diferencias en la VR a ET-1 (p>0.05; Tabla 2; fig. 2B). Al estímulo con PE aumentó la pD2 (pD2: NT, 5.7±0.008; ET, 6.2±0.09; TU, 6.1±0.13, p=0.004) y Emax (Emax: NT, 91±12%KCl; ET, 137±6.5% y TU, 117±18%; p=0.04; Tabla 2; fig. 2C) en ET y TU. A U46619 se presentó un aumento de

sensibilidad (pD2: NT, 7.08±0.1; ET, 7.3±0.09; TU, 7.2±0.1, p=0.06; Tabla 2; fig. 2D) en ET y TU.

Relajación

Se evidenció un aumento en sensibilidad a CCh (Emax: NT, 1.3±8%; ET, 49.6±14% y TU, 41.5±13% de relajación; p=0.009; Tabla 2; fig. 3A) en ET y TU. Al estímulo con BK disminuyó la pD2 (pD2: NT, 6.2±0.16; ET, 6.01±0.2; TU, 6.05±0.12, p=0.02) y Emax (Emax: NT, 91±20%l; ET, 53.4±5.6% y TU, 44.08±1% de relajación; p=0.03; Tabla 2; fig. 3B) en ET y TU. Al estímulo con isoproterenol aumentó la sensibilidad (pD2: NT, 6.5±0.17; ET, 8.3±0.3; TU, 7.7±0.18, p=0.001) y Emax (Emax: NT, 8.4±2%; ET, 28.2±5% y TU, 29.5±9.2% de relajación; p=0.005; Tabla 2; fig. 3C) en ET y TU. No se encontraron diferencias en la VR a VEGF (P>0.05; Tabla 2; fig. 3D).

Inmunofluorescencia

En la cuantificación de expresión se evidenció aumento en la íntima de los receptores α1, TP y VEGFR2 en ET, y TP, β2 y VEGFR1 en TU (fig. 4). En la túnica media aumentó la expresión de α1 y TP en ET y solo TP en TU. No se encontraron diferencias en la expresión de ETA y ETB, ni en adventicia para ningún receptor. A su vez, se evidencio un aumento de expresión de PTEN en la íntima y media de ET y TU (fig. 5 A,B). No se encontraron diferencias en la expresión de GSK3B (fig. 5 A,C). Se encontró aumento de expresión de NF-kB en la túnica media de ET y TU (fig. 5 A,D).

Expresión génica

En la cuantificación de ARNm se encontró sobreexpresión de ECE-1 en TU (fig. 6A). sobreexpresión de VEGF (fig. 6B) en arterias ET. C: Desregulación de la expresión del gen COX-2 (fig. 6C) en las arterias TU y ET.

Discusión

El tumor remodela los vasos sanguíneos que le irrigan, promoviendo engrosamiento de la pared vascular y reduciendo la relajación a BK y aumentando la VR a PE, TXA2, CCh, e isoproterenol.

En las variables antropométricas se hizo evidente que hay más casos de CAc en mujeres, en contraste con un mayor número de hombres en casos no tumorales, sin embargo, nuestra muestra no es representativa de la población por lo que es probable que este hallazgo esté condicionado por simple azar. Es interesante que en la clasificación de la patología un 80% de los casos corresponden a fases intermedias de la enfermedad, un grupo con baja variabilidad desde la parte clínica. La posible interferencia de la diferencia de la edad (18 años en la) sobre la función vascular en los grupos de CA y NT fue descartado mediante un trabajo complementario (capítulo tres- Cupitra, 2020B) en el que comparamos la VR de aorta en conejos jóvenes adultos y viejos. Además, los dos grupos fueron en general comparables en el peso, la talla y el índice de masa corporal, por esta razón, las diferencias vasculares deben derivar principalmente del hecho de que uno de los grupos tenía CA y el otro no.

La señalización tumoral induce hiperplasia en las túnicas íntima y media

Se encontró hiperplasia de la túnica media e íntima en arterias de pacientes con CAc. Este aumento en el grosor de las túnicas íntima y media sugiere que los factores promotores de proliferación y angiogénesis participan en la señalización tumoral como VEGF y ET-1 (Rapisarda, 2012; Rosanò, 2013), también induce alteraciones de la pared vascular que posiblemente estén asociadas a cambios funcionales, los cuales pueden guardar relación con la vasculatura intratumoral, donde se ha descrito la formación de vasculatura aberrante, que reduce la perfusión a tumor y posiblemente promueve proliferación al promover un ambiente hipóxico en el tumor (Nagy, 2012). Un hallazgo similar fue el de (Wilbers, et al., 2014) quien reportó hiperplasia arterial en pacientes cancerosos posterior a irradiación. Esto es muy llamativo pues en nuestros casos no hubo pacientes irradiados, pero indicaría que la hiperplasia puede no estar presente en todos los casos de CAc.Atribuimos este remodelamiento a la cantidad de factores de crecimiento generados por el tumor para promover su supervivencia, por ejemplo, el aumento de actividad adrenérgica que promueve la transición epitelial a mesenquimal (Cole, 2012).

La VR a KCl, PE y U46619 aumenta en las arterias de pacientes con cáncer

La VR al estímulo con KCl mostró que las arterias de pacientes con cáncer son más reactivas que las de pacientes NT, sugiriendo que el microambiente tumoral altera la contracción independiente de receptor en pacientes con cáncer. Este resultado es esperable, pues el estrés oxidativo típico de la hipoxia del microambiente tumoral activa kinasas, como HSP27, que promueven la proliferación y resistencia a anticancerosos, y favorecen los mecanismos de contracción en músculo liso (Nogueira, 2013; Lianos, 2015), además de que dicho estrés generado por las ROS podría promover disfunción endotelial, lo que haría esperable un aumento en esta vía de respuesta contráctil.

Encontramos diferencias en la sensibilidad a ET-1 en las arterias TU. Este es un resultado desafiante dado que la sobreexpresión de ET-1 en tumor debería tener efecto sobre el lecho vascular. En la expresión de los receptores ETA y ETB no se mostró diferencias estadísticas, pero sí una tendencia al aumento de ETA en las túnicas íntima y media. Además, se encontró un aumento en la expresión génica de ECE-1, lo sugiere aumento de la expresión de este receptor y la ECE-1 como compensación a la pérdida de sensibilidad al agonista, indicando que la exposición crónica de las arterias a la ET-1 generada en el tumor indujo resistencia al estímulo, y posiblemente contribuyó con la hiperplasia en la pared vascular. Por otro lado, estos resultados son contrastantes con lo publicado por (Ferrero, 2008) que reportó aumento en expresión del receptor ET-B en arterias que irrigan CAc.

En donde sí evidenciamos importantes diferencias es en la sensibilidad a PE y al análogo del TXA2 en las arterias TU y ET, mostrando un aumento en la VR a ambos agonistas. Destacamos, que en el bloqueo con LNAME, con prazosina y con seratrodast no se encontraron diferencias estadísticas, esto sugiere que la mayor reactividad a PE y TXA2 no se debe en su totalidad a una probable disfunción endotelial o a alteraciones en la unión ligando receptor de cada agonista con su receptor. Complementariamente, la cuantificación de los receptores α1 y TP, se encontró aumento en la expresión de ambos receptores en las túnicas íntima y media, estos resultados, particularmente los de media explicarían el aumento en sensibilidad reportado para estos agonistas. Lo anterior indica que el ambiente

tumoral parece favorecer una condición hipertensa en las arterias que van al tumor a través de la constricción por vía adrenérgica y por TXA2. En la literatura no hemos encontrado evidencia clara sobre el rol de la señalización alfa-adrenérgica en el control vascular en cáncer, aunque sí se ha reportado la importancia de los receptores beta-adrenérgicos participando en la iniciación y progresión del tumor, y aumentos súbitos de hasta 10 veces en los niveles basales de epinefrina y norepinefrina, haciendo muy probable una afectación al vaso que irriga el tumor (Cole, 2012). Es importante recalcar que el único agonista relajante que mostró diferencias estadísticas en nuestro trabajo fue el isoproterenol, cuya función sucede a través de beta, en concordancia con el aumento en la expresión de este receptor.

El tumor reduce la relajación por óxido nítrico y aumenta la dilatación adrenérgica y colinérgica

En la VR a agonistas relajantes, encontramos que el 70% de las arterias de pacientes con cáncer no generaban al menos un 50% de relajación a BK, indicando que la mayor parte de esta población de estudio tenía posible disfunción endotelial. Teniendo en cuenta lo anterior, los experimentos de relajación se realizaron en arterias de pacientes que mostraran al menos un 40% de la relajación a BK 10 µM en el inicio del experimento. En la RV a CCh se evidenció relajación en las arterias TU y ET, mientras que en las arterias NT dicha relajación fue virtualmente inexistente, esto indicaría que la señalización en tumor fortalece la respuesta colinérgica en las arterias. Complementariamente, nuestros resultados coinciden con lo mostrado por (Hall, 2006) y (Tottrup, 2004) quienes reportan ausencia de relajación a CCh en mesentéricas de pacientes con cáncer de intestino. Lo anterior sugiere que la ganancia en relajación a CCh no es mandataria para las arterias en todos los tumores y es probable que esté condicionada al avance de la enfermedad.

En la relajación a BK se evidenció una disminución en sensibilidad y Emax en las arterias TU y ET. Cuando se bloqueó con LNAME se evidenció una reducción en Emax >30% en todos los grupos, en contraste con un aumento de la relajación cuando de bloqueó con indometacina, sugiriendo que la dilatación mediada por BK depende parcialmente de óxido

nítrico y es inhibida por la vía de prostanoides. Complementariamente, cuando se bloqueó con LNAME e indometacina se inhibió parcialmente la relajación, sugiriendo que hay otros mecanismos de relajación activados por BK en arterias TU, ET y NT, posiblemente el factor hiperpolarizante derivado del endotelio.

En la relajación a isoproterenol se evidenció un aumento en sensibilidad y eficacia en las arterias TU y ET. Esto posiblemente se deba al aumento en la expresión de su receptor β2 como un mecanismo compensatorio a la disfunción endotelial generada por el cáncer. Lo anterior también indica que el cáncer favorece la señalización adrenérgica en las arterias, dado que se ha reportado la importancia de los receptores beta-adrenérgicos (Cole, 2012), haciendo muy probable estos cambios en los vasos que irrigan el tumor, también promuevan el desarrollo del mismo.

No encontramos diferencias estadísticas a la relajación con VEGF, sin embargo, a nivel endotelial encontramos resultados contrastantes en la expresión de sus receptores, donde el receptor VEGFR1 aumento en las arterias TU y en VEGFR2 en las ET. Estos resultados explicarían el aumento de expresión génica de VEGF en arterias ET frente a TU y NT, sugiriendo que en las ET se favorecen los mecanismos angiogénicos, como es el caso de VEGF/VEGFR2, mientras que se inhibe en las TU a través de VEGFR1. Estas modificaciones podrían favorecer un ambiente hipóxico en el tumor retroalimentando así vías de señalización como VEGF/PTEN/GSK3B/NF-kB que facilitan el desarrollo tumoral y las adaptaciones vasculares (Chang, 2019).

Conclusión

El ambiente tumor induce hiperplasia en las túnicas íntima y media, que junto con la ganancia en contracción a PE y TXA2 favorecen un ambiente hipertenso en estas arterias. A su vez, la influencia tumoral reduce la relajación endotelial mediada por BK, compensada por el aumento en dilatación adrenérgica y colinérgica. La promoción del ambiente contráctil en las arterias, al parecer reduce el flujo a tumor, facilitando en el nicho tumoral ambiente hipóxico, que condiciona dos ambientes vasculares, el primero encargado de la irrigación y de

favorecer la proliferación tumoral, y el segundo, en la periferia tumoral promoviendo angiogénesis, y facilitando la migración del tumor a nuevas zonas.

Referencias

Chang H., Cai Z., Roberts T.M. (2019). The mechanisms underlying PTEN loss in human tumors suggest potential therapeutic opportunities. Biomolecules, Volume 9.

Cole SW, Sood AK. Molecular pathways: Beta-adrenergic signaling in cancer. Clin Cancer Res. 2012

Cupitra NI, Calderón JC, Narvaez-Sanchez R. Increased receptor expression supports vascular reactivity of the rabbit aorta during preservation. Eur J Cardiothorac Surg. 2020A Nov 14:ezaa386. doi: 10.1093/ejcts/ezaa386. Epub ahead of print. PMID: 33188691.

Cupitra NI, Calderón JC, Narvaez-Sanchez R. Influence of Ageing on Vascular Reactivity and Receptor Expression in Rabbit Aorta: A Complement to Elastocalcinosis and Smooth Muscle Mechanisms. Clin Interv Aging. 2020B Apr 20;15:537-545. doi: 10.2147/CIA.S236173. PMID: 32368020; PMCID: PMC7182455.

Hall, J., Jones, T. H., Channer, K. S., & Jones, R. D. (2006). Mechanisms of agonist-induced constriction in isolated human mesenteric arteries. Vascular Pharmacology, 44(6), 427–433. doi:10.1016/j.vph.2006.02.004

Lianos GD, Alexiou GA, Mangano A, Mangano A, Rausei S, Boni L, et al. The role of heat shock proteins in cancer. Cancer Letters. 2015.

Maeda, H., Akaike, T., Wu, J., Noguchi, Y., & Sakata, Y. (1996). Bradykinin and nitric oxide in infectious disease and cancer. Immunopharmacology, 33(1-3), 222-230.

Maeda, H., Akaike, T., Wu, J., Noguchi, Y., & Sakata, Y. (1996). Bradykinin and nitric oxide in infectious disease and cancer. Immunopharmacology, 33(1-3), 222-230.

Nogueira V, Hay N. Molecular pathways: Reactive oxygen species homeostasis in cancer cells and implications for cancer therapy. Clin Cancer Res. 2013;

Olsson A-K, Dimberg A, Kreuger J, Claesson-Welsh L. VEGF receptor signalling - in control of vascular function. Nat Rev Mol Cell Biol. 2006;7(5):359–71.

Rapisarda A, Melillo and G. Role of the VEGF/VEGFR axis in cancer biology and therapy. Guid Mol Cancer Tumor Angiogenes. Academic Press; 2012;114:237.

Rosanò L, Spinella F, Bagnato A. Endothelin 1 in cancer: biological implications and therapeutic opportunities. Nat Rev Cancer [Internet]. 2013;13(9):637–51. Available from: http://www.ncbi.nlm.nih.gov/pubmed/23884378

Sakai H, Suzuki T, Takahashi Y, Ukai M, Tauchi K, Fujii T, et al. Upregulation of thromboxane synthase in human colorectal carcinoma and the cancer cell proliferation by thromboxane A2. FEBS Lett. 2006;

Sonveaux, P. (2008). Provascular strategy: targeting functional adaptations of mature blood vessels in tumors to selectively influence the tumor vascular reactivity and improve cancer treatment. Radiotherapy and Oncology, 86(3), 300-313.

Stewart, J. M., & Gera, L. A. J. O. S. (2006). Bradykinin and cancer. Handbook of Biologically Active Peptides, 443-6.

Tottrup A, Kraglund K (2004). Endothelium-dependent responses in small human mesenteric arteries. Physiol Res. 53(3):255-63. PMID: 15209532.

Wagland, R., Richardson, A., Ewings, S., Armes, J., Lennan, E., Hankins, M., & Griffiths, P. (2016). Prevalence of cancer chemotherapy-related problems, their relation to health-related quality of life and associated supportive care: a cross-sectional survey. Supportive Care in Cancer, 24(12), 4901-4911.

WHO (2020). Cardiovascular diseases (CVDs). WHO [Internet]. World Health Organization; [cited 2020 Sep 18]; Available from: https://www.who.int/cardiovascular_diseases/en/

Wilbers J, Dorresteijn LD, Haast R, Hoebers FJ, Kaanders JH, Boogerd W, et al. Progression of carotid intima media thickness after radiotherapy: A long-term prospective cohort study. Radiother Oncol [Internet]. Elsevier; 2014 Dec 1 [cited 2019 Aug 21];113(3):359–63. Available from: https://www.sciencedirect.com/science/article/pii/S0167814014004241

Tablas.

Tabla 1. Variables antropométricas de pacientes con CAc y pacientes no cancerosos.

Characteristics		Patients		Sig.
		CA	NT	
Nº of patients		25	13	
Age (years)		67±3	49±6	p<0.05
Gender	F	15	4	-
	M	10	8	
Diagnosis of pathology	Adenocarcinoma	25	-	
	Diverticulitis	-	4	
	Obstruction by flanges	-	5	
	Trauma	-	3	
	Others	-	1	
Location	Right colon	11	8	
	Left colon	8	1	
	Sigmoid colon	3	3	
	Transverse colon	3	1	
TNM classification	pT0N0	1	-	
	pT2N1	4	-	
	pT3N0	7	-	
	pT3N1	5	-	
	pT4N0	5	-	
	pT4N2	3	-	

Tabla 2. pD2 y respuesta máxima a KCl, PE, U46619, ET-1, CCh, BK, isoproterenol, VEGF y sus bloqueantes en arteria mesentérica de pacientes NT, TU y ET.

Agonist		pD2				Emax (% KCl 40mM)			
		NT	ET	TU	p	NT	ET	TU	p
Contraction	KCl	1.6±0.04	1.8±0.02	1.8±0.03	0.02γ	128±10.2	130.1±7	152±11.3	0.21
	PE	5.75±0.08	6.2±0.09	6.1±0.13	0.004γ	91.09±12	137.7±6.5	117.7±18.8	0.04γ
	PE+LNAME[b]	6.02±0.18	6.2±0.05	6.15±0.02	0.3	91.1±12.2	95.59±5.6	93.98±7.2	0.9
	PE+Prazosin[c]	4.6±0.03	4.4±0.03	4.3±0.06	0.9	18.03±4	14.1±3.6	28.7±6.7	0.9
	U46619	7.089±0.12	7.36±0.09	7.21±0.11	0.06γ	128.6±8.5	123.9±14	110.8±11.3	0.7
	U46619+LNAME[b]	7.247±0.2	7.88±0.13	7.58±0.07	0.25	144.3±5.7	147.57.1	165.1±32.5	0.9
	U46619+seratrodast[c]	6.4±0.2	6.41±0.07	6.5±0.96	0.7	34.01±3.3	26.14±5	41.42±3	0.3
	ET-1	7.061±0.11	7.07±0.13	6.76±0.04	0.06λ	106.8±15.3	91.29±11.8	96±6.6	0.6
Dilation[a]	CCh	6.33±0.16	6.22±0.17	6.27±0.13	0.8	1.31±8	49.6±14	41.5±13.6	0.009γ
	BK	6.2±0.16	6.01±0.2	6.05±0.12	0.02γ	91.01±20	53.45±5.6	44.08±8.2	0.03γ
	BK+LNAME[c]	7.01±0.2	6.36±0.18	6.3±0.09	0.9	58.65±2.3	38.41±15.8	28.97±4	0.1
	BK+Indomethacin[c]	6.8±0.24	6.5±0.11	6.3±0.25	0.9	97.75±7.7	57.68±8.2	80.09±2	0.9
	BK+LNAME-Indomethacin[b]	7.07±0.26	7.3±0.15	6.3±0.16	0.8	44.8±5.6	38.8±9.6	28.3±4.7	0.3
	Isoproterenol	6.54±0.17	8.38±0.3	7.78±0.18	0.001γ	8.46±2	28.2±5	29.5±9.2	0.005γ
	VEGF	10.17±0.5	10.32±0.13	10.29±0.23	0.9	51.44±24.6	41.36±5.6	42.61±9.4	0.8

M: concentración molar. [a]% de relajación en relación con la precontracción con U46619. [b] indica n= 2 pacientes, 4 anillos. [c]indica n= 3, 6. Los demás experimentos tienen un n= 5, 10. Resultados en media±SEM. γ indica diferencias estadísticas en TU y ET frente a NT; λ indica

diferencias estadísticas en TU frente a NT. Oneway ANOVA seguido del post-hoc de Dunnett, nivel de significancia P <0,05.

Figuras.

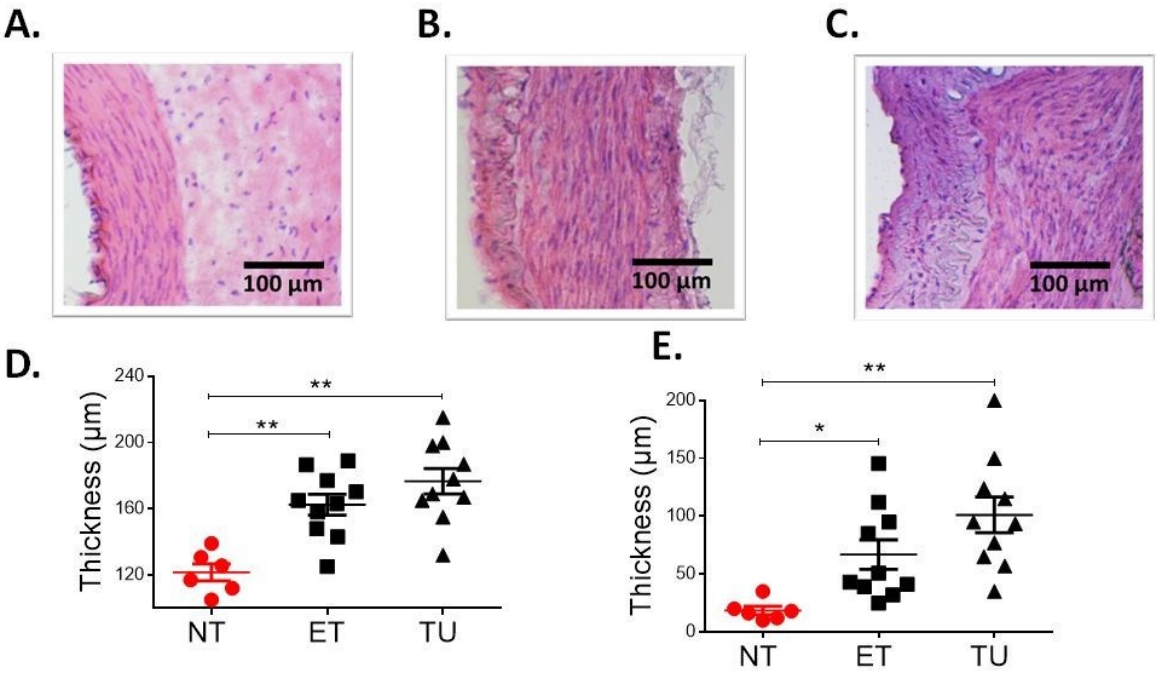

Figura 1. Estudio histológico vascular. A) Arteria NT; B) arteria ET; C) Arteria TU; D) Grosor de la túnica media en las arterias NT, ET y TU; E) Grosor de la túnica íntima en arterias NT, ET y TU. One-way ANOVA seguido del post-hoc de Dunnett. * indica p <0,05. ** indica p <0,01.

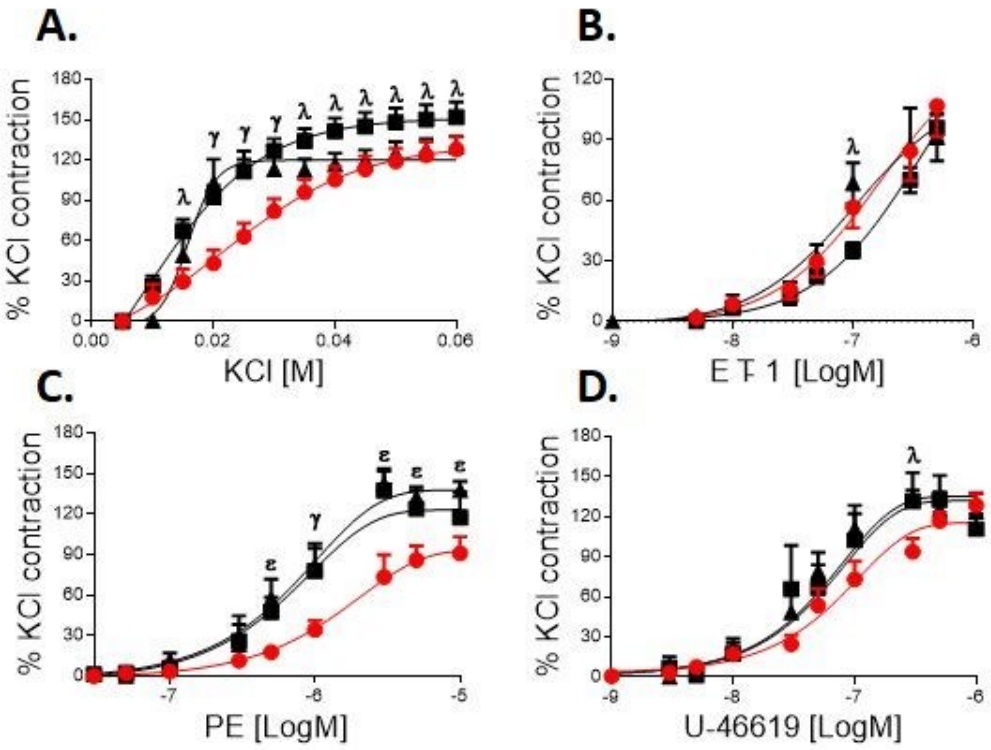

Figura 2. Curvas de concentración-respuesta a KCl (A), ET-1 (B), PE (C) y U46619 (D). NT (●, 5 patients, 10 rings), ET (▲, 5, 10) and TU (■, 5, 10). λ indica mayor sensibilidad y Emax a KCl o menor sensibilidad a ET-1 o mayor sensibilidad a U46619 en TU en comparación con NT. γ indica mayor sensibilidad a KCl o mayor pD2 a PE en TU y ET en comparación con NT. ξ indica mayor sensibilidad y eficacia a PE en ET en comparación con NT. Two-way ANOVA seguido del post-hoc de Dunnett, nivel de significancia P<0,05.

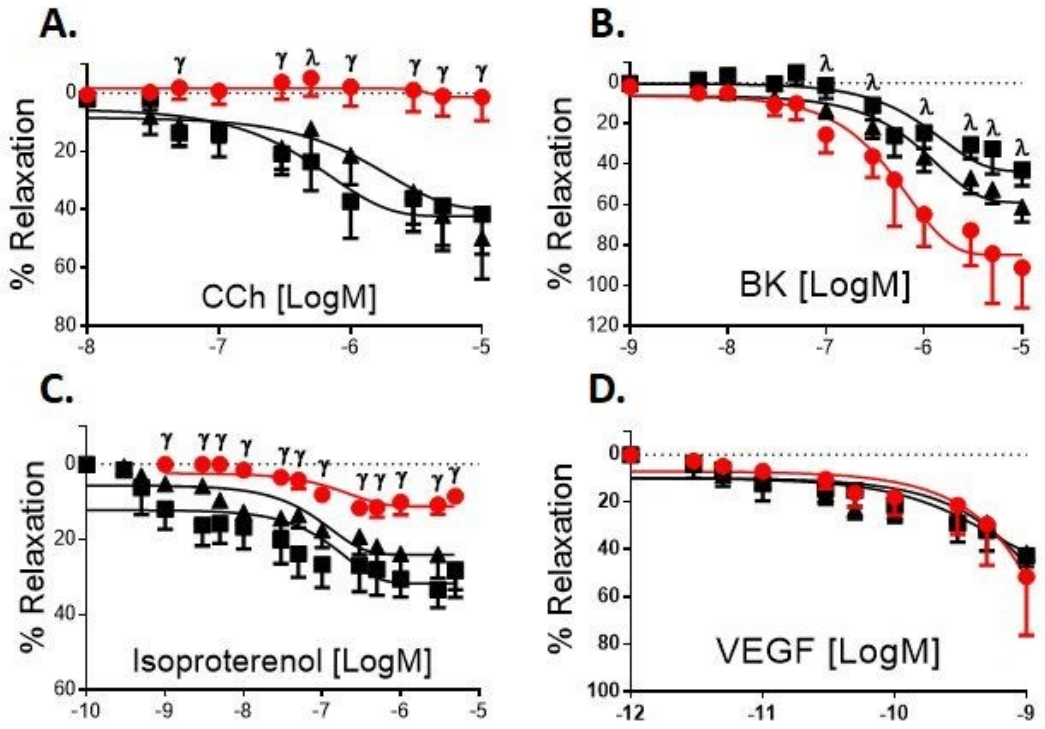

Figura 3. Curvas de concentración-respuesta a CCh (A), BK (B), isoproterenol (C), VEGF (D). NT (●, 5 patients, 10 rings), ET (▲, 5,10) and TU (■, 5,10). λ indica mayor sensibilidad a CCh o menor sensibilidad a BK en TU, en comparación con NT. γ indica mayor sensibilidad y Emax a CCh o mayor pD2 y Emax a isoproterenol en TU y ET, en comparación con NT. Two-way ANOVA seguido del post-hoc de Dunnett, nivel de significancia $P<0,05$.

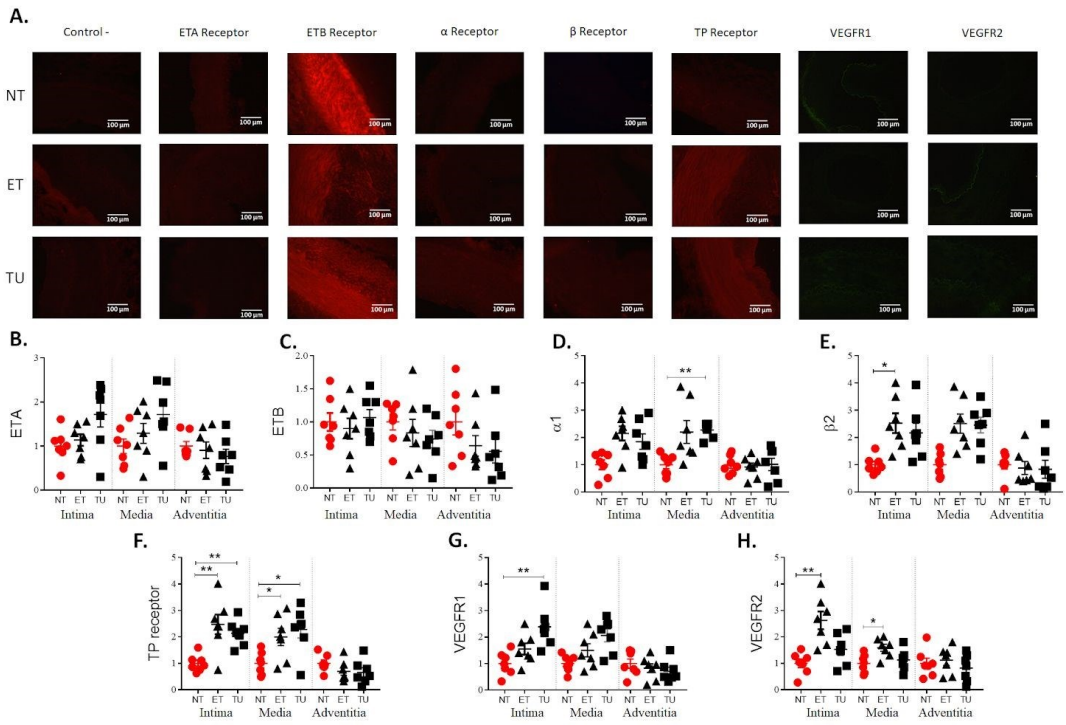

Figura 4. Cuantificación de la expresión proteica de los receptores ETA, ETB, α1, β2, TP, VEGFR1 y VEGFR2 en la pared de arterias mesentéricas de NT (●), ET (▲) y TU (■). A, imágenes representativas de inmunofluorescencia para identificar receptores ETA, ETB, α1, β2, TP, VEGFR1 y VEGFR2. B, C, D, E, F, G y H, cuantificación de la fluorescencia de los receptores ETA, ETB, α1, β2, TP, VEGFR1 y VEGFR2, respectivamente, en las túnicas de la pared de arteria mesenterica. El número de experimentos es 7 en todos los casos. (A) La longitud de las barras de calibración del blanco es equivalente a 100 µm. Analizado con One-way ANOVA seguido del post-hoc de Dunnett. * indica p <0,05. ** indica p <0,01.
La expresión se normalizó a NT.

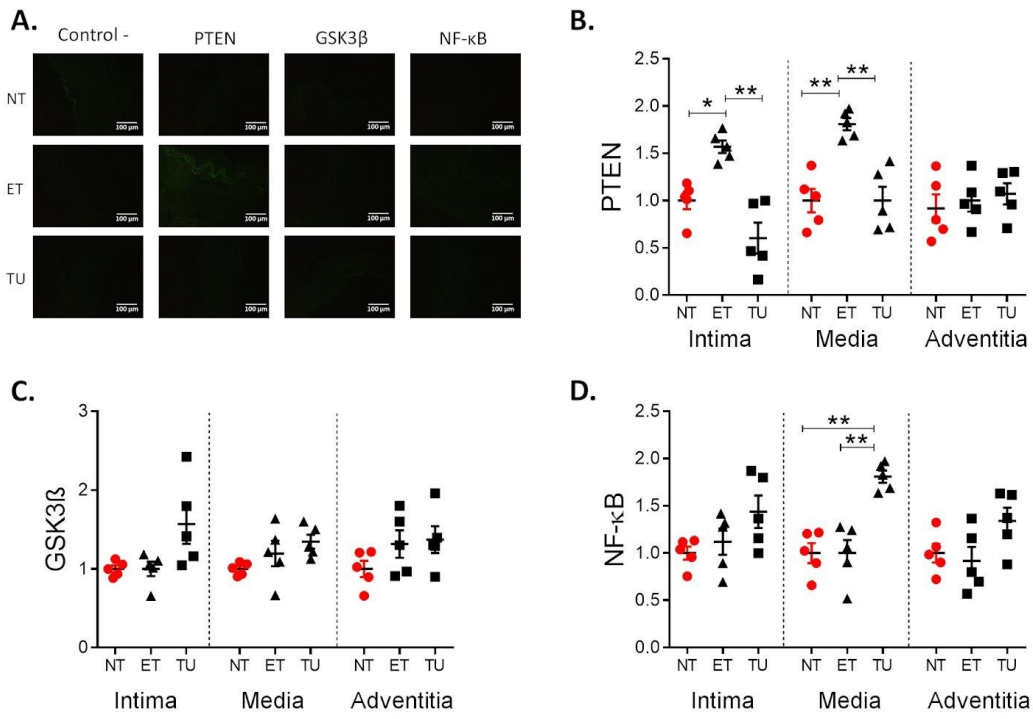

Figura 5. Cuantificación de la expresión proteica de PTEN, GSK3β, y NF-kB en la pared de arterias mesentéricas de NT (●), ET (▲) y TU (■). A, imágenes representativas de inmunofluorescencia para identificar PTEN, GSK3β, y NF-kB. B, C y D, cuantificación de la fluorescencia de PTEN, GSK3β, y NF-kB, respectivamente, en las túnicas de la pared de arterias mesentéricas. El número de experimentos es 5 en todos los casos. (A) La longitud de las barras de calibración del blanco es equivalente a 100 µm. Analizado con One-way ANOVA seguido del post-hoc de Dunnett. * indica p <0,05. ** indica p <0,01. La expresión se normalizó a NT.

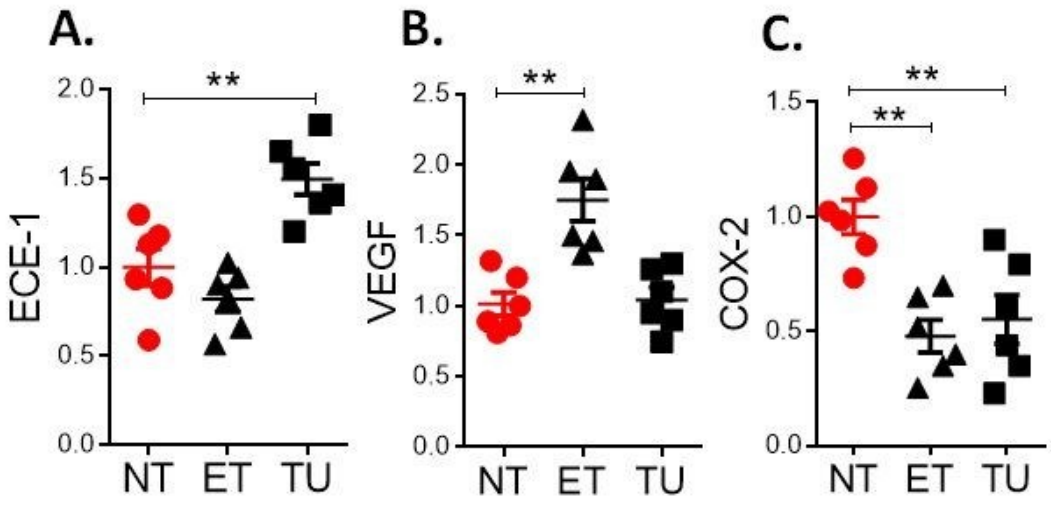

Figura 6. Niveles de expresión génica de ECE-1 (A), VEGF (B) y COX-2 (C) en arterias mesentéricas de NT (●), ET (▲) y TU (■). A: Sobreexpresión de ECE-1 en TU. B: sobreexpresión de VEGF en arterias ET. C: Desregulación de la expresión del gen COX-2 en las arterias TU y ET. Analizado con One-way ANOVA seguido del post-hoc de Dunnett. ** indica $p<0,01$. La expresión se normalizó a NT.

Capítulo seis: Discusión General

Discusión general

Esta tesis se enfocó en caracterizar los mecanismos de adaptación vascular inducidos en arterias que irrigan CAc en humanos, generando una plataforma de trabajo que podría ayudar a profundizar en la fisiopatología del cáncer y a explorar nuevas aproximaciones farmacológicas. Entre las principales características de este trabajo se destacan:

1. Usando como modelo vascular aorta de conejo se determinó que durante la preservación se deteriora VR mediada por prostanoides a las 24 horas. A su vez este deterioro es compensado por el aumento en la VR adrenérgica y sus receptores (Cupitra, 2020A). En el marco del proyecto principal, estos resultados permitieron definir la ventana de tiempo óptima dentro de la cual se preserva la respuesta fisiológica, permitiendo validar la fiabilidad de los resultados obtenidos de arterias de la mesentérica en humanos y cerdos utilizados en los capítulos cuatro y cinco. Además, permitió determinar que solo es recomendable montar experimentos en baño de órganos las primeras 24 horas, si se quiere evaluar la VR adrenérgica o endotelial.
2. Usando como modelo vascular aorta de conejos jóvenes, adultos y viejos se determinó que durante el envejecimiento la VR a prostanoides, óxido nítrico, y a β-agonistas disminuye (Cupitra, 2020B). Estos resultados en el marco del proyecto principal permitieron definir que los hallazgos reportados en el capítulo cinco no se deben a los 18 años de diferencia entre los pacientes con cáncer y los pacientes control, siendo esperable que el aumento en VR a U46619, CCh, Isoproterenol y la reducción a BK se deba a la influencia del tumor.
3. Se caracterizaron las diferencias en VR de arteria mesentérica de humanos no tumorales, cerdos, conejos y ratas, identificando a las arterias de cerdos como el modelo vascular más comparable con el humano. En el marco del proyecto principal, y por la limitación en la frecuencia de pacientes control, el cerdo podría ser un modelo apropiado para evaluar diferentes estrategias terapéuticas, entre ellas aquellas que requieran de un control vascular sano en humanos.

Este trabajo se enfocó en evaluar los mecanismos de adaptación vascular en arterias que irrigan los tumores. Los resultados expuestos en el capítulo cinco nos permiten proponer el modelo que se presenta en la figura 1. El tumor indujo hiperplasia en las túnicas íntima y media en la pared vascular, exacerbó la VR contráctil, redujo la relajación endotelial y aumento la relajación muscarínica y β2 adrenérgica, dos mecanismos que fisiológicamente tienen poca participación vascular en humanos, todo para favorecer el desarrollo tumoral.

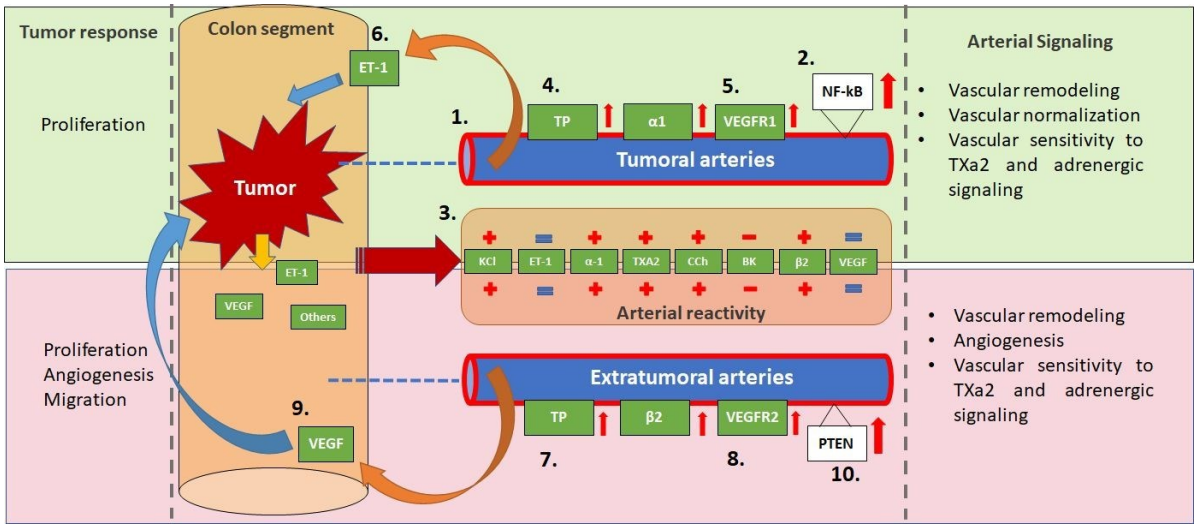

Figura 1. Mecanismos de adaptación vascular en arterias que irrigan tumores en cáncer de colon en humanos.

Como se evidencia en la figura 1, estos mecanismos de adaptación se dividen en dos fases, una tumoral (verde) y otra extratumoral (rojo). La fase tumoral se caracteriza por un marcado engrosamiento de la pared vascular promovida desde la señalización tumoral **(1)**, y por la expresión de factores de transcripción como el NF-kB **(2) ,** asociados a remodelamiento en hipoxia (Diebold, 2008). A su vez, este remodelamiento se complementa con el aumento de la sensibilidad del vaso a los estímulos de agonistas contráctiles como fenilefrina, tromboxano A2, junto con una disminución del 50% en la relajación a BK en los pacientes que no presentaron disfunción endotelial **(3)** (30% de los pacientes). Este condicionamiento vascular promovió el aumento de la VR muscarínica y β2 adrenérgica, probablemente como compensación a la reducción de relajación endotelial. Estas modificaciones vasculares sugieren que en la vasculatura que irriga al tumor se facilita un ambiente procontráctil, el cual

podría reducir el flujo hacia el tumor, induciendo un ambiente hipóxico que a su vez promueve el crecimiento tumoral.

Curiosamente, aunque ET-1 y VEGF son importantes promotores del desarrollo tumoral (Asham, 2001; Itatani, 2018), la VR a ET-1 disminuyó en sensibilidad y VEGF no presentó diferencias, indicando que su rol más relevante se da en otros procesos asociados al cáncer y no en la regulación del tono vascular. Esta promoción de la contractilidad se beneficia del aumento en la expresión de los receptores α1 y TP en las túnicas íntima y media **(4)**. El aumento selectivo del receptor VEGFR1 en la íntima de estas arterias sugiere que hay una regulación negativa de la angiogénesis **(5)** (Koch, 2011), esto se complementa con la mayor expresión del receptor TP el cual tiene actividad antiangiogénica y proliferativa (Sakai, 2006). El aumento en la expresión génica de la ECE-1 indicaría que desde la arteria se está promoviendo la proliferación del tumor inducida por ET-1 **(6)**, y explicaría a su vez la disminución en sensibilidad evidenciada en la VR, posiblemente generada como resistencia al aumento crónico de ET-1.

La fase extratumoral (>5cm del tumor), al igual que en la tumoral, promueve un ambiente procontráctil, presentando engrosamiento de la pared vascular, aumento de sensibilidad a agonistas contráctiles, disminución del 35% en la relajación a BK y compensación muscarínica y β2 adrenérgica relajación **(3).** Sugiriendo al igual que en la tumoral que se reduce el flujo hacia el tumor, induciendo un ambiente hipóxico que promueve el desarrollo del cáncer. Esta promoción de la contractilidad se beneficia del aumento en la expresión de los receptores TP en las túnicas íntima y media **(7)**. El aumento selectivo del receptor VEGFR2 en la íntima de estas arterias sugiere que hay promoción de la angiogénesis mediada por el mismo VEGF **(8)** (Nagy, 2012), pero se contrapone con la mayor expresión del receptor TP. El aumento en la expresión génica de la VEGF **(9)** indicaría que desde la arteria se está promoviendo angiogénesis en la periferia tumoral, condicionando este espacio a una próxima migración de la masa tumoral. Una particularidad de la fase extratumoral es el aumento en la expresión de PTEN **(10)** un regulador negativo de NF-kB (Chang, 2019), que estaría indicando un primer esfuerzo de la arteria por suprimir las adaptaciones vasculares dirigidas desde el tumor.

Conclusión

En este trabajo se determinó que el ambiente tumor induce hiperplasia en las túnicas íntima y media, que se complementa con un aumento en contracción a KCl, PE y U46619, y reduce la relajación endotelial mediada por BK, compensada por el aumento en dilatación adrenérgica y colinérgica, favoreciendo un ambiente hipertenso en estas arterias. La promoción del ambiente contráctil en las arterias, al parecer reduce el flujo a tumor, facilitando en el nicho tumoral ambiente hipóxico, que a su vez condiciona dos ambientes vasculares a través de HIF-1α, el primero encargado de la irrigación y que podría favorecer la proliferación tumoral, y el segundo, en la periferia tumoral promoviendo angiogénesis, facilitando la migración del tumor a nuevas zonas.

Perspectivas

Los resultados de este trabajo de investigación abren las puertas a nuevos estudios que permitan abordar el potencial terapéutico de los procesos asociados a las adaptaciones vasculares en cáncer. Como perspectivas se plantean las siguientes:

- Aumentar la batería de vías de señalización vascular asociadas a cáncer
- Caracterizar aguas abajo los segundos mensajeros implicados en las adaptaciones en VR en el cáncer
- Determinar si las adaptaciones vasculares en CAc son comparables con las de otros tipos de cáncer
- Determinar el potencial terapéutico de sustancias sobre las adaptaciones vasculares en cáncer

Referencias: capítulos uno y seis

Asham, E., Shankar, A., Loizidou, M., Fredericks, S., Miller, K., Boulos, P. B., ... & Taylor, I. (2001). Increased endothelin-1 in colorectal cancer and reduction of tumour growth by ET A receptor antagonism. British journal of cancer, 85(11), 1759-1763.

Buchinger-Kähler V, Stoldt VR, Muth T, Schipke JD. Function and Viability of Vessels in Different Preservation Solutions-An Experimental Study on Human Great Saphenous Veins. J Angiol Vasc Surg 2016;1(003);1-7.

Chang H., Cai Z., Roberts T.M. (2019). The mechanisms underlying PTEN loss in human tumors suggest potential therapeutic opportunities. Biomolecules, Volume 9.

Cole SW, Sood AK. Molecular pathways: Beta-adrenergic signaling in cancer. Clin Cancer Res. 2012

Cupitra NI, Calderón JC, Narvaez-Sanchez R. Increased receptor expression supports vascular reactivity of the rabbit aorta during preservation. Eur J Cardiothorac Surg. 2020A Nov 14:ezaa386. doi: 10.1093/ejcts/ezaa386. Epub ahead of print. PMID: 33188691.

Cupitra NI, Calderón JC, Narvaez-Sanchez R. Influence of Ageing on Vascular Reactivity and Receptor Expression in Rabbit Aorta: A Complement to Elastocalcinosis and Smooth Muscle Mechanisms. Clin Interv Aging. 2020B Apr 20;15:537-545. doi: 10.2147/CIA.S236173. PMID: 32368020; PMCID: PMC7182455.

Dao HH, Essalihi R, Bouvet C, Moreau P. Evolution and modulation of age-related medial elastocalcinosis: impact on large artery stiffness and isolated systolic hypertension. Cardiovascular research. 2005;66(2):307-317.

Diebold I, Djordjevic T, Hess J, Görlach A. Rac-1 promotes pulmonary artery smooth muscle cell proliferation by upregulation of plasminogen activator inhibitor-1: role of NFkappaB-dependent hypoxia-inducible factor-1alpha transcription. Thromb Haemost. 2008 Dec;100(6):1021-8. PMID: 19132225.

Donato AJ, Machin DR, Lesniewski LA. Mechanisms of dysfunction in the aging vasculature and role in age-related disease. Circulation research. 2018;123(7):825-848.

Ferrero E, Labalde M, Fernández N, Monge L, Salcedo A, Narvaez-Sanchez R, et al. Response to endothelin-1 in arteries from human colorectal tumours: role of endothelin receptors. Exp Biol Med (Maywood). 2008;233:1602–7.

Itatani, Y., Kawada, K., Yamamoto, T., & Sakai, Y. (2018). Resistance to anti-angiogenic therapy in cancer—alterations to anti-VEGF pathway. International journal of molecular sciences, 19(4), 1232.

Koch, S., Tugues, S., Li, X., Gualandi, L., & Claesson-Welsh, L. (2011). Signal transduction by vascular endothelial growth factor receptors. Biochemical journal, 437(2), 169-183.

Nagy JA, Dvorak HF. Heterogeneity of the tumor vasculature: The need for new tumor blood vessel type-specific targets. In: Clinical and Experimental Metastasis. 2012. p. 657–62.

Olsson A-K, Dimberg A, Kreuger J, Claesson-Welsh L. VEGF receptor signalling - in control of vascular function. Nat Rev Mol Cell Biol. 2006;7(5):359–71.

Rapisarda A, Melillo and G. Role of the VEGF/VEGFR axis in cancer biology and therapy. Guid Mol Cancer Tumor Angiogenes. Academic Press; 2012;114:237.

Rauen U, Groot H. New insights into the cellular and molecular mechanisms of cold storage injury. J. Investig. Med 2004;52:299–309.

Romanque, P., Piguet, A. C., & Dufour, J. F. (2008). Targeting vessels to treat hepatocellular carcinoma. Clinical science, 114(7), 467-477.

Rosanò L, Spinella F, Bagnato A. Endothelin 1 in cancer: biological implications and therapeutic opportunities. Nat Rev Cancer [Internet]. 2013;13(9):637–51. Available from: http://www.ncbi.nlm.nih.gov/pubmed/23884378.

Russell JC, Proctor SD (2006). Small animal models of cardiovascular disease: tools for the study of the roles of metabolic syndrome, dyslipidemia, and atherosclerosis. Cardiovascular Pathology.

Sakai H, Suzuki T, Takahashi Y, Ukai M, Tauchi K, Fujii T, et al. Upregulation of thromboxane synthase in human colorectal carcinoma and the cancer cell proliferation by thromboxane A2. FEBS Lett. 2006;

Virmani R, Kolodgie FD, Farb A, Lafont A (2003). Drug eluting stents: are human and animal studies comparable? Heart [Internet]. BMJ Publishing Group Ltd; 89(2):133–8. Available from: http://www.ncbi.nlm.nih.gov/pubmed/12527658.

Voss NCS, Kold-Petersen H, Boedtkjer E. Enhanced nitric oxide signaling amplifies vasorelaxation of human colon cancer feed arteries.

WHO (2020). Cardiovascular diseases (CVDs). WHO [Internet]. World Health Organization; [cited 2020 Sep 18]; Available from: https://www.who.int/cardiovascular_diseases/en/.

Anexo uno:

Estrada O; Giulio C; Dorta-Ledezma R; Gonzalez-Mujica F; Motta N; Zea E; Cupitra NI; Contreras W; Narvaez-Sanchez R; Calderón JC, 2019. Compound Isolated from Phyllanthus tenellus Demonstrates Metabolic and Vascular Effects In Vitro.

Artículo publicado en Planta Medica; IF: 2.68

Enlace: https://www.thieme-connect.com/products/ejournals/abstract/10.1055/a-1019-9401

En agosto de 2016, previo a la aprobación de la recolección de arterias humanas por parte de la IPS universitaria- Clínica León XIII, se programó una pasantía de tres meses en el Laboratorio de fisiología celular del Centro de Biofísica y Bioquímica en el Instituto Venenzolano de Investigaciones Científicas, bajo la tutoría del PhD. Omar Estrada. El objetivo fue capacitar al estudiante en el montaje de arterias en baño de órgano aislado. Uno de los resultados de la pasantía fue el aporte experimental al trabajo “Compound Isolated from Phyllanthus tenellus Demonstrates Metabolic and Vascular Effects In Vitro”.

A continuación, artículo correspondiente al anexo uno

Thieme

A Compound Isolated from *Phyllanthus tenellus* Demonstrates Metabolic and Vascular Effects *In Vitro*

Authors

Omar Estrada[1], Camilo Di Giulio[1], Radharani Dorta-Ledezma[1], Freddy Gonzalez-Mujica[2], Norma Motta[2], Elsa Zea[2], Nelson Cupitra[3], Whendy Contreras[1], Raúl Narvaez-Sanchez[3], Juan C. Calderón[3]

Affiliations

1 Centre of Biophysics and Biochemistry, Venezuelan Institute for Scientific Research, Caracas, Venezuela
2 Faculty of Medicine, Central University of Venezuela, Caracas, Venezuela
3 Physiology and Biochemistry Research group-PHYSIS, Faculty of Medicine, University of Antioquia, Medellín, Colombia

Key words

Phyllanthus tenellus, Phyllantaceae, metabolic syndrome, pinocembrin, human platelets, vascular reactivity

received May 18, 2019
revised September 23, 2019
accepted September 26, 2019

Bibliography

DOI https://doi.org/10.1055/a-1019-9401
Published online | Planta Med © Georg Thieme Verlag KG Stuttgart · New York | ISSN 0032-0943

Correspondence

Dr. Omar Estrada
Cell Physiology Laboratory, Centre of Biophysics and Biochemistry, Venezuelan Institute for Scientific Research
K11 de la Carretera Panamericana, Apartado 20632, 1020-A Altos de Pipe, Venezuela
Phone: + 58 212 504 1230, Fax: + 58 212 504 1093
oestrada@ivic.gob.ve

Supporting information available online at http://www.thieme-connect.de/products

ABSTRACT

Common chronic conditions such as metabolic syndrome and diabetes are increasingly associated to metabolic and cardiovascular complications. Although *Phyllanthus tenellus* leaves have been used in decoctions as a popular remedy to control blood glucose levels and hypertension, its use needs a scientific basis. This study was therefore undertaken to report a phytochemical analysis of *P. tenellus* leaves and to test if the main active compound has potential to simultaneously tackle several pathophysiological features of metabolic syndrome and diabetes-related metabolic and vascular disorders such as hyperglycaemia, increased platelet activation, and endothelial dysfunction. We performed a partition of the methanolic extract of *P. tenellus* leaves among different organic solvents followed by chromatographic separation guided by the rat liver microsomal glucose-6-phosphatase assay. Two known tannins were identified by spectroscopic methods as pinocembrin-7-*O*-[3′′-*O*-galloyl-4′′,6′′-(*S*)-hexahydroxydiphenoyl]-α-D-glucose, named P7OG by us, and gemin D. The structural determination of the isolated compounds was based on spectral data. The ability of the main active component, P7OG, to inhibit human platelet aggregation and to modify vascular reactivity of rat aortic rings incubated with high glucose (D-glucose 55 mM) was then evaluated. P7OG was further able to inhibit platelet aggregation induced by adenosine 5′-diphosphate and collagen, showed vasorelaxant effects in arteries precontracted with phenylephrine, and reverted the endothelium-dependent impairment effect of high glucose in rat aortic rings. In conclusion, one tannin isolated from *P. tenellus* showed promising metabolic, antiaggregant, and vascular effects, which suggests the potential beneficial use of *P. tenellus* to tackle complex cardiometabolic diseases.

Introduction

MS is a highly prevalent, chronic condition that is becoming a serious problem in public health worldwide. It is related to genetic predisposition, physical inactivity, and inadequate eating habits, which induce insulin resistance, glucose and lipid disorders, fat accumulation, and arterial hypertension, increasing the risk of diabetes and cardiovascular disease [1,2]. The vascular wall is one of the main targets where MS exerts its disastrous effects, such as hypertension, increased platelet aggregation, stroke, infarction, atherosclerosis, etc. Among the mechanisms implicated in the development of cardiovascular complications in patients with MS and diabetes, there are two very important ones. One is platelet hyperreactivity, which accelerates atherosclerosis and thrombosis leading to ischaemic events mediated by an enhanced platelet production of COX 1 and 2 as a source of aspirin-escaping thromboxane formation [3]. The other mechanism is the impairment of endothelial-dependent vasodilation, induced by hyperglycaemia in several ways, mainly due to lessening of NO bioavailability. This diminution is due to an increased production of reac-

ABBREVIATIONS

1D NMR	one dimensional nuclear magnetic resonance spectroscopy
AA	arachidonic acid
ACh	acetylcholine
ADP	adenosine 5′-diphosphate
AIF	acetone-insoluble fraction
AF	acetone-soluble fraction
COX	cyclooxygenase
G-6-Pase	glucose-6-phosphatase
HG	high glucose
HG-Krebs	Krebs high-glucose solution
KHB	Krebs Henseleit solution
MWSF	methanol: water-soluble fraction
MWIF	methanol: water-insoluble fraction
MS	metabolic syndrome
ME	methanolic extract
NO	nitric oxide
P7OG	pinocembrin-7-O-[3′′-O-galloyl-4″,6″-(S)-hexahydroxydiphenoyl]-α-D-glucose
PRP	platelet-rich plasma
RP-18	reverse phase 18
PE	phenylephrine
PPARs	peroxisome proliferator activated receptors

tive oxygen species that scavenges part of the NO and reduces the activity of the rest. This last condition can be mimicked in the lab using incubation of arterial rings with HG (55 mM) [4].

The treatment of chronic metabolic conditions includes lifestyle changes, such as a healthy diet and regular physical activity [5]. However, when cardiometabolic disease is established, it is necessary to include medication to help the patient recover to normal values and decrease symptoms, and help the body reverse the damaging changes established due to the disease. The medication has problems itself, such as staggering costs [6] in addition to secondary effects. In this sense, the search for new drugs that reduce symptoms and complications associated with them would be desirable.

Based on the perception that phytotherapy is less expensive and better than modern medicine, rural communities of Latin America use medicinal plants to treat metabolic diseases [6]. However, there are only a few phytochemical and pharmacological studies that scientifically support the medicinal properties of the plants that are associated with the prevention of progression of hyperglycaemic complications [7, 8]. *Phyllanthus tenellus* Roxb. (Phyllanthaceae) is a small shrub of widespread distribution throughout most tropical and subtropical countries, such as Venezuela and Colombia [9]. In South America, the decoction of the leaves of *Phyllanthus* has been used as a popular remedy to control blood glucose levels and hypertension [10–12]. The *Phyllanthus* genus represents one of the largest sources of tannins, flavonoids, lignins, triterpenoids, and securinine-type alkaloids, with more than 500 isolated compounds, few of which have been associated with antidiabetic or cardiovascular effects [13]. A phytochemical study reported the presence of tannins in its leaves [14]; however, there are scarce studies dealing with their biological effects. This study was therefore undertaken to perform a phytochemical analysis of *P. tenellus* leaves, guided by a rat liver microsomal G-6-Pase bioassay that may be a useful method to determine substances that reduce glycaemia [15].

The main active compound in *P. tenellus* was evaluated for its capacity to inhibit human platelet aggregation *ex vivo* and its ability to prevent the effect of HG in vascular reactivity experiments in rat aortic rings. We wanted to understand if one molecule can simultaneously tackle some MS and diabetes-related pathologic conditions, such as the hyperglycaemia, increased platelet activation, and endothelial dysfunction.

Results

▶ **Table 1** shows the effect of the guided fractionation on the activity of G-6-Pase. Only the MWSF (54 % inhibition), not the MWIF, had an effect on G-6-Pase. After evaporation of the solvent, only

▶ **Table 1** Effects of *P. tenellus* tannins on hepatic microsomal G-6-Pase and human platelet aggregation.

Compound	Intact microsomes G-6-Pase activity (%)		G-6-P IC_{50} (μM) (Intact microsomes)	Aggregation IC_{50} (μM)	
				ADP	Collagen
Extract	1.06 ± 0.02	(59)	–	–	–
MWSF	1.02 ± 0.02	(54)	–	–	–
MWIF	2.10 ± 0.40	(4)	–	–	–
AF	0.80 ± 0.20	(69)	–	–	–
AIF	2.60 ± 0.10	(0)	–	–	–
Phlorizin	2.00 ± 0.10	(23)	486	–	–
P7OG	0.43 ± 0.04	(83)	17.20	26	61
Gemin D	1.80 ± 0.07	(32)	106	–	–

G-6-Pase activity is expressed as μmol phosphate released/h/mg of protein and each value represents the average of 5–9 separate experiments ± standard deviation. Numbers in parentheses refer to percentage of inhibition. The IC_{50} was determined using a G-6-Pase assay in intact microsomes with 1 mM G-6-P in the presence of increasing concentrations (including values below and above the IC_{50}) of the compounds. The results are the means of three different experiments ± standard deviation and expressed in μM.

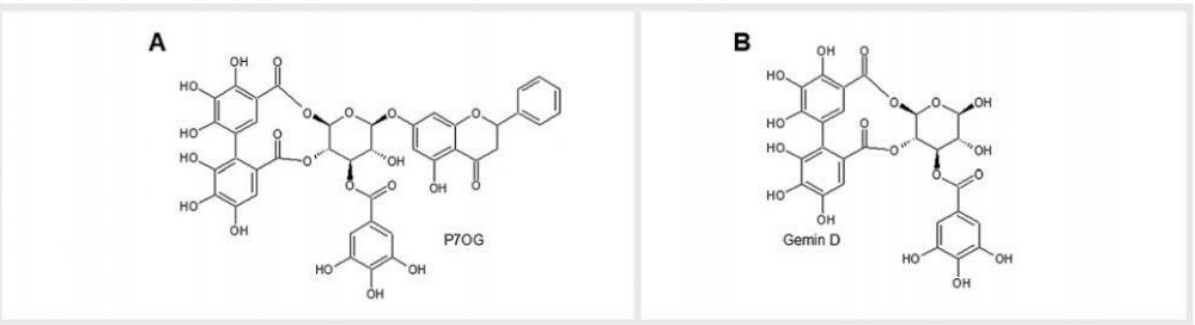

▶ **Fig. 1** Structures of the active compounds isolated from *P. tenellus*. **A** Pinocembrin-7-*O*- [3″-*O*-galloyl-4″,6″-(*S*)-hexahydroxydiphenoyl]-α-D-glucose (P7OG) and **B** gemin D.

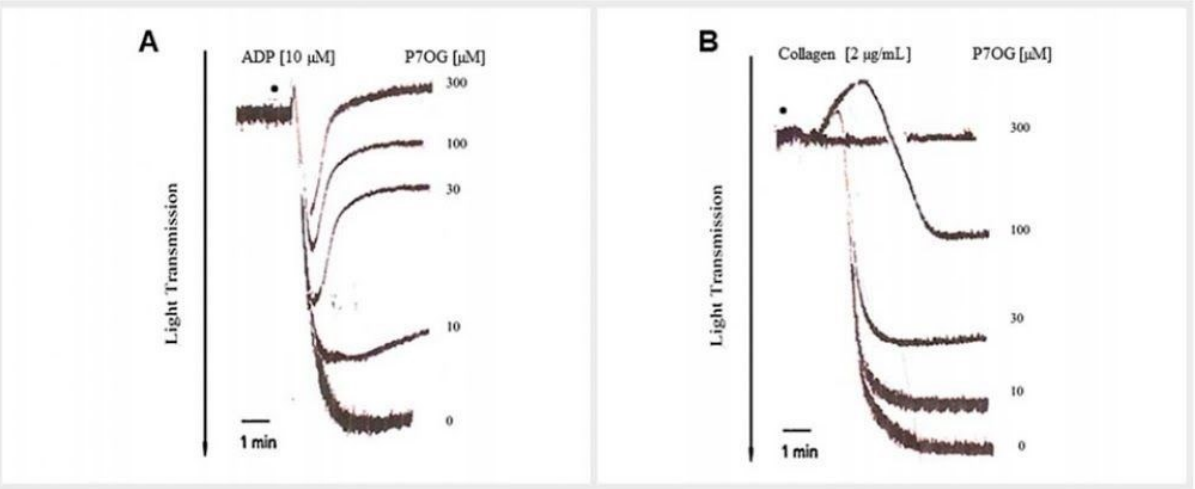

▶ **Fig. 2** Representative original tracing of the platelet aggregation responses was monitored by change in the light transmission over time. It shows the concentration-dependent inhibition of compound P7OG on human platelet aggregation induced by ADP (**A**) and collagen (**B**) in PRP. These original tracings are representative of ten curves done for each agonist. Platelets in PRP were preincubated with increasing concentrations (0–300 µM) of P7OG or 0.25% DMSO (control, **Fig. 8S**, Supporting Information) for 10 min, then platelet aggregation was stimulated by the addition of ADP (10 µM) or collagen (2 µg/mL) at 37 °C under 1000 rpm stirring.

the AF (69% inhibition), not the AIF, showed an effect on the G-6-Pase assay. From the AF (1 g), two known tannins were obtained by chromatographic separation. The structures of the isolated compounds were characterised by 1D NMR experiments and identified by comparison with spectroscopic data available in the literature [14, 16] as pinocembrin-7-O-[3″-O-galloyl-4″,6″-(S)-hexahydroxydiphenoyl]-α-D-glucose, named P7OG by us (243.5 mg), and gemin D (151 mg) (▶ **Fig. 1** and **Figs. 1S–8S**, Supporting Information). As also shown in ▶ **Table 1**, P7OG exhibited the greatest inhibition effect on the G-6-Pase (83% inhibition) assayed in intact microsomes among the isolated compounds tested. The positive control phlorizin exhibited a lower effect. On the other hand, in disrupted microsomes, the tested compounds had no effect on the G-6-Pase enzyme (data not shown). Thus, the IC_{50} determination was carried out using only intact microsomes. IC_{50} values of the isolated compounds were less than 25 times compared to the positive control.

In PRP, stimulation of human platelet aggregation with ADP or collagen was effectively inhibited by P7OG in a concentration-dependent manner. In ▶ **Fig. 2**, the left panel (A) shows that P7OG has no effect on the well-known ability of ADP to induce platelet shape change, even at the maximal dose (300 µM) at which P7OG completely inhibited the aggregation response stimulated by ADP. For semiquantification of the inhibitory effects of P7OG, the percent of reduction in the maximum aggregation amplitude of ADP and collagen responses were measured 10 min after the addition of the stimulus, at each concentration of P7OG used. From the data presented in ▶ **Fig. 2**, IC_{50} values of 26 ± 5 µM and 61 ± 8 µM (n = 10) were estimated as the potency of P7OG to inhibit platelet aggregation responses induced by ADP and collagen, respectively, which were significantly different ($p < 0.05$)

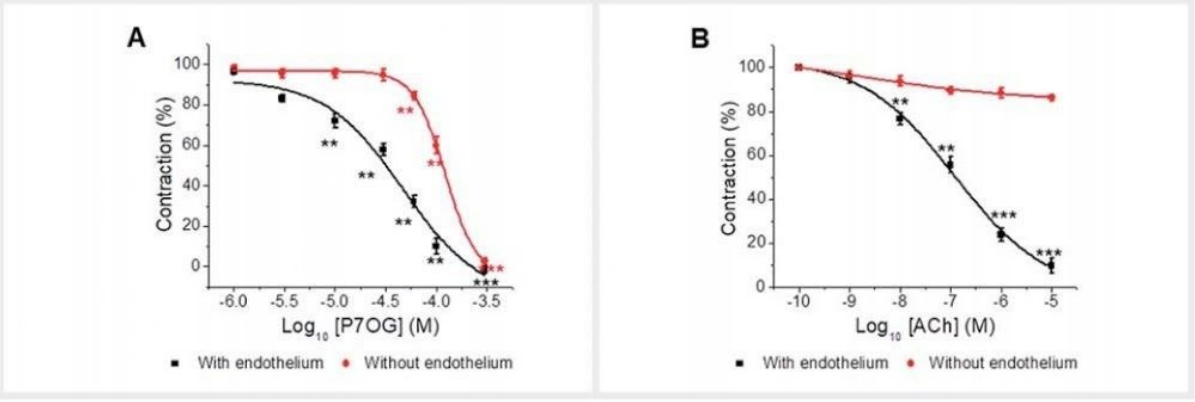

▶ **Fig. 3** Vasorelaxant effect of P7OG on isolated rat aortic rings. **A** Cumulative concentration-responses to P7OG (1 to 300 µM) in preparations with (black) and without (red) endothelium stimulated with PE (1 µM). Results are expressed as the mean ± SEM of five experiments. **B** The control curves show the effectiveness of endothelium removal (red) and the typical endothelium-induced relaxation in healthy vessels (black). Results are expressed as the mean ± SEM of six experiments. Unpaired t test with Welch's correction (* $p < 0.05$, ** $p < 0.01$, and *** $p < 0.001$).

from each other. In contrast, platelet aggregation induced by epinephrine, U-46619, or AA was not inhibited by P7OG 300 µM (not shown).

The effects of P7OG on rat aortic rings were studied with two sets of experiments. First, in arteries with intact endothelium (E+, black) or without endothelium (E-, red) precontracted with PE, cumulative concentration-response curves to P7OG (1–300 µM) were constructed. In E+ arteries, P7OG showed a significant relaxant effect (IC_{50} 35 ± 4 µM, E_{max} 92 ± 4%, n = 5) and had a minor effect on E- rings (IC_{50} 105 ± 7 µM, E_{max} 95 ± 4%, n = 5) (▶ **Fig. 3A**). ▶ **Fig. 3B** shows (the control) the known effect of ACh on E+ and E- aortic rings. P7OG up to 100 µM had no effect on baseline tension in rat aortic rings (not shown). Part of the control rings were similarly treated with PE 1 µM, and then the vehicle (DMSO 0.5%) was added as described [17]. The solvent had no effect on the precontractile force.

The second experiment was designed to evaluate the effect of P7OG on the impairment of endothelium-dependent relaxation induced by HG. As shown in ▶ **Fig. 4**, when aortic rings were preincubated for 6 h with HG (red closed circle), the E_{max} of ACh decreased from 89 ± 5% (n = 5) to 44 ± 11% (n = 6). However, the aortic rings incubated with P7OG (red open circles) improved the capability of relaxation induced by ACh in HG-Krebs solution, indicating that the deleterious effects of HG levels were noticeably attenuated. P7OG mildly improved the relaxation ability of the control rings (black symbols).

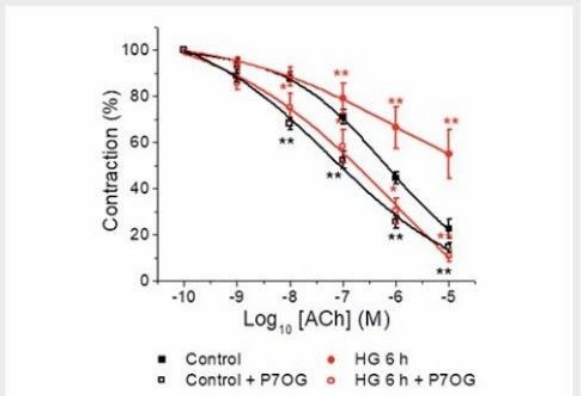

▶ **Fig. 4** Vasorelaxation induced by increasing concentrations of ACh on PE-contracted rat aortic rings preincubated for 6 h with a solution with D-glucose 5.5 mM (control, closed black squares), D-glucose 5.5 mM plus P7OG 10 µM (control + P7OG, open black squares), D-glucose 55 mM (HG 6 h, closed red circles), and D-glucose 55 mM plus P7OG 10 µM (HG 6 h + P7OG, open red circles). Results are expressed as the mean ± SEM of five or six experiments. Unpaired t test with Welch's correction (* $p < 0.05$, ** $p < 0.01$, and *** $p < 0.001$).

Discussion

The pathophysiology of metabolic chronic diseases such as MS and diabetes involves hyperglycaemia, increased platelet activation, and endothelial dysfunction that lead to metabolic and vascular complications in several population groups [1, 2, 18]. We performed this study to evaluate if *P. tenellus*, used in folk medicine as an antidiabetic plant, has potential uses to simultaneously tackle part of the MS and diabetes-related features. Our main findings were: i) two tannins with an effect on G-6-Pase were isolated and its structure determined, ii) the compound P7OG showed a potent inhibitory effect on G-6-Pase, iii) P7OG inhibited platelet aggregation responses induced by ADP and collagen, and iv) P7OG also showed intrinsic vasorelaxant properties and reverted the HG-induced endothelial dysfunction in rat aortic rings.

Phytochemical and molecular considerations on the effects of *Phyllanthus tenellus* compounds

Using bioassay-guided fractionation of the ME of *P. tenellus*, we report the isolation of P7OG as the main component responsible for

the enzymatic inhibition of G-6-Pase of this extract. The inhibition of G-6-Pase by P7OG in intact microsomes, but not in disrupted ones, is a clear indication that they interact with the G-6-P transporter (T1) of the G-6-Pase system with no effect on the catalytic subunit. It is interesting to point out that these tannins behave in a similar way to phlorizin, only inhibiting the T1 transporter [19]. The comparison of the structures of P7OG and gemin D suggests that the lowest IC_{50} and the highest percentage of inhibition of P7OG on G-6-Pase is explained by the addition of the flavonoid moiety on the ellagitannin skeleton. These findings suggest that this combination of tannins and flavonoid moieties is in concordance with the particular interaction between the polyphenolic residue on the G-6-P transporter (T1), because the complex formation between proteins and tannins, in which gallic acid is usually one of the main components, is well known [20]. This inhibitory effect of P7OG on G-6-Pase may lead to reduced glycaemic values in patients with chronic metabolic diseases.

Based upon the central roles played by platelets in the complications arising in patients with MS and diabetes, we evaluated the possible action of P7OG on *in vitro* human platelet aggregation. Experiments carried out using PRP clearly showed that P7OG inhibited platelet aggregation induced by ADP or collagen. When platelets were stimulated by AA, U-46619, or epinephrine, no inhibition response was seen, even in high concentrations (300 µM) of P7OG, suggesting that P7OG does not inhibit COX activity. The biological reason for its selective effect on platelet aggregation needs to be studied further. This protective effect of P7OG may lead to reduced cardiovascular (mainly ischaemic) complications in patients with MS and diabetes, which needs to be tested in other experimental models.

HG levels in blood have deleterious effects on vascular endothelial cells generating impaired endothelium-dependent relaxation. These alterations appear not to be caused by hyperosmotic conditions, as both normal glucose and HG-incubated cells have been shown to have the same osmotic pressure [4]. Endothelial dysfunction is the main cause of vascular disease due to hyperglycaemia and diabetes. In this study, we evaluated the effect of P7OG on the normal endothelium and on the endothelial dysfunction induced by HG in aortic rings isolated from nondiabetic rats. P7OG had a vasorelaxant effect on both E- and E+ preparations. However, the lower IC_{50} obtained for the E+ arteries suggests that the relaxant effect was mainly mediated by the endothelium. On the other side, the aortic rings incubated with P7OG retained or improved its capability of relaxation induced by ACh in HG-Krebs solutions, indicating that the deleterious effects of HG levels were attenuated. P7OG is a complex tannin and its effect is in accordance with experimental results that demonstrate that tannins could act as an antioxidant, preventing lipid peroxidation and cell death without affecting the production of reactive oxygen species. Therefore, it is possible that the effect of P7OG against HG-induced endothelial dysfunction in the rat aorta is related to inhibiting the decrease of NO synthase activity. A complementary way, evidenced in other molecules with positive effects on improving vasodilation in spite of HG, is the beneficial effect resulting from interactions with PPAR transcription factors [4]. A future work is to determine if P7OG has an effect on the expression of one isoform of PPARs.

There are current problems with the pharmacological treatment of chronic metabolic diseases. Most of the drugs act on a single target and this is not enough to control the condition. P7OG is a compound with antidiabetic, antiplatelet, vasorelaxant, and endothelium protective properties, which makes it a potential drug to tackle several of the key elements of the pathophysiological sequence of conditions such as MS and subsequent complications such as diabetes and ischaemic events. Then, P7OG would be very useful in a large group of patients with several metabolic and cardiovascular comorbidities. Tackling several conditions with a single compound would reduce the problems associated with polymedication, such as high costs, adverse effects, discontinuance, or change in medications. P7OG is now an interesting candidate drug for future clinical studies.

In conclusion P7OG, isolated from *P. tenellus*, showed promising metabolic, antiaggregant, and vascular effects, which suggests its potential of beneficial use to tackle cardiometabolic diseases such as MS and diabetes. The use of a broad spectrum, single molecule in such a complex disease would be advantageous over other treatments that rely on polymedication.

Materials and Methods

Plant material

P. tenellus leaves were collected in September 2008 at the Venezuelan Central University Campus (Caracas, Venezuela) and were identified by Dr Stephen Tillett. A voucher specimen was deposited in the 'Manuel Ovalles' Herbarium at the Pharmacy Faculty of the Venezuelan Central University (voucher number: MYF21992).

Extraction and isolation

Compounds isolation and reagents

The isolation of the active compounds of *P. tenellus* (32 g) was initiated by its fractionation based on differences in solubility at room temperature using methanol : water 1 : 1 (1 L × 3), a procedure that generated an MWSF (26.1 g) and an MWIF (5.3 g). Since only the MWSF had an effect on G-6-Pase, this fraction was extracted with acetone at room temperature (250 mL × 3), obtaining two new fractions, a brownish residue (9.8 g) named AIF and a yellowish solution from which a yellowish residue named AF was yielded (15.7 g). After evaporation of the solvent, only AF showed an effect on the G-6-Pase assay. Subsequently, the fraction AF (1 g) was chromatographed on RP-18 column chromatography and eluted with a acetonitrile-water mixture (2 : 3) to yield two fractions, A and B. These fractions were evaporated in vacuum using a rotary evaporator to obtain Gemin D and pinocembrin-7-O-[3″-O-galloyl-4″,6″-(S)-hexahydroxydiphenoyl]-α-D-glucose, respectively.

^{1}H and ^{13}C NMR spectra were obtained using a Bruker DRX 500 (500 MHz for ^{1}H and 125 MHz for ^{13}C) in deuterated dimethylsulfoxide (DMSO-d_6; Sigma-Aldrich). ADP was obtained from Sigma. Collagen was from Helena Laboratories. All solvents used were of HPLC grade quality and obtained commercially from Sigma-Aldrich. The following drugs used for vascular reactivity experiments were also purchased from Sigma-Aldrich: phlorizin, D-glucose, ACh, and PE. Reversed phase C18 was used for low-pressure

column chromatography and silica gel 60 RP18 F254 (Merck) for TLC on glass (Merck). TLC plates were sprayed with a saturated solution of ceric sulfate in 65% sulfuric acid (Sigma-Aldrich) and heated to 120 °C.

Experimental procedures with humans and animals

Humans and animals

The human part of the study was approved by the Bioethical Committee of the Venezuelan Institute for Scientific Research (IVIC; minutes number 1316, March 2009), following the guidelines of the Declaration of Helsinki and Tokyo for investigations in humans. All volunteers, healthy adults, gave informed consent. Humans did not take any drugs during the previous 2 weeks of the study. By clean venipuncture, blood samples were obtained for platelet aggregation assays.

The animal part of the study was evaluated and approved by the Bioethics Commission for Investigations in Animals at the IVIC (Protocol 201417, approval on November 2014), in accordance with the Code on Bioethics and Biosecurity (2008) established by the Bioethics Commission National Fund on Science and Technology (FONACIT), under the national legislation. Male Sprague-Dawley rats weighing 240–350 g were used for liver microsomal G-6-Pase and vascular reactivity assays and were obtained from the animal care service of IVIC. They were housed at room temperature (21 ± 2 °C) and light-dark (12 : 00–12 : 00 h), with a maximum of four rats per acrylic, transparent, rectangular cage, with wood-derived bedding. Food and tap water were freely available at the conventional animal facilities of the IVIC.

Microsome purification and glucose-6-phosphatase assays

Liver microsomes were purified as described elsewhere [21] from rats fasted overnight. The microsomal fraction was resuspended in 0.25 mM sucrose, 1 mM $MgCl_2$, and 5 mM HEPES, pH 6.5, to give a final protein concentration of 20 mg/mL and frozen at − 80 °C until use. Protein concentration was estimated using the modification of the Lowry method [22]. Enzymatic G-6-P assays were performed according to the method described by Burchell et al. [23] with intact and disrupted microsomes. For IC_{50} determinations, solutions of 1 mM of compounds were made in 10% DMSO and added to the assay tube at a final concentration of 50 µM. The final concentration of DMSO in the control and experimental assays was 0.5%. Phlorizin, prepared from a stock solution of 2.5 mM made in water, was used as a positive control at the same concentration as the isolated compounds [24]. The G-6-Pase assay was carried out with 1 mM G-6-Pase using intact microsomes as described previously in the presence of increasing concentrations of the abovementioned extract, fractions, and compounds. All microsomes used were at least 95% intact as determined by the hydrolysis of mannose-6-phosphate [25].

Blood collection and platelet preparation

Blood was obtained by clean venipuncture from 10 healthy human donors. PRPs were obtained according to the method of Cazenave et al. [26] with modifications. Briefly, blood samples were collected, discarding the first 2 or 3 mL, into 3.2% (109 mM) trisodium citrate dihydrate (1 : 9 v/v, citrate to blood) and centrifuged at 160 × *g* for 15 min, with no break, at room temperature. PRP (the upper phase) was isolated and the remaining lower phase was further centrifuged at 1500 × *g* for 15 min at room temperature to obtain PPP, which is used to determine 100% light transmittance in platelet aggregation assays.

Aggregation assays

Platelet aggregation was monitored by Born's method [27]. Briefly, 400 µL of PRP (3×10^5 platelets/µL) were incubated and stirred at 1000 rpm for 1 min at 37 °C in an optical aggregometer (Chrono-Log 490) connected to a dual channel recorder. The aggregometer was calibrated so that PRP gave 10% light transmission while PPP gave 90% light transmission. Inhibition experiments were done by incubating the platelets with increasing concentrations of the active compounds (0–300 µM) or 0.25% DMSO (control) for 10 min before the addition of ADP (10 µM), collagen (2 µg/mL), epinephrine (50 µM), AA (0.5 mM), or U-46619 (1 µM) at 37 °C under 1000 rpm stirring.

Vascular reactivity assays

The rats were anaesthetised with sodium pentobarbital (60 mg/kg, intraperitoneal) and the chests were opened by midline incision to isolate the descending thoracic aorta. After removal of the superficial fat and connective tissue, the rings with intact endothelium (E+) were placed in a 10-mL organ chamber containing physiological salt solution, constantly bubbled with a mixture of 95% O_2/5% CO_2 and maintained at 37 °C. The composition of physiological salt solution was as follows (mM): NaCl, 118; KCl, 4.7; KH_2PO_4, 1.2; $MgSO_4$, 1.2; $NaHCO_3$, 15; glucose, 5.5; $CaCl_2$, 2.5. The rings were stretched until an optimal basal tension of 2 g was reached, previously determined by length-tension relationship experiments, and then were allowed to equilibrate for 2 h with the bath fluid being changed every 15–20 min. Mechanical stability of the system was tested by adding KCl 50 mM, three times. Aortic rings were repeatedly washed and allowed to reequilibrate for an additional 30 min. Endothelial integrity was assessed qualitatively by the degree of relaxation caused by ACh (10 µM) in the presence of the contractile tone induced by PE (1 µM). In some rings (E-), the endothelial layer was removed immediately after dissection by gently rubbing the luminal surface with a small wooden stick. Only one experiment was carried out in each aorta ring. Isometric tensions were recorded on a polygraph (PowerLab 4/26; PanLab) by means of a force displacement transducer ML201. Data were fed to a computer and a LabChart system (PanLab) was used to convert acquired data into digital form. For P7OG assays, PE 1 µM precontrated E+ and E- rings were exposed to increasing (1–300 µM) P7OG concentrations. For HG experiments, the first ring (control), was incubated in KHB, the second ring was incubated in KHB with high glucose (HG; 55 mM), and the third ring was incubated in KHB with HG plus P7OG 10 µM. A KHB plus P7OG 10 µM group was also recorded. All rings were incubated for 6 h. After this period, rings were precontracted with PE 1 µM, and once a stable contraction was achieved, cumulative concentration-response curves to ACh were obtained. Maximum relaxation (E_{max}) and concentration producing the half-maximal effect (EC_{50}) were determined from each concentration-response curve. The relaxation from the precontracted level to baseline was considered 100% relaxation.

Statistics

Values are expressed as means and standard error of the mean (SEM). Statistical analysis was performed applying one-way ANOVA using GraphPad Prism (version 6.1) software. Statistical comparisons between two data means were made using an unpaired t test with Welch's correction, and p values less than 0.05 were considered statistically significant. The vasorelaxing response was expressed in terms of percent decrease of the maximal contraction caused by PE (1 μM). The IC_{50} value was defined as the concentration of the compound that reduced the maximum contraction elicited by PE by 50% and was calculated from a concentration-response curve, which was analysed by nonlinear regression (curve fit) using GraphPad Prism (Version 6.1).

Supporting Information

1D NMR spectra for the isolated compounds and DMSO control experiments for platelet aggregation assays are available as Supporting Information.

Acknowledgements

We would like to dedicate this work to the memory of Professor Masahisa Hasegawa. May his work and aspirations be fulfilled. The present work was supported by grants 20071585 from *FONACIT*, Venezuela and CODI-University of Antioquia grant to R. N. S., according to minutes 666 from September 10, 2013, code 2581. We thank Dr. Sara Pekerar (IVIC) for the helpful cooperation in the NMR experiments.

Conflict of Interest

The authors declare no conflict of interest.

References

[1] Lakka HM, Laaksonen DE, Lakka TA, Niskanen LK, Kumpusalo E, Tuomilehto J. The metabolic syndrome and total and cardiovascular disease mortality in middle-aged men. JAMA 2002; 288: 2709–2716

[2] Alberti KG, Eckel RH, Grundy SM, Zimmet PZ, Cleeman JI, Donato KA. Harmonizing the metabolic syndrome: a joint interim statement of the International Diabetes Federation Task Force on Epidemiology and Prevention; National Heart, Lung, and Blood Institute; American Heart Association; World Heart Federation; International Atherosclerosis Society; and International Association for the Study of Obesity. Circulation 2009; 120: 1640–1645

[3] Santilli F, Vazzana N, Liani R, Guagnano M, Davi G. Platelet activation in obesity and metabolic syndrome. Obes Rev 2012; 3: 27–42

[4] Wu Y, Xue L, Du W, Huang B, Tang C, Liu C. Polydatin restores endothelium-dependent relaxation in rat aorta rings impaired by high glucose: a novel insight into the PPARβ-NO signaling pathway. PLoS One 2015; 10: e0126249

[5] Sperling L, Mechanick J, Neeland I, Herrick C, Despres J, Ndumele C, Vijayaraghavan K, Handelsman Y, Puckrein G, Araneta M, Blum Q, Collins K, Cook S, Dhurandhar N, Dixon D, Egan B, Ferdinand D, Herman L, Hessen S, Jacobson T, Pate R, Ratner R, Brinton E, Forker A, Ritzenthaler L, Grundy S. The Cardiometabolic Health Alliance: working toward a new care model for the metabolic syndrome. J Am Coll Cardiol 2015; 66: 1050–1067

[6] Buffery D. Cardiometabolic health in 2014: clinical and economic implications. Am Heart Drug Benefits 2014; 7: 427–428

[7] Eddouks M, Maghrani M, Lemhadri A, Ouahidi ML, Jouad H. Ethnopharmacological survey of medicinal plants used for the treatment of diabetes mellitus, hypertension and cardiac diseases in the south-east region of Morocco (Tafilalet). J Ethnopharmacol 2002; 82: 97–103

[8] Barbosa-Filho JM, Vasconcelos THC, Alencar AA, Batista LM, Oliveira RAG, Guedes DN, Falcão HS, Moura MD, Diniz MF, Modesto-Filho J. Plants and their active constituents from South, Central, and North America with hypoglycemic activity. Rev Bra Farmacogn 2005; 15: 392–413

[9] Hoffmann P, Kathriarachchi H, Wurdack KJ. A phylogenetic classification of *Phyllanthaceae* (*Malpighiales; Euphorbiaceae sensu lato*). Kew Bull. 2006; 61: 37–53

[10] Sarin B, Verma N, Martín JP, Mohanty A. An overview of important ethnomedicinal herbs of *Phyllanthus* species: present status and future prospects. Sci World J 2014; 2014: 839172

[11] Calixto JB. The plants of the genus Phyllanthus as a potential source of new drugs. Ciênc Cult 1997; 49: 422–432

[12] Shanmugam S, Manikandan K, Rajendran K. Ethnomedicinal survey of medicinal plants used for the treatment of diabetes and jaundice among the villagers of Sivagangai District, Tamilnadu. Ethnobot Leaflets 2009; 13: 189–194

[13] Mao X, Wu LF, Guo HL, Chen WJ, Cui YP, Shi LQ, Liang WY, Yang GH, Shao YY, Zhu D, She GM, You Y, Zhang LZ. The genus *Phyllanthus*: an ethnopharmacological, phytochemical, and pharmacological review. Evid Based Complement Alternat Med 2016; 2019: 7584952

[14] Huang Y, Chen C, Hsu F, Chen C. Two tannins from *Phyllanthus tenellus*. J Nat Prod 1998; 61: 523–524

[15] McCormack JG, Westergaard N, Kristiansen M, Brand CL, Lau J. Pharmacological approaches to inhibit endogenous glucose production as a means of anti-diabetic therapy. Curr Pharm Des 2001; 7: 1451–1474

[16] Wang H, Liu Y, Feng C. Isolation and identification of a novel flavonoid from *Penthorum chinense* P. J Asian Nat Prod Res 2006; 8: 757–761

[17] Estrada O, González-Guzmán JM, Salazar-Bookaman M, Fernández A, Cardozo A, Alvarado-Castillo C. Pomolic acid elicits endothelium-dependent relaxation in rat aortic rings. Phytomedicine 2011; 18: 464–469

[18] Narvaez-Sanchez R, Calderón JC, Vega G, Trillos MC, Ospina S. Skeletal muscle as a protagonist in the pregnancy metabolic syndrome. Med Hypotheses 2019; 126: 26–37

[19] Arion WJ, Lange AJ, Walls HE. Microsomal membrane integrity and the interactions of phlorizin with the glucose-6-phosphatase system. J Biol Chem 1980; 255: 10387–10395

[20] Spencer CM, Cai Y, Martin R. Polyphenol complexation some thoughts and observations. Phytochemistry 1988; 27: 2397–2409

[21] Marcucci OL, González-Mujica F, Perez-Ayuso E. Alterations of liver nuclear envelopes accompanying thioacetamide administration in rats. Act Cien Ven 1983; 34: 109–117

[22] Markwell M, Hass S, Bieber L, Tolbert N. A modification of the Lowry procedure to simplify protein determination in membrane and lipoprotein sample. Anal Biochem 1978; 87: 206–210

[23] Burchell A, Hume R, Burchell B. A new microtechnique for the analysis of the human hepatic microsomal glucose-6-phosphatase system. Clin Chim Act 1988; 173: 183–192

[24] Estrada O, Hasegawa M, Gonzalez-Mujica F, Motta N, Perdono E, Solórzano A, Méndez J, Méndez B, Zea EG. Evaluation of flavonoids from *B. megalandra* leaves as inhibitors of glucose-6-phosphatase system. Phytother Res 2005; 19: 859–863

[25] Gonzalez-Mujica F, Motta N, Márquez A, Capote-Zulueta J. Effects of *Bauhinia megalandra* aqueous leaf extract on intestinal glucose absorption and uptake by enterocyte brush border membrane vesicles. Fitoterapia 2003; 74: 84–90

[26] Cazenave J, Ohlmann P, Cassel D, Eckly A, Hechler B, Gachet C. Preparation of washed platelet suspensions from human and rodent blood. Methods Mol Biol 2004; 272: 13–28

[27] Born G. Aggregation of blood platelet by adenosine diphosphate and its reversal. Nature 1962; 194: 927–929

Anexo dos:

Romero-Imbachi MR; Cupitra NI; Ángel K; González B; Estrada O; Calderón JC; Guerrero-Vargas J; Beltrán J; Narvaez-Sanchez R, 2020. *Centruroides margaritatus* scorpion complete venom exerts cardiovascular effects through alpha-1 adrenergic receptors.

Artículo publicado en Comparative Biochemistry and Physiology Part C: Toxicology &

Pharmacology; IF: 2.89

Enlace: https://www.sciencedirect.com/science/article/abs/pii/S1532045620302398

En agosto de 2018, se participó como cotutor en el trabajo de grado “efecto vasomotor inducido por el veneno total de Centruroides margaritatus en anillos aórticos de ratas (Rattus norvegicus) cepa Wistar” de Margarita Rosa Romero Imbachí, estudiante de biología de la Universidad del Cauca. Durante su pasantía en el laboratorio del grupo PHYSIS, donde se acompañó en el desarrollo de los experimentos en VR de aorta de ratas, orientando y capacitando a la estudiante, con el acompañamiento de JC Calderón, MD PhD y bajo la dirección de R Narvaez-Sanchez- MD PhD. De esta interacción se dio como resultado la formación de una estudiante de pregrado y la publicación del trabajo “Centruroides margaritatus scorpion complete venom exerts cardiovascular effects through alpha-1 adrenergic receptors”

A continuación, el artículo correspondiente al anexo dos.

Contents lists available at ScienceDirect

Comparative Biochemistry and Physiology, Part C

journal homepage: www.elsevier.com/locate/cbpc

Centruroides margaritatus scorpion complete venom exerts cardiovascular effects through alpha-1 adrenergic receptors

Margarita Rosa Romero-Imbachi [a,b], Nelson Cupitra [a], Karen Ángel [b], Beatriz González [c], Omar Estrada [c], Juan C. Calderón [a], Jimmy Guerrero-Vargas [b], José Beltrán [b], Raul Narvaez-Sanchez [a,*]

[a] Physiology and Biochemistry Research Group-PHYSIS, Faculty of Medicine, University of Antioquia, Medellin, Colombia
[b] Herpetological and Toxinological Research Group, Faculty of Natural, Exact and Educational Sciences, University of Cauca, Popayán, Colombia
[c] Laboratory of Cellular Physiology, Center for Biophysics and Biochemistry, Venezuelan Institute for Scientific Research, Venezuela

ARTICLE INFO

Keywords:
Artery
Centruroides margaritatus
Scorpion venom
Vasomotor

ABSTRACT

Centruroides margaritatus scorpion stings are common in Colombia. However, the cardiovascular toxicity of the venom has not been clarified. Aim: To study the effect and mechanisms of action of the complete venom of *C. margaritatus* (CmV) on the murine cardiovascular system. Methods: We evaluated the *in vivo* effect of CmV LD50 on the mean arterial pressure (MABP), heart rate, and surface electrocardiogram in male adult normotensive Wistar rats. *Ex vivo*, we evaluated the vascular reactivity of rat aortic rings to increasing concentrations (1 to 60 μg/mL) of CmV using the blockers L-NAME, indomethacin, seratrodast, and prazosin. Results: In the first hour of poisoning, CmV increased the MABP. In the second hour after poisoning, the heart rate decreased as the normalized PR interval and QT corrected increased. After that, cardiovascular shock was demonstrated by a drastic fall in the MABP and signs of cardiac conduction system block. In aortic rings, CmV caused a direct vasoconstrictor effect mediated by alpha-1 adrenergic receptors and counteracted by nitric oxide. Conclusion: The direct vascular and probably the cardiac alpha-1 effects likely explain the transient hypertension and the maintenance of cardiac function, while interval lengthening may be due to K^+ channel blockage. Afterwards, the effects of both the alpha-1 pathway and the K^+ channel pathway converged, resulting in fatal cardiovascular shock. This knowledge could aid in understanding the dynamics of the effects of the venom and in designing treatments to address its cardiovascular effects.

1. Introduction

Scorpion stings are the second most frequent human accident involving poisonous animals. More than a million cases are reported every year worldwide, causing more than three thousand deaths per year (Chippaux and Goyffon, 2008; Minghui et al., 2019). The species of the Buthidae family are dangerous due to the toxicity of their venom. Within this family, species of the genus *Centruroides* are very common in South America; of these, *Centruroides margaritatus* is particularly abundant in western Colombia (Armas et al., 2012), where their synanthropic habits cause a high frequency of accidents.

C. margaritatus complete venom (CmV) has a relatively high lethal dose 50 (LD50) between 42.8 and 59.9 mg/kg when subcutaneously injected into mice (Guerrero-Vargas, 2002; Marinkelle and Stahnke, 1965). It produces mainly local pain, excitability, piloerection, sweating, dizziness, nausea or vomiting and less frequently causes salivation, tachycardia or a weak pulse (Guerrero-Vargas et al., 2014; Marinkelle and Stahnke, 1965). The study of the proteome of the venom of several *Centruroides* species, such as *C. noxius*, *suffusus*, *exilicauda* and *margaritatus*, has demonstrated the presence of peptides such as margatoxins (MgTx) without proteolytic or phospholipase activity but with an effect on several voltage-gated ion channels, especially K^+ channels (Corona et al., 2001; Garcia-Calvo et al., 1993; Guerrero-Vargas, 2008; Gurrola et al., 1999; Nastainczyk et al., 2002), which play a crucial role in

Abbreviations: CCh, carbachol; CmV, complete venom of *C. margaritatus*; DMSO, dimethyl sulfoxide; HR, heart rate; KH, Krebs-Henseleit solution; LD50, lethal dose 50; L-NAME, Nω-nitro-l-arginine methyl ester hydrochloride; MABP, mean arterial pressure; MgTx, margatoxins; NO, nitric oxide; PE, phenylephrine; QTc, QT corrected; VEGF, vascular endothelial growth factor.

* Corresponding author at: Carrera 51 D #62-29 office 203, Medellín, Colombia.
E-mail address: raul.narvaez@udea.edu.co (R. Narvaez-Sanchez).

https://doi.org/10.1016/j.cbpc.2020.108939
Received 1 September 2020; Received in revised form 23 October 2020; Accepted 3 November 2020

returning the depolarized cell to a resting state. This composition leads to diverse neurological and neuromuscular effects, which have been described (Escobar et al., 2008, 2003; Guerrero-Vargas et al., 2014; Marinkelle and Stahnke, 1965).

Several lines of evidence suggest that CmV could have important effects on the cardiovascular system: i) MgTx has the ability to block K^+ channels in endothelial cells, since in human HUVECs, it blocks VEGF-induced hyperpolarization and Ca^{2+} influx, which may reduce the production of VEGF-induced nitric oxide (NO) (Erdogan et al., 2005); ii) in isolated rat kidneys, CmV venom increases renal vascular resistance (Galíndez-Cerón et al., 2019); iii) scorpion venoms, including some from species of the *Centruroides* genus such as *C. margaritatus*, can alter serum electrolytes (Boyer et al., 2013; Sitprija and Sitprija, 2016; Romero-Imbachi, 2018), which could induce cardiovascular alterations and explain some outcomes observed in poisoned children (Osnaya-Romero et al., 2016); and iv) the most common signs of envenomation reflect dysautonomia, with a predominance of the activation of the sympathetic nervous system, which extensively innervates the cardiovascular system. Prior works directly addressing the cardiovascular effects of CmV have shown that sublethal doses induce electrocardiographic alterations in rats, such as long QTc, sinusal and ventricular tachycardias or bundle branch blocks (Arenas, 2010; Bonilla, 2014). The prolongations in the intervals are compatible with the blockade of the K^+ channels by CmV and would contribute to the transient increase in the pressure of the left ventricle that has been observed in rats during the first hour of envenomation (Bonilla, 2014).

Although preliminary evidence suggests that CmV should have a measurable effect on cardiovascular function in mammals, this has not been explored in depth, and the possible mechanisms by which the venom may affect the cardiovascular system have not been explored either. We hypothesize that CmV increases the heart rate (HR), mean arterial blood pressure (MABP) and the risk of arrhythmias in part through alterations in the conduction system of the heart and a direct vascular contractile effect. To test this hypothesis, in this work, we used *in vivo* and *ex vivo* experimental models to study the effect of sublethal doses of CmV on cardiovascular function in rats.

2. Methods

2.1. Animal care and handling

Nineteen normotensive male Wistar rats (300 ± 50 g) were housed in groups in polypropylene boxes at a temperature of 22 ± 2 °C under 12 h of light with access to normal food and water *ad libitum*. The procedures were carried out according to the bioethical requirements of the Colombian Ministry of National Health according to resolution 008430 of 1993 and were approved by the Research Ethics Committee of the University of Cauca through act No. 9 of 12/14/2016 (ID 4681). For all tests, the rats were anesthetized with 60 mg/kg sodium pentobarbital (Penthal, Invet, Colombia) intraperitoneally (IP).

2.2. Drugs

Carbamoylcholine (212385-M; carbachol, CCh), phenylephrine hydrochloride (P6126, PE), Nω-nitro-l-arginine methyl ester hydrochloride (N5751, L-NAME), indomethacin (I8280), prazosin hydrochloride (P7791), and seratrodast (SML1379) were obtained from Sigma–Aldrich Co. (St. Louis, MO, USA). U-46619 (ab144540) was purchased from Abcam (Cambridge, USA). The stock solutions of indomethacin and seratrodast were prepared with dimethyl sulfoxide (DMSO). The maximum concentration of DMSO in the bath was 0.3%. The stock solutions of the other drugs were prepared in distilled water and supplemented with ascorbic acid (10 μM) to avoid oxidation. The saline solution contained 0.9% NaCl.

2.3. Venom preparation

Crude venom was obtained from 80 adult scorpions collected in the municipality of Patía, Department of Cauca, southwest Colombia (collection permit R0152 02/15/2015 from the National Authority for Environmental Licenses, Colombia). They were kept in captivity at the Biomedical Research Center of the University of Cauca. The venom was extracted by electrical stimulation of the telson according to a method described previously (Guerrero-Vargas, 2002) using a DC Square Wave Stimulator 1999 electrical pulse generator (824151IS, Lafayette Instrument Company). The CmV was obtained by centrifugation at 15,000 rpm at 4 °C for 15 min, lyophilized, and stored at −20 °C until use. For each experiment, the CmV was reconstituted in saline solution. The doses were established according to the LD50 (42.8 mg/kg) previously determined by our group (Guerrero-Vargas, 2002).

2.4. Invasive hemodynamics and electrocardiographic measurements

Invasive measurements of MABP are considered the gold standards in a rat model (Parasuraman and Raveendran, 2012). The invasive right femoral MABP and surface electrocardiogram (EKG) were recorded before and after intraperitoneal administration of a single dose of CmV (40 mg/kg). The final volume of the vehicle or venom administered to rats was 0.2 mL. Briefly, once anesthetized, an intratracheal probe was inserted into the animals to maintain ventilation. The right femoral artery was cannulated using a polyethylene catheter prefilled with heparin (50 U/mL) and attached to a fluid-filled pressure transducer (MLT0670, AD Instruments, Sydney, Australia) connected to a precalibrated bridge amplifier (FE117 BP Amp, AD Instruments) to record the MABP and HR using the PowerLab data acquisition system (PL3516/P PowerLab 16/35, AD Instruments). Simultaneously, the EKG was recorded using 3 electrodes (MLA1214, AD Instruments) in the standard position that were connected to a bioamplifier (FE136 Animal Bio Amp, AD Instruments). The data were sampled at a frequency of 500 Hz. The rat body temperature was maintained at 37 °C throughout the procedure using a heating blanket.

After the stabilization of the cardiovascular parameters, all measurements were recorded for 45–50 min before the intraperitoneal administration of the venom, after which the signals were recorded for 190–200 min. Data were analyzed with Labchart Pro 7.2 software (ADInstruments). The DII of the recorded EKG was used to calculate the HR, QRS, PR, and QT intervals with the same software. Bazett's equation was selected to calculate the QT corrected (QTc) interval. The HR and MABP results are shown as absolute values, and the EKG results are shown as normalized values. Analyses were done comparing all data points to the first control value.

2.5. Ex vivo vascular reactivity

The isolated rings of the aorta are the model of choice to evaluate the potential direct effects of substances on arteries since they are not affected by the presence of other tissues (Ramírez et al., 2007). Furthermore, the use of specific blockers of molecules that modulate vascular reactivity allows to reliably dissect the mechanisms of action in vascular tissue. Anesthetized rats were killed by cervical dislocation. The descending aorta was rapidly dissected without branching zones and conserved at 4 °C in Krebs-Henseleit (KH) solution, which had the following composition (mM): NaCl 118; KCl 4.7; KH_2PO_4 1.2; $MgSO_4$ 1.2; $NaHCO_3$ 25.0; glucose 11.1; $CaCl_2$ 2.5; pH 7.4. Under a stereomicroscope, excess perivascular tissue was removed from the aortic segment, which was then cut into rings that were 3–5 mm in length. The rings were used for relaxation and contraction experiments that began within the first hour after sacrifice.

The rings were placed in a LE13206 PANLAB organ bath (Barcelona, Spain) with 10 mL of KH solution at 37 °C and bubbled with carbogen, as described previously (Cupitra et al., 2020). The contractile response was

digitized with a Powerlab PL-3504 (AD Instruments) and analyzed with the dose-response module of LabChart 8 software (AD Instruments). Each preparation was stabilized at 2 g of resting tension for 90 min before initiating the agonist stimulation; during this period, the KH solution was replaced every 20 min. After stabilization, the arterial ring was stimulated twice with 40 mM KCl for 20 min and washed between each stimulus. Then, for all arterial rings, 1 μM PE and 10 μM CCh were consecutively added to the bath to confirm the presence of the endothelium. For studies in vessels with intact endothelium, if relaxation resulting from CCh was not 70% or greater, the ring was discarded. In experiments that required the absence of functional endothelium, aortic rings were denuded by gently rubbing the lumen with the closed tips of microforceps, and the success of the procedure was confirmed if the response to CCh was abolished. After that, the following evaluations were made.

Protocol 1. Blocking effect of CmV on contractile and relaxing agonists: Intact rings were preincubated with CmV at a single concentration of 50 μg/mL for 20 min. Then, separate rings were exposed to KCl at cumulative concentrations from 5 to 60 mM, to PE at concentrations from 1 nM to 10 μM and to U-46619 at concentrations from 0.1 nM to 100 nM. Relaxation studies were performed after contraction was induced by 1 μM PE using 1–10 μM CCh.

Protocol 2. Effect of CmV on vascular tone: Concentration-response curves were generated by exposing aortic rings with endothelium (intact), without endothelium (denuded), or with endothelial blockage (using 10 μM indomethacin and/or 100 μM L-NAME) to cumulative concentrations of CmV (1, 5, 10, 20, 30, 40, 50 and 60 μg/mL).

Protocol 3. Vasomotor mechanisms affected by CmV: CmV concentration-response curves were generated with rings with endothelial blockage after a 20 min preincubation with 1 μM prazosin or 3 μM seratrodast.

2.6. Statistical methods

The number of experiments is shown as (#animals, #rings). The results are presented as dot plots of the mean ± SEM. Normality assumptions were confirmed with D'Agostino-Pearson and Shapiro-Wilk tests. Concentration-response curves were fitted with nonlinear

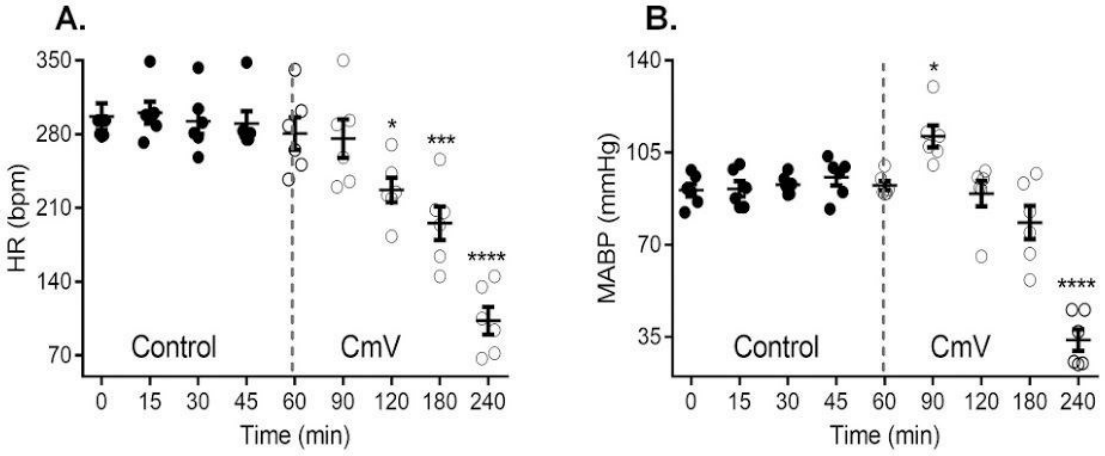

Fig. 1. Effect of CmV on heart rate (HR, panel A) and mean blood pressure (MABP, panel B) in rats. In animals that showed a stable cardiovascular condition (closed circles), the injection of the venom (indicated by the black dotted vertical lines) induced an early, transient increase in MABP, followed by a cardiovascular shock with severe bradycardia and hypotension (open circles). Significance level of $^{*}p < 0.05$; $^{***}p < 0.001$, $^{****}p < 0.0001$.

regression using a sigmoidal four-parameter (4PL) model with the equation Y = Bottom + (Top − Bottom) / (1 + 10^((LogIC50-X)*HillSlope)), where Top represents the maximum contraction (Emax) and the negative Log10 value of the molar concentration that produces 50% of the maximum response reflects sensitivity (pD2). The HR, MABP, EKG variables, pD2 and Emax were analyzed with one-way ANOVA followed by Tukey's *post hoc* test. Concentration-response curves were analyzed with two-way ANOVA followed by Tukey's *post hoc* test to compare the time/concentration. The significance level was always $p < 0.05$. The GraphPad Prism 7 statistical package v7.0 was used.

3. Results

3.1. In vivo effect of CmV on the HR and MABP

CmV at the LD50 induced a significant reduction in the HR after 60 min of injection in rats, which showed very stable values during the control period (Fig. 1A). The control values were 296.8 ± 12.5, 300.3 ± 10.6, 292.3 ± 12 and 290.2 ± 11.6 bpm at 0, 15, 30 and 45 min, respectively. After the CmV injection was finished at 60 min, the HR values observed after 10, 40, 70, 130 and 190 min were 280.7 ± 15.4, 275.8 ± 18.3, 227.0 ± 11.7, 195.5 ± 15.7 and 103.0 ± 13.1 bpm, respectively. The MABP showed an evident reversible mean increase of 16% compared to the 45-min control measurement after 40 min of injection, as shown in Fig. 1B. The control values were 90.8 ± 2.4, 91.2 ± 3, 92.9 ± 1.5 and 95.6 ± 3 mmHg. After CmV injection, the MABP values were 92.5 ± 1.7, 111.2 ± 4.1, 89.5 ± 4.8, 78.5 ± 6.3 and 33.8 ± 4.1 mmHg. All animals showed cardiovascular collapse after 130 min of injection.

3.2. In vivo effect of CmV on the EKG

Approximately 150 min after the injection of CmV, there was an increase in the normalized PR interval and QRS complex duration, as shown in panels A and B of Fig. 2. There was a trend toward an increase in the QTc ($p = 0.054$, Fig. 2C) and no changes in the P amplitude (Fig. 2D), P duration, T peak to T end interval, T amplitude or ST height (not shown). Additionally, after that time, three animals showed a change indicating a negative predominance of the QRS (not shown).

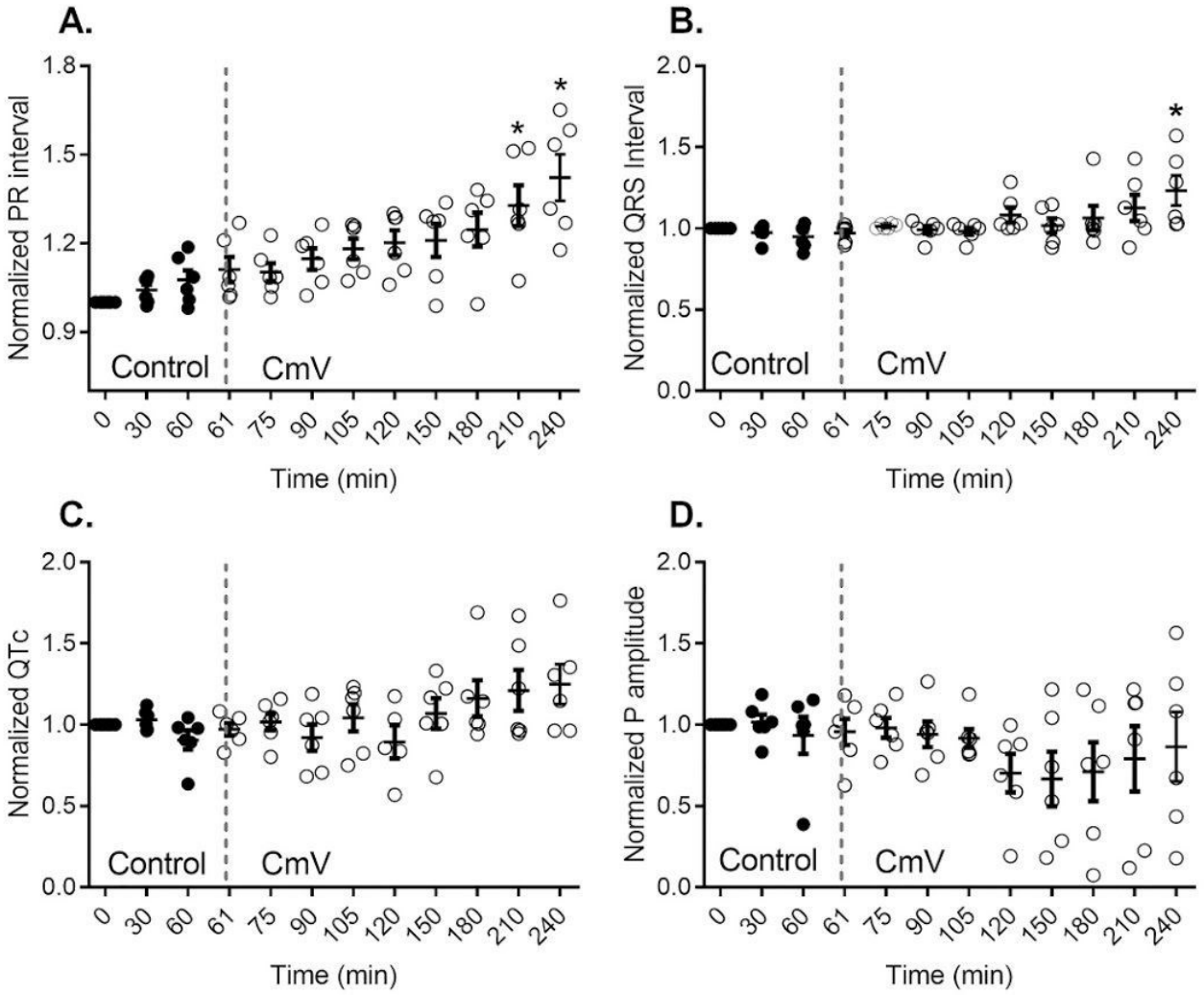

Fig. 2. Effect of CmV on EKG variables in rats. There was a clear, late increase in the normalized values of the PR interval (panel A) and QRS interval (B). Although not significant, also a reproducible, late increase in the QTc can be found (C). No change was found in a very variable P wave (D). The meaning of closed and open circles, as well as black vertical dotted lines, as in Fig. 1. Significance level of $^*p < 0.05$.

3.3. Ex vivo effect of CmV as a vascular blocker

Preincubation with venom did not show any effect (Fig. 3A) on the vascular reactivity induced by KCl, FE, U-46619 or CCh, as shown in detail in the upper rows of Table 1.

3.4. Ex vivo effect of CmV on vascular tone

Fig. 3A shows that CmV induced a small contraction in the intact ring equivalent to 5.5 ± 1.9% of the KCl Emax. In contrast, in a ring denuded of endothelium, CmV induced a strong contractile response equivalent to 37.1 ± 5.6% of the KCl Emax. This was similar to what we observed when we performed endothelial blockage with L-NAME and indomethacin (36.6 ± 3% of the KCl Emax). If we used only L-NAME and then incubated the ring with CmV, the contraction was equivalent to 25 ± 4.7% of the KCl Emax, and if we used only indomethacin prior to adding the venom, a negligible contraction equivalent to 2.5 ± 0.8% of the KCl Emax was elicited. It follows that CmV has an important contractile effect when the vessels are devoid of NO. The middle rows of Table 1 show the EC50 and Emax values observed in these experiments. The vehicle used for the application of CmV did not show any vasomotor effect.

3.5. Ex vivo vasomotor mechanisms affected by CmV

If we added seratrodast during the preincubation with L-NAME + indomethacin, the further addition of the venom induced a contractile response equivalent to 45.5 ± 5.8% of the KCl Emax (lower rows of Table 1 and Fig. 3B), which was not significantly different from the 36.6 ± 3% response reported above, suggesting that there are no other pathways that participate in the endothelial response. There was also no change in the sensitivity when comparing these two experiments (Table 1). However, if we added prazosin to the endothelial blockage experiment, the CmV-induced contractile response was dramatically reduced to 9.2 ± 3.5% of the KCl Emax, and the EC50 was significantly increased to 45.86 ± 3.2 μg/mL (Table 1 and Fig. 3B), strongly suggesting that the alpha-1 adrenergic receptor mediates most of the contractile effect of CmV.

Table 1
Vasomotor and antagonistic effects of CmV in rat aorta.

Agonists	pD2 or EC50 (μg/mL)	p value	Emax (% KCl)	p value
KCl	1.83 ± 0.3[c]	NS	134 ± 5	NS
KCl + CmV[#]	1.85 ± 0.4[c]		128 ± 4.1	
Phenylephrine	7.6 ± 0.2[c]	NS	123.8 ± 8	NS
Phenylephrine + CmV[#]	7.1 ± 0.5[c]		112.7 ± 11.5	
U-46619	7.2 ± 0.2[c]	NS	156.4 ± 11	NS
U-46619 + CmV[#]	7.6 ± 0.3[c]		129.5 ± 18	
Carbachol	6.3 ± 0.2[c]	NS	60.7 ± 2	NS
Carbachol + CmV[#]	6 ± 0.1[c]		53 ± 8.4	
Intact endothelium + CmV	36.1 ± 4.2	NA	5.5 ± 1.9	NA
Denuded endothelium + CmV	32.1 ± 6.1	NS[a]	37.1 ± 6.5	***[a]
L-NAME[¥] + indomethacin[¥] + CmV	29.8 ± 3.9	NS[a]	36.6 ± 3	***[a]
L-NAME[¥] + CmV	34.8 ± 9.3	NS[a]	25 ± 4.7	**[a]
Indomethacin[¥] + CmV	30.2 ± 5.1	NS[a]	2.5 ± 0.8	NS[a]
Prazosin[¥] + CmV	45.9 ± 3.2	***[b]	9.2 ± 3.5	***[b]
Seratrodast[¥] + CmV	36.7 ± 5.3	NS[b]	45.5 ± 5.8	NS[b]

Results as mean ± SEM. NA, not applicable; NS, non-significant.
[¥] Rings pre-incubated for 20 min with this antagonist.
[#] Rings preincubated for 20 min with 50 μg/mL CmV.
[a] Significant difference compared to Intact endothelium + CmV.
[b] Significant difference compared to L-NAME¥ + indomethacin¥ + CmV.
[c] Values presented as pD2 + SEM.
** $p < 0.01$.
*** $p < 0.001$.

4. Discussion

CmV induced the following cardiovascular alterations in rats during *in vivo* and *ex vivo* experiments: i) an irreversible reduction of the HR, ii) a reversible increase in the MABP, iii) an increase in the normalized PR and QTc interval, as well as in the QRS complex duration, iv) a direct contractile effect on aortic rings devoid of NO, and v) the direct activation of alpha-1 adrenergic pathways in the isolated aortic rings.

4.1. Cardiovascular effects of CmV

Although the clinical signs of CmV intoxication suggest activation of the sympathetic nervous system, we did not find an increase in the HR in rats but did observe a significant and temporary increase in diastolic pressure approximately 45 min after poisoning, which is the usual amount of time needed for signs to manifest when some venoms are administered intraperitoneal or subcutaneously, for example venoms of

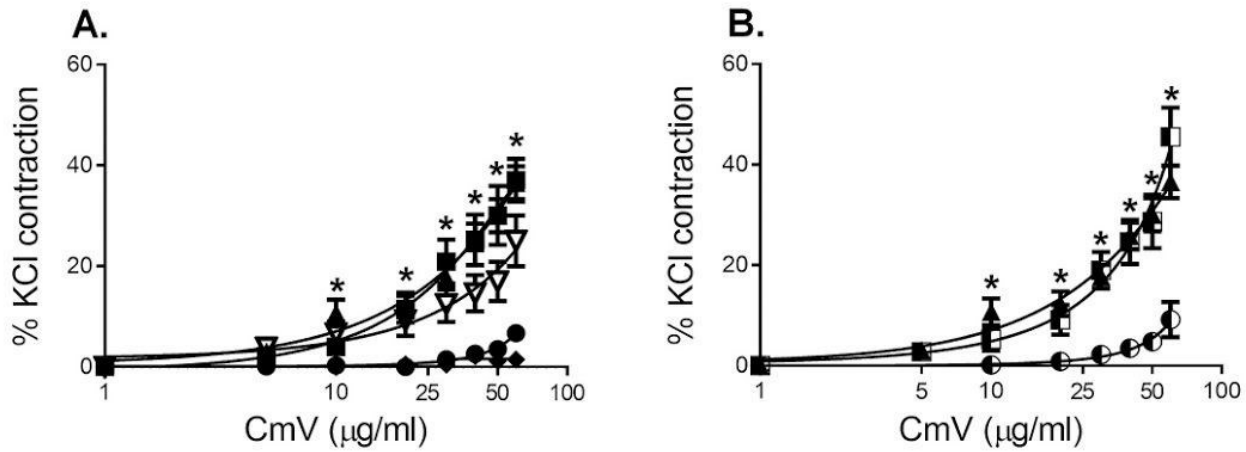

Fig. 3. Vasoconstrictive effect of CmV on rat aorta. In A, we show the effect of increasing concentrations of the venom on vessels with intact endothelium (●), denuded endothelium (■), or intact endothelium but exposed to L-NAME (▽), indomethacin (◆) and L-NAME+indomethacin (endothelial blockage, ▲). In B, we show the effect of increasing concentrations of the venom on vessels with endothelial blockage plus prazosin (◐) and seratrodast (◧). EC50 and Emax values calculated from these experiments can be seen in the Table 1. Significance level of $^*p < 0.01$.

the scorpions *Androctonus australis hector* (Elatrous et al., 2015) or *Buthus occitanus tunetanus* (Nasr et al., 2009).

This pressure increase could be explained by the inotropic effect of CmV, which has been shown with CmV (Bonilla, 2014) to be concomitant with an increase in peripheral vascular resistance, as has been reported, for instance, in the vasculature of kidneys (Galíndez-Cerón et al., 2019). Such effects are probably mediated by alpha-1 signaling, which is not heavily involved in HR regulation but increases inotropism and induces vasoconstriction through a Ca^{2+} signaling pathway (O'Rourke et al., 1992).

The prolongations in the intervals are compatible with the blockage of K^+ channels by CmV, similar to those found in aorta using venoms of *Leiurus quinquestriatus hebraeus* (Strong et al., 1989), prolonging the duration of the action potential probably through a reduction in rectifying K^+ currents or an increase in Ca^{2+} channel currents (Antzelevitch, 2007). The K^+ channel isoforms most involved in QT prolongation are 1.7 and 1.11, and although MgTx has only been shown to function as a 1.3 isoform blocker, it might also have the ability to block one or both of these channels. This pathophysiology is also compatible with the increase in the pressure/time relationship of the left ventricle that has been previously observed with CmV (Bonilla, 2014), and with other venoms such as that of the scorpion *Tityus serrulatus* (Teixeira et al., 2001).

Therefore, the positive inotropism and the increase in vascular contractility mediated by alpha-1 signaling seem to explain the increase that we observed for the MABP. Other mechanisms that may contribute to the explanation of the effect of CmV on the HR and MABP, such as neurological and inflammatory responses, have been described for venoms from other scorpions of the Buthidae family, such as *Tityus discrepans* (D'Suze et al., 2003), *Centruroides infamatus* (Ledesma Espinoza, 2013) and *Androctonus australis hector* (Nouira et al., 2005), and it would be interesting to explore these mechanisms in future studies. Likewise, hypercalcemia has been recorded in rats exposed to CmV at the LD40 dose (Romero-Imbachi, 2018). If both hypercalcemia and a high MABP occur in the same time frame of envenomation, it is then possible that the increase in Ca^{2+} prevents an even higher increase in the MABP (Vicente and de Artiñano, 1993) and could be a mechanism explaining the transiency of CmV-induced rat hypertension observed within the first hour of treatment. From the second hour on, the increase in the normalized PR interval and QRS complex duration could influence the severe decrease in the HR and the MABP changes observed 2 h after envenomation. Some late electrolyte changes, such as hypokalemia, have been described after exposure to venom from other Buthidae scorpions such as *Palamneus gravimanus* (More et al., 2004) and may help explain these late changes.

4.2. Mechanisms of the vascular effects of CmV

We showed a direct vasoconstrictor effect of CmV that was only noticeable in rings with mechanical or pharmacological removal of NO, as observed for other Buthidae scorpion venoms as *Androctonus crassicauda* (Ay et al., 1996). Consistent with what has been discussed, our experiments with prazosin showed the very important contribution of alpha-1 adrenergic receptors to the vasoconstrictor effect induced by CmV. A complementary mechanism to explain the vasoconstriction induced by CmV is based on the modulation of smooth muscle K^+ conductance as a function of the endothelium-dependent relaxing factor (Berridge, 2009), since MgTx is an inhibitor of K^+ channels (Dueñas-Cuellar, 2014; Guerrero-Vargas, 2008) and can act on smooth muscle, favoring vasoconstriction (Novakovic et al., 2006). Since there are different isoforms of MgTx and different types of K^+ channels, it would be interesting to explore the real impact of MgTx blockage of these channels on vascular physiology and to define the proportion of the effect attributable to adrenergic activity in response to CmV.

4.3. Final remarks

Although measurable, it seems that the cardiovascular toxicity of CmV is lower than that observed for venom from other species, even within the *Centruroides* genus. This may explain why some authors who used very low doses of venom in preliminary assays have misleadingly concluded that CmV has no effect on the cardiovascular system (Ferreira Santos et al., 2019). Our results may help guide future fractionation and final isolation of toxins, as well as the understanding of the mechanisms of the cardiovascular toxicity induced by CmV.

5. Conclusion

CmV produces measurable cardiovascular toxicity in rats, which is manifested as transient hypertension with no changes in the cardiac rhythm, and this can be explained in part through the activation of cardiac and vascular alpha-1 adrenergic receptors in the first hour of envenomation. After that, many alterations of the cardiac conduction system lead to severe bradycardia, hypotension and EKG alterations, which are likely induced by the blockage of K^+ channels in the heart and smooth muscle.

Declaration of competing interest

The authors declare that they have no known competing financial interests or personal relationships that could have appeared to influence the work reported in this paper.

Acknowledgments

The authors are grateful for the sponsorship of the University of Antioquia (Medellin, Colombia) and the University of Cauca (Popayan, Colombia), for the support received.

References

Antzelevitch, C., 2007. Ionic, molecular, and cellular bases of QT-interval prolongation and torsade de pointes. Europace 9, iv4–iv15.

Arenas, C., 2010. Determinación de las alteraciones electrocardiográficas causadas por el veneno del escorpión Centruroides margaritatus en ratas *Rattus norvegicus* Cepa Wistar (Unpublished bachelor's thesis, Universidad del Cauca, Popayán, Colombia). Universidad del Cauca.

Armas, L.F., Sarmiento, D.L., Flórez, E., 2012. Composición del género Centruroides Marx, 1890 (Scorpiones: Buthidae) en Colombia, con la descripción de una nueva especie. Boletín la SEA 105–114.

Ay, I., Tuncer, M., Onur, R., 1996. Effects of Androctonus crassicauda scorpion venom on endothelium-dependent and -independent vascular responses of rabbit aorta. Gen. Pharmacol. 27, 519–523.

Berridge, M.J., 2009. Inositol trisphosphate and calcium signalling mechanisms. Biochim. Biophys. Acta, Mol. Cell Res. (6), 933–940.

Bonilla, J.M., 2014. Evaluación por hemodinámica sistémica del efecto del veneno del escorpión Centruroides margaritatus, en ratas wistar (Unpublished bachelor's thesis, Universidad del Cauca, Popayán, Colombia). Universidad del Cauca.

Boyer, L.V., Theodorou, A.A., Chase, P.B., Osnaya, N., Berg, M., Mallie, J., Carbajal, Y., de Jesus-Hernandez, T., Olvera, F., Alagon, A., 2013. Effectiveness of Centruroides scorpion antivenom compared to historical controls. Toxicon 76, 377–385.

Chippaux, J.P., Goyffon, M., 2008. Epidemiology of scorpionism: a global appraisal. Acta Trop. 107 (2), 71–79.

Corona, M., Valdez-Cruz, N.A., Merino, E., Zurita, M., Possani, L.D., 2001. Genes and peptides from the scorpion Centruroides sculpturatus Ewing, that recognize Na+-channels. Toxicon 39, 1893–1898.

Cupitra, N.I., Calderón, J.C., Narvaez-Sanchez, R., 2020. Influence of ageing on vascular reactivity and receptor expression in rabbit aorta: a complement to elastocalcinosis and smooth muscle mechanisms. Clin. Interv. Aging 15, 537.

D'Suze, G., Moncada, S., González, C., Sevcik, C., Aguilar, V., Alagón, A., 2003. Relationship between plasmatic levels of various cytokines, tumour necrosis factor, enzymes, glucose and venom concentration following Tityus scorpion sting. Toxicon 41, 367–375.

Dueñas-Cuellar, R., 2014. Identificação e caracterização de peptídeos bioativos presentes na peçonha do escorpião Colombiano Centruroides margaritatus (Gervais, 1841). Doctoral thesis. Universidade de Brasília, Brasília, Brasil. Retrieved from. http://repositorio.unb.br/handle/10482/15868.

Elatrous, S., Ouanes-Besbes, L., Ben Sik-Ali, H., Hamouda, Z., Benabdallah, S., Tilouche, N., Jalloul, F., Fkih-Hassen, M., Dachraoui, F., Ouanes, I., Abroug, F.,

2015. Study of severe scorpion envenoming following subcutaneous venom injection into dogs: hemodynamic and concentration/effect analysis. Toxicon 104, 1–6.
Erdogan, A., Schaefer, C.A., Schaefer, M., Luedders, D.W., Stockhausen, F., Abdallah, Y., Schaefer, C., Most, A.K., Tillmanns, H., Piper, H.M., 2005. Margatoxin inhibits VEGF-induced hyperpolarization, proliferation and nitric oxide production of human endothelial cells. J. Vasc. Res. 42, 368–376.
Escobar, E., Velásquez, L., Rivera, C., 2003. Separación e identificación de algunas toxinas del veneno de Centruroides margaritatus (Gervais, 1841; Scorpiones: Buthidae). Rev. Peru. Biol. 10, 209–216.
Escobar, E., Flores, L., Rivera, C., 2008. Péptidos antibacterianos de los venenos de Hadruroides mauryi y Centruroides margaritatus. Rev. Peru. Biol. 15, 139–142.
Ferreira Santos, C., Céron, J.D.G., Bindá, A.H., Possani, L.D., Vidal, J.B., Fonteles, M.C., Nascimento, N.R.F., 2019. Cardiovascular effects of the scorpions Centruroides margaritatus, Centruroides limpidus and Centruroides noxius crude venom. FASEB J. 33, 812–814.
Galíndez-Cerón, J.D., Jorge, R.J.B., Chavez-Acosta, M.H., Jorge, A.R.C., Alves, N.T.Q., Prata, M.M.G., Rodrigues, F.A. d P., Havt, A., Sampaio, T.L., Martins, A.M.C., 2019. Renal alterations induced by the venom of Colombian scorpion Centruroides margaritatus. Curr. Top. Med. Chem. 19, 2049–2057.
Garcia-Calvo, M., Leonard, R.J., Novick, J., Stevens, S.P., Schmalhofer, W., Kaczorowski, G.J., Garcia, M.L., 1993. Purification, characterization, and biosynthesis of margatoxin, a component of Centruroides margaritatus venom that selectively inhibits voltage-dependent potassium channels. J. Biol. Chem. 268, 18866–18874.
Guerrero-Vargas, J., 2002. Aislamiento, Purificación y Evaluación de Neurotoxinas del Escorpión Centruroides margaritatus (Buthidae) del Municipio de El Patía, Departamento del Cauca, Colombia (Unpublished bachelor's thesis, Universidad del Cauca, Popayán, Colombia). Universidad del Cauca.
Guerrero-Vargas, J.A., 2008. Análise Proteômica Parcial da Peçonha do Escorpião Colombiano Centruroides margaritatus. Master's thesis. Universidade de Brasília, Brasília, Brasil. Retrieved from. https://repositorio.unb.br/handle/10482/1235.
Guerrero-Vargas, J.A., Buitrago, J.R., Ayerbe, S., Daza Flórez, E., Beltrán, J.T.B., 2014. Scorpionism and dangerous species of Colombia. In: Gopalakrishnakone, P. (Ed.), Toxinology. Springer, Dordrecht. https://doi.org/10.1007/978-94-007-6647-1_22-1.
Gurrola, G.B., Rosati, B., Rocchetti, M., Pimienta, G., Zaza, A., Arcangeli, A., Olivotto, M., Possani, L.D., Wanke, E., 1999. A toxin to nervous, cardiac, and endocrine ERG K+ channels isolated from Centruroides noxius scorpion venom. FASEB J. 13, 953–962.
Ledesma Espinoza, L.A., 2013. Efectos curativos y preventivos de antioxidantes (α-tocoferol y quercetina) en los signos y síntomas cardiovasculares presentados en la intoxicación por el veneno de Centruroides infamatus (Master's thesis, Universidad Autonoma de Aguascalientes, Aguascalientes, Mexico). Universidad Autónoma de Aguascalientes. Retrieved from: http://bdigital.dgse.uaa.mx:8080/xmlui/handle/11317/924.
Marinkelle, C.J., Stahnke, H.L., 1965. Toxicological and clinical studies on Centruroides margaritatus (Gervais), a common scorpion in western Colombia. J. Med. Entomol. 2, 197–199.
Minghui, R., Malecela, M.N., Cooke, E., Abela-Ridder, B., 2019. WHO's snakebite envenoming strategy for prevention and control. Lancet Glob. Health 7, e837–e838.
More, S.S., Kiran, K.M., Gadag, J.R., 2004. Dose-dependent serum biochemical alterations in Wistar albino rats after Palamnevs Gra Vimanus (Indian black scorpion) envenomation. J. Basic Clin. Physiol. Pharmacol. 15, 263–276.
Nasr, H. Ben, Serria, H., Chaker, S., Riadh, B., Zouheir, S., Kamel, J., Tarek, R., Khaled, Z., 2009. Some biological effects of scorpion envenomation in late pregnant rats. Exp. Toxicol. Pathol. 61, 573–580.
Nastainczyk, W., Meves, H., Watt, D.D., 2002. A short-chain peptide toxin isolated from Centruroides sculpturatus scorpion venom inhibits ether-??-go-go-related gene K+ channels. Toxicon 40, 1053–1058.
Nouira, S., Elatrous, S., Besbes, L., Boukef, R., Devaux, C., Aubrey, N., Elayeb, M., Abroug, F., 2005. Neurohormonal activation in severe scorpion envenomation: correlation with hemodynamics and circulating toxin. Toxicol. Appl. Pharmacol. 208, 111–116.
Novakovic, A., Gojkovic-Bukarica, L., Peric, M., Nezic, D., Djukanovic, B., Markovic-Lipkovski, J., Heinle, H., 2006. The mechanism of endothelium-independent relaxation induced by the wine polyphenol resveratrol in human internal mammary artery. J. Pharmacol. Sci. 101, 85–90.
O'Rourke, B., Reibel, D.K., Thomas, A.P., 1992. α-Adrenergic modification of the Ca2+ transient and contraction in single rat cardiomyocytes. J. Mol. Cell. Cardiol. 24, 809–820.
Osnaya-Romero, N., Acosta-Saavedra, L.C., Goytia-Acevedo, R., Lares-Asseff, I., Basurto-Celaya, G., Perez-Guille, G., Possani, L.D., Calderón-Aranda, E.S., 2016. Serum level of scorpion toxins, electrolytes and electrocardiogram alterations in Mexican children envenomed by scorpion sting. Toxicon 122, 103–108.
Parasuraman, S., Raveendran, R., 2012. Measurement of invasive blood pressure in rats. J. Pharmacol. Pharmacother. 3, 172.
Ramírez, J.H., Palacios, M., Gutiérrez, O., 2007. Implementación de la técnica en órgano aislado vascular como herramienta para la validación de plantas medicinales: Estudio del efecto vasodilatador de la Salvia scutellarioides. Colomb. Med. 38, 28–33.
Romero-Imbachi, M.R., 2018. Efecto Vasomotor Inducido Por el Veneno Total de Centruroides Margaritatus en Anillos aórticos de Ratas (*Rattus norvegicus*) Cepa Wistar (Unpublished bachelor's Thesis, Universidad del Cauca, Popayán, Colombia). Universidad del Cauca.
Sitprija, V., Sitprija, S., 2016. Animal toxins and renal ion transport: another dimension in tropical nephrology. Nephrology 21, 355–362.
Strong, P.N., Weir, S.W., Beech, D.J., Hiestand, P., Kocher, H.P., 1989. Effects of potassium channel toxins from Leiurus quinquestriatus hebraeus venom on responses to cromakalim in rabbit blood vessels. Br. J. Pharmacol. 98 (3), 817–826.
Teixeira Jr., A.L., Fontoura, B.F., Freire-Maia, L., Machado, C.R.S., Camargos, E.R.S., Teixeira, M.M., 2001. Evidence for a direct action of Tityus serrulatus scorpion venom on the cardiac muscle. Toxicon 39 (5), 703–709.
Vicente, M.P., de Artiñano, M.A.A., 1993. Demonstration of the alpha-vasoconstriction-lowering effect of calcium in the pithed rat. J. Vasc. Res. 30, 303–308.